REPUBLIC OF TURKEY
MARMARA UNIVERSITY
INSTITUTE OF HEALTH SCIENCES

THREE-DIMENSIONAL EVALUATION OF THE SIZE AND DIMENSIONAL CHANGES OF THE VOMER BONE IN MIDFACIAL DEFICIENCY INDIVIDUALS

AMMAR RIYAD MOHI
PhD THESIS

DEPARTMENT of ORAL AND MAXILLOFACIAL RADIOLOGY

SUPERVISOR
Prof. Dr. Şebnem ERÇALIK YALÇINKAYA

ISTANBUL-2017

TEZ ONAYI

Kurum : Marmara Üniversitesi Sağlık Bilimleri Enstitüsü

Programın seviyesi : Doktora

Anabilim Dalı : Ağız, Diş ve Çene Radyolojisi A.B.D.

Tez Sahibi : Dr. Ammnar Riyad MOHİ

Tez Başlığı : Three dimensional evaluation of the size and dimensional changes of the Vomer Bone in midfacial deficiency individuals

Sınav Yeri : DİŞ Hekimliği Fakültesi Ağız, Diş Ve Çene Radyolojisi A.B.D.

Sınav Tarihi : 29.11.2017

Tez tarafımızdan okunmuş, kapsam ve kalite yönünden Doktora Tezi olarak kabul edilmiştir.

Danışman (Unvan, Adı, Soyadı)	Kurumu	İmza
Prof. Dr. Şebnem ERÇALIK YALÇINKAYA	Marmara Üniversitesi	

Sınav Jüri Üyeleri (Unvan, Adı, Soyadı)

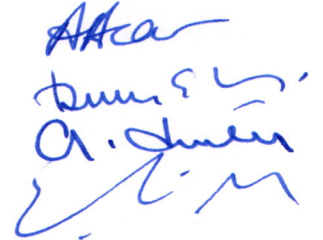|		
Prof. Dr. Ahu ACAR	Marmara Üniversitesi	
Prof. Dr. Tamer L. ERDEM	Okan Üniversitesi	
Yrd. Doç. Dr. Asım DUMLU	Marmara Üniversitesi	
Yrd. Doç. Dr. Mehmet Ali ELÇİN	Aydın Üniversitesi	

Yukarıdaki jüri kararı Enstitü Yönetim Kurulu'nun 07./.12./.2017 tarih ve 13 sayılı kararı ile onaylanmıştır.

Prof. Dr. Göksel ŞENER
Sağlık Bilimleri Enstitüsü Müdürü

-Sınav evrakları 3 iş günü içinde ıslak imzalı tek kopya halinde Enstitüye teslim edilmelidir.
-Bu form bilgisayar ortamında doldurulacaktır.

BEYAN

Bu tez çalışmasının kendi çalışmam olduğunu, tezin planlanmasından yazımına kadar bütün aşamalarda etik dışı davranışımın olmadığını, bu tezdeki bütün bilgileri akademik ve etik kurallar içinde elde ettiğimi, bu tez çalışmasıyla elde edilmeyen bütün bilgi ve yorumlara kaynak gösterdiğimi ve bu kaynakları da kaynaklar listesine aldığımı, yine bu tezin çalışılması ve yazımı sırasında patent ve telif haklarını ihlal edici bir davranışımın olmadığı beyan ederim.

17 KASIM 2017

Ammar MOHI

DECLERATION

I declare that this thesis study belongs to me. There is no immoral attitude in all stages from the planning stage of thesis to the writing stage. I gained all the information in the terms of academic and ethical rules. I stated sources for the information gained not with this study. I showed the source in the list of sources, and again there is no copyright infringement in study and writing stage.

17 NOV. 2017

Ammar MOHI

I. ACKOWNLEDGEMENTS

II. CONTENTS   **Page No**

III. ABBREVIATIONS

>: Greater than

≥: Equal to or greater than

<: Smaller than

2D: Two Dimensional

3D: Three Dimensional

AOI: Area of Interest

CBCT: Cone Beam Computed Tomography

CT: Computer Tomography

DICOM: Digital Imaging and Communications in Medicine

Et al: And others

FH: Frankfort Horizontal

FOV: Field of View

HP: Horizontal Plane

HU: Hounsfield Units

KV: Kilovolt

MIMICS: Materialise Interactive Medical Image Control System

MRI: Magnetic Resonance Imaging

MS-CT: Multi-Slice Computed Tomography

MTF: Modulation Transfer Function

n: Number

mm: Millimeters

mm^3: Cubic millimeters

p: probability

r: Correlation Coefficient

SD: Standard Deviation

Sig.: Significance

IV. LIST OF FIGURES AND GRAPHS

V. LIST OF TABLES

Three-Dimensional Evaluation of the Size and Dimensional Changes of Vomer Bone in Mid-Facial Deficiency Individuals.

Dr.Ammar Riyad MOHI / Prof. Dr. Şebnem Erçalık YALÇINKAYA

1. SUMMARY

Aim: The aim of this study was 1) To evaluate the vomer bone shape and size changes in relation to midfacial deficiency features. 2) To determine the correlation between different cranial and midfacial skeletal parameters of the vomer bone in both linear and angular measurements. 3) To compare the 3D reconstructed vomer bone models of three groups. **Material and Method**: CBCT images of 96 patients with normal occlusion and Class III malocclusion were collected from the archive of Orthodontic Department, Faculty of Dentistry, Marmara University. The age of patients was between 16-30 years old. All images were classified into three groups using ANB angle Steiner's analysis: Normal (type A) group, Mild (type B) and Severe (type C) midfacial hypoplasia groups. Firstly, 13 skeletal points in cranial, midfacial and vomer region level were selected. Then linear and angular reference planes were drawn for shape outline analysis and later the 3D reconstructed models of vomer bone size were measured using Mimics 19.0V software and data were statistically analyzed. **Results**: There were high significant differences between anterior variables ($P< 0.01$) followed by posterior variables ($P<0.05$) of the vomer bone with high positive correlation in linear and angular parameters in all planes of the severe group (type C) and it was higher in males than females. No statistical correlation within different age was found ($P>0.01$). The size of the 3D reconstructed model of the vomer bone was larger and had elongated pattern in severe group (type C) when compared to other groups ($p<0.001$). **Conclusion**: Based on the findings of this study, it was concluded that the vomer bone had an eventual role in preserving the midface contour of class III malocclusion midface complex in all planes.

Keywords: Mimics, Orthodontics, Vomer Bone, Midfacial Hypoplasia.

Vomer Kemiğinin Konumunun ve Boyutlarının Orta-Yüz Yetersizliği Olan Bireylerde Üç Boyutlu Olarak Değerlendirilmesi

Dr.Ammar MOHI / Prof.Dr.Şebnem YALÇINKAYA

2. ÖZET

Amaç: Bu çalışmanın amacı, 1) Orta-yüz yetersizliği olan bireylerde vomer kemiğinin konumsal ve boyutsal morfometrik değişimlerini değerlendirmek, 2) Farklı kranial ve midfasiyal iskeletsel parametrelerde, lineer ve açısal ölçümlerle gruplararası korelasyonun belirlemek ve 3) Vomer kemiğininin 3B rekonstrüksiyon modelini üç farklı yüz profilinde karşılaştırmaktır. **Gereç ve Yöntem:** Marmara Üniversitesi Diş Hekimliği Fakültesi Ortodontik A. D. arşivinden seçilmiş, normal okluzyonu ve Angle Sınıf III malokluzyonu olan 16-30 yaş arasındaki 96 hastanın CBCT görüntüleri değerlendirildi. Steiner analiziyle hastalar üç gruba ayrıldı: Normal (tip A), Hafif (tip B) ve Şiddetli (tip C) orta-yüz yetersizliği. Kranial, midfasiyal ve vomer bölgesinde, 13 iskeletsel nokta seçilerek doğrusal ve açısal referans düzlemleri çizildi. Vomer kemiğinin 3B rekonstrüktif boyutları, MIMICS 19.0V yazılımıyla ölçüldü ve veriler istatistiksel olarak analiz edildi. **Bulgular**: Lineer ve açısal ilişkide vomer kemiğinin anterior ($p < 0.01$) ve posterior ($P < 0.05$) düzeysel parametreleri arasında istatistiksel olarak anlamlı ilişki olduğu saptandı ve bu korelasyonun erkeklerde ve şiddetli (tip C) orta-yüz yetersizliği grubunda daha belirgin olduğu görüldü ($p<0.01$). Vomer kemiğinin 3B rekonstriktif modelinin şiddetli (tip C) grupta daha geniş ve daha uzun şekilde ölçüldüğü ve istatistiksel olarak diğer gruplardan farklı olduğu saptandı ($p<0.001$). **Sonuç:** Bu çalışmanın bulguları tüm düzlemlerde orta-yüz bölgesinde, vomer kemiğinin aktif rolünün önemini göstermektedir.

Anahtar Sözcükler: MIMICS, Ortodonti, Vomer Kemik, Orta-Yüz Yetersizliği.

3. INTRODUCTION AND AIMS

Class III malocclusion may display a midface hypoplasia, in combination with normal or prognathic mandible. Midfacial hypoplasia is characterized by deficiency of skeletal height, width, and anterioposterior relationships, which requires multidirectional correction (McNamara and James 1987; Bailey, Proffit and White 1995; Ngan and Moon 2015).

The midfacial skeleton morphology may be affected by several factors such as age, gender, facial growth pattern, pathological/functional alterations, decreased or increased muscular activity, occlusal force, and dental occlusion changes (Wada et al. 1980; Tanaka et al. 2008). The remodeling and reconfiguration of the midfacial bones may compensate under adaptation responses to outline the final configuration of midface and adjacent structures (Enlow DH and Bang S 1965; Sato et al. 2001).

The vomer bone as a central structure of the midfacial complex has a role as sustaining a good occlusion and balanced stomatognathic system (Ackerman, Proffit, Sarver 1999; Proffit L 2000). Several studies reported the dimenssional variations of vomer bone outline or anatomical alteration in relation to the development of dentofacial frame discrepancy (Fawcett E 1911; Hansen et al. 2004).

Basili et al. (2009) published a key study regarding the vomer bone relation in the architecture of craniofacial structures in caucasic human skulls. They were measured the vomer bone actual structure variables using dry skull measurements and were concluded that the sagittal relationship between the vomer bone and cranium may influence other adjacent structures of the craniofacial system. Thus, the morphology of vomer bone and midfacial relationship could be compromised, in significant to the sagittal discrepancies, due to sliding or compression forces of the surrounding tissues cross through the vomer bone. This could favor a continuous adaptation of midface compartement by dimensional changes of its compartments through remodeling process (Tanaka and Sato 2008; Hall and Precious 2013).

In the earlier studies, the analysis of malocclusion evaluated by use of conventional radiographs analysis which have limitations such as structural superimpositions in two-

dimension, particularly in some regions such as the midfacial complex and also loss of accuracy (Sato S 2001). Currently, CBCT as three- dimenssion diagnostic element provide theoretical advantages over conventional imaging of the midfacial compartment. CBCT provides a high resolution imaging that allows the qualification and quantification of facial bone tissues in almost real dimensions without significant magnification or distortion (Adams et al. 2004; Muramatsu et al. 2008; Van Vlijmen et al. 2009; Basili et al. 2009). Newly computer based analysis softwares like MIMICS() have a high level of imagin resolution and fine details appearance with an accurate size and shape demonstration (Takada et al. 1993; Barteczko et al. 2004, Polat and Kaya 2007; Lagravère et al. 2008; Periago et al. 2008).

In view of these different publications, it is clear that the vomer long neglected to be determined alone away from the septum or confused with him. Little studies, seemed to intervene predominantly with the anterior-posterior growth of the middle third of the face (Foster and Holton 2016).

In fact, it is necessary to take into account the active and real role of the vomer bone position in development of facial integrity and how the vomer bone act as a main strut in midfacial complex to enforce the skeleton properly. Based on that clinical evidence analyses, the midfacial deficiency advocate the active role of vomer bone to be avaliable in Angle Class III malocclusion.

This study used the 3D image CBCT construction technique of MIMICS software to evaluate the midfacial hypoplasia in relation to vomer bone shape and size alteration of Cl III malocclusion in comparison to normal control group with aiming :

1) To evaluate the vomer bone morphometric changes of shape and size in relation midfacial hypoplasia features of different study groups.

2) To determine the correlation between different cranial and midfacial skeletal parameters of the vomer bone in both linear and angular measurements.

3) To compare three different facial profile of 3D reconstructed model of vomer bone using Mimics 19.0v Software analysis tool.

4. LITERATURE REVIEW

4.1 Human Craniofacial Integrity

The human skull is a complex of structures that forming of a mosaic of semi-independent but closely integrated functional units (Enlow and Hans 1996; Sperber and Guttmann 2001; Hallgrimsson et al. 2007). The inter-relationship of these units and their modifications can be induced by intrinsic or extrinsic factors (Lieberman et al. 2008).

The cranial sutures are the major sites of growth during the rapid expansion of the neurocranium and the development of the maxillary complex. (Opperman LA 2000) This growth is controlled by a highly complex intercellular signaling system that governs the different regions and suture margins (Jiang et al. 2002). The mechanical forces of functional and environmental origin play an important role in the development an integrity of facial skeleton (Langford et al. 2003a; Mao and Nah 2004; Lieberman 2008).

Early studies focused on the morphological differences among cranial units (Moss ML 1958; McNeill and Newton 1965), while others approached the anthropology concepts (Cheverud and Midkiff 1992; Cheverud et al. 1992). However, recent studies dealt with the alteration of the covariances in different units of midface complex, showing a pervasive integration that overlay and modify the deformation (Martinez-Abadias et al. 2009).

The majority of previous studies on deformation have detected changes in the growth of the base of the skull and of the viscerocranium. McNeill and Newton (1965), detected a more obtuse angle of the base of the skull and an increase in its width, but found no correlation with any specific type of deformation. Moss ML (1958), reported kyphosis of the base of the skull that was related to the type of deformation to which the vault was subjected. In contrast, Schendel et al. (1980), found alterations of the jaws in deformed skulls, supporting the hypothesis that the integration within cranial units led to subtle changes in maxillary structures.

Björk and Björk (1964), reported that the incisal midline was maintained by a compensatory asymmetric growth of the jaws in artificially deformed skulls with marked

5

asymmetry of the vault and base of the skull; this coincides a close interaction between function and the shape and size of the jaws (Dixon, Hoyte and Rönning 1997; Langford et al. 2003a; Paschetta et al. 2010).

4.1.1 Midfacial Complex Embryology Concepts

The facial bones develop intramembranously from ossification centers in the neural crest mesenchyme of the embryonic facial prominences. An epithelial-mesenchymal interaction between the ectomesenchyme of the facial prominences and the overlying ectodermal epithelium is essential for the differentiation of the facial bones as appear in Figure 4.1 (Kjaer et al. 1999).

Bone	Site and Number of Ossification Centers		Initial Appearance
	Primary	Secondary	
Frontal	Superciliary arch (2)		8 weeks
		Trochlear fossa (2)	8.5 weeks
		Zygomatic process (2)	9 weeks
		Nasal spine (2)	10–12 yr
Parietal	Eminence (2)		8 weeks
Occipital (interparietal)	Supranuchal squamous (medial) (2)		8 weeks
		Supranuchal squamous (lateral) (2)	12 weeks
Temporal (desmocranial portion)	Squamous/zygomatic (1)		8 weeks
	Tympanic ring (4)		12 weeks
Nasal	Central (1)		8 weeks
Lacrimal	Central (1)		8–12 weeks
Maxilla	Body (1)		7 weeks
		Zygomatic (1)	8 weeks
		Orbitonasal (1)	8 weeks
		Nasopalatine (1)	8 weeks
Premaxilla	Intermaxillary (2)		7 weeks
Palatine	Junction of horizontal and perpendicular plates (1)		8 weeks
Vomer	Alae (2)		8 weeks
Mandible	Body (1)		6–7 weeks
		Coronoid, condylar (cartilage)	10–14 weeks
		Mental ossicles (cartilage)	7 mo pc
Zygomatic	Body (1)		8 weeks

pc = post conception.

Figure 4.1: Intramembranous Ossification Centers (Craniofacial development/ Sperber 2001).

The ossification centers for the upper third of the face are those of the frontal bone, which also contributes to the anterior part of the neurocranium. In the frontonasal prominence, intramembranous single ossification centers appear in the 8th week post conception for each of the nasal and lacrimal bones in the membrane covering the cartilaginous nasal capsule (Arnold et al. 1998).

The embryonic facial maxillary prominences develop numerous intramembranous ossification centers. Single ossification centers appear for each of the palatine bones, and two centers appear bilaterally for the vomer in the maxillary mesenchyme surrounding the cartilaginous nasal septum in the 8th week post conception (Gill et al. 1994).

A primary intramembranous ossification center appears for each maxilla in the 7th week, at the termination of the infraorbital nerve just above the canine tooth dental lamina. Secondary zygomatic, orbitonasal, nasopalatine, and intermaxillary ossification centers appear and fuse rapidly with the primary centers (Kjaer and Niebuhr 1999).

The two intermaxillary ossification centers generate the alveolar ridge and primary palate region that is homologous with the premaxilla in other mammals. In humans, this area encloses the four maxillary incisor teeth; in the neonate, it is demarcated by a lateral fissure from the incisive foramen to the area between the lateral incisor and canine teeth and forms the so-called os incisivum (Du Raan FJ 2017).

The nasal cavity and (in particular) the nasal septum have considerable influence in determining facial form. In the fetus, a septomaxillary ligament arising from the sides and anteroinferior border of the nasal septum and inserting into the anterior nasal spine, transmits septal growth "pull" to the maxilla (Niida et al. 1991; Guis et al. 1995).

Facial growth is directed downward and forward by the septal cartilage, which expands its vertical length sevenfold between the 10th and 40th weeks post conception. At birth, the nasal cavity lies almost entirely between the orbits. Growth of the nasal septal cartilage continues but at a decreasing rate until the age of 6 years, lowering the nasal cavity floor below the orbits (Sandikcioglu, Mølsted and kjaer 1994).

This pull created by nasal septal growth can be separate the frontomaxillary, frontonasal, frontozygomatic, and zygomaticomaxillary sutures in varying degrees. The growth potential of the nasal septal cartilage is clearly demonstrated in cases of bilateral cleft lip

and palate: the tip of the nose, columella, philtrum, prolabium, and primary palate form a globular process that, freed from its lateral attachments to the maxillae, protrudes conspicuously on the face as a result of vomerine and nasal septal growth (Siegel et al. 1991).

This growth normally dissipates into adjacent facial structures, which indicates some resistance to it. It is of interest that the nasal septum deflects from the midline during late childhood, indicating some resistance to septal growth thrust. The spheno-occipital synchondrosis cartilage forces also act variously in separating the facial sutures. Furthermore, these sutures later subjected to forces exerted by the masticatory muscles (i.e., masticatory pressures transmitted through adjacent bones) (Del Santo et al. 1998).

Growth of the maxilla depends on the influence of several functional matrices that act upon different areas of the bone, thus theoretically allowing its subdivision into "skeletal units" appear in Figure 4.2.
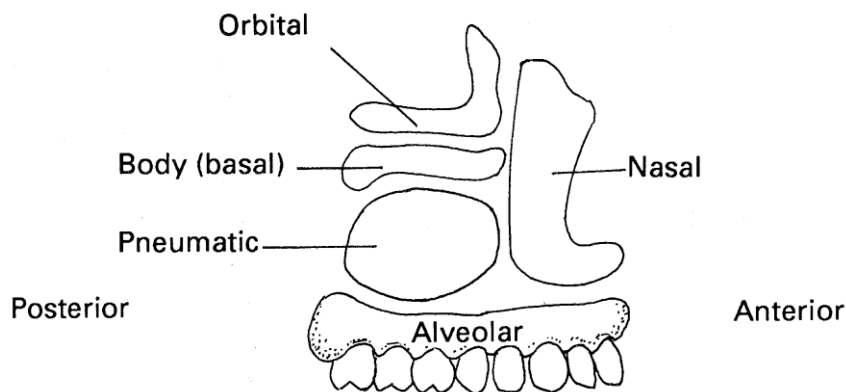
Figure 4.2: Schema of "skeletal units" of the maxilla.

The complex action of these functional forces on the facial bones results in different effects on different sutures. The growth pattern of the dental alveolar arch differs from that of the facial skeleton, being related to the sequence of tooth eruption. Resorption along the anterior surface of the bodies of the maxillae creates the supra-alveolar concavity, thus emphasizing the projection of the anterior nasal spine of the maxilla (Kjaer and Niebuhr 2005).

Sadler TW (1911) and Scammon RE (1930), earlier demonstrated this type of somatic development many years ago; there is rapid pre- and postnatal activity, followed by slowing until adolescent acceleration which continues to a tapering off near adulthood. One should be cognizant of the fact that this type of assessment elucidates craniofacial development in a collective sense, and one has simply viewed expansive growth as the net effect of surface activity alone.
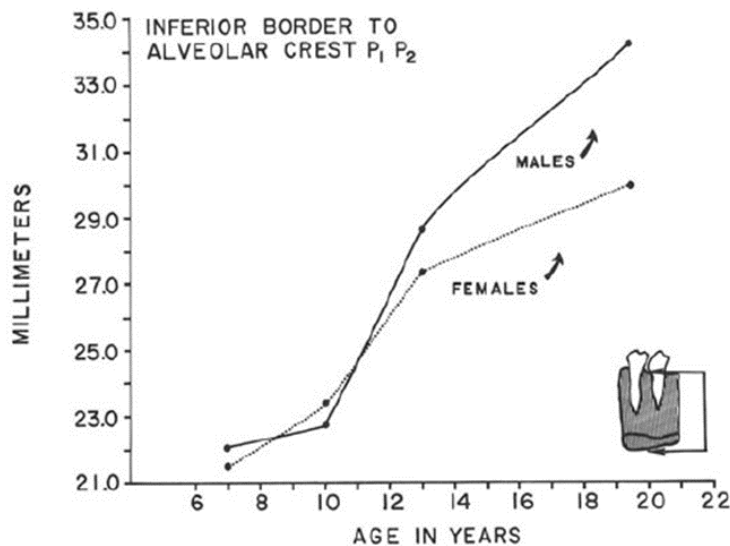
Figure 4.3: Surface measurements depict enlargement plotted relative to age.

The growth pattern shown by the maxilla, as the major bone in the upper face, provides an example of the Operation of the three mechanisms of bone movement. If the movement of a Landmark on the anterior surface of the maxilla from soon after birth to adult life is examined (point A), all three growth mechanisms are found to participate in the movement. Firstly, the Landmark (point A) will move mainly in downward direction by bone deposition on the inferior-facing surfaces of the maxilla. An equivalent, integrated degree of bone resorption is found on the superiorly facing surfaces as shown in Figure 4.3 (Brodbent and Golden 1975).
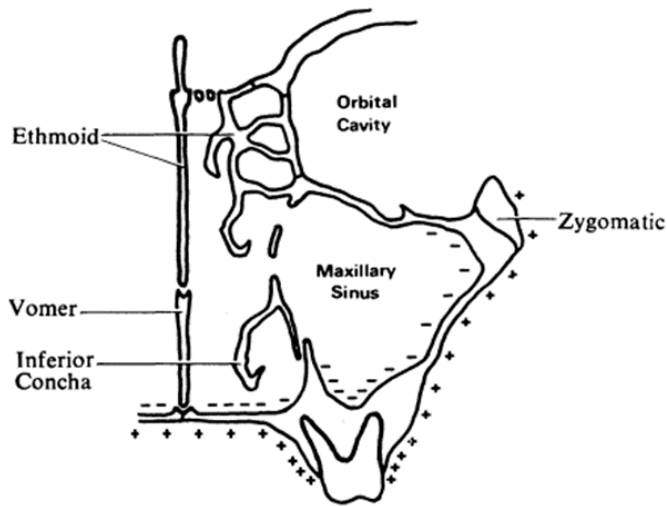
Figure 4.4: Growth of the upper facial skeleton. Surface deposition, +; resorption, -.

This remodeling is associated with the increase in maxillary height which occurs with the enlargement of the maxillary sinus and the development and eruption of the dentition. Secondly, the Landmark will move following sutural growth at the circumnasal suture system. The effect on point A of growth at these sutures is in a downward and forward direction, but in this instance the movement is achieved by the bodily movement of the whole maxilla (Enlow et al. 1977).

Finally, the landmark is repositioned in a forward direction by endochondral bone formation at the sphenooccipital synchondrosis. In this instance, the whole anterior cranial base has been repositioned forward by an enlargement of the middle cranial fossa (Savara and Thomas 1972).

Furthermore, it will be appreciated that the movement of one point on the surface of the maxilla in a downward and forward direction does not mean that all the points in the maxilla are growing in the same direction at the same rate. For instance, at stages during the development of the molar teeth, the posterior aspect of the maxilla is growing rapidly in a distal direction as shown in Figure. 4.4 (Ricketts RM 1972 and 1973).
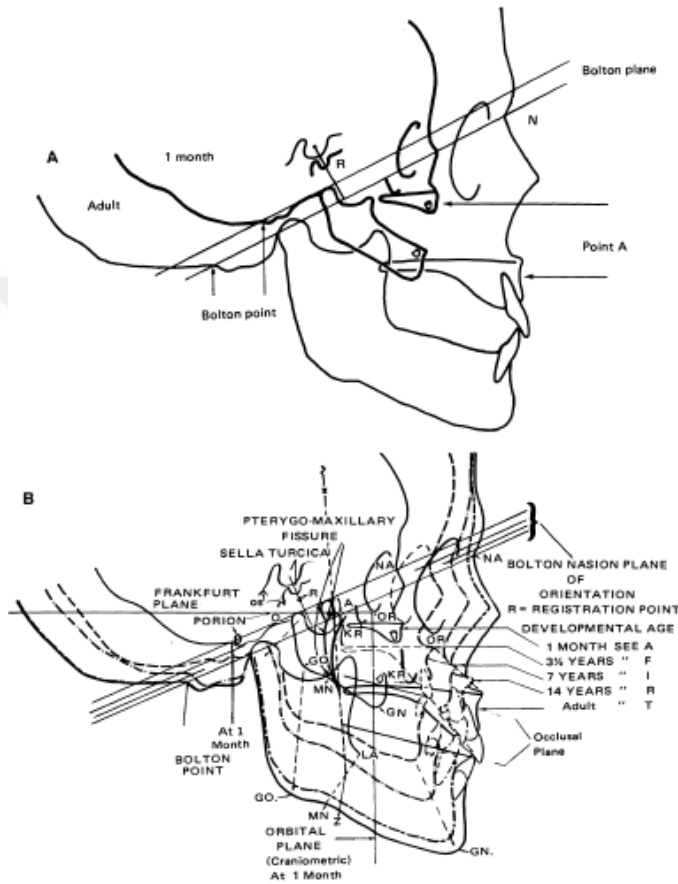
Figure 4.5: Superimposition of radiograph tracings, A) Point of maxilla, B) Composite tracing showing mean growth trends (postnatal Growth Falkner and Tanner 1978).

In the midline of the nasomaxillary complex, the septal cartilage articulated in infancy with the ethmoid sphenoid, vomer, and premaxilla bones (Figure 4.5). This structure is derived from the cartilage of the embryonic nasal capsule and formed from primary cartilage. At the septoethmoidal junction, the cartilage is replaced by bone in a zone of endochondral ossification (Baume LJ 1961). Furthermore, the cartilage is attached anteriorly to the premaxilla by a septopremaxillary ligament (Latham RA 1969). The growth potential of cartilage region has been prompted by several authors. Scott JH

(1958), suggested that the nasal septum acts as a primary growth center for the normal development of the upper facial region. This view is supported by experiments involving the resection of all or part of the nasal septum in experimental animals, with a resulting distortion in the normal growth pattern of the facial region (Sarnat and Wexler 1967). As similar, Gange and Johnston (1974), reported about the septopremaxillary attachment in rats.
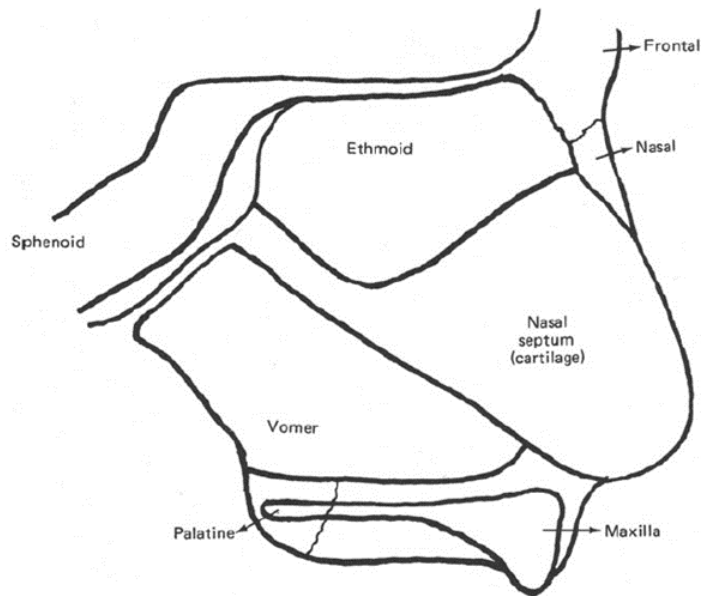
Figure 4.6: The nasal septum and adjacent bones in a young child (postnatal Growth /Falkner and Tanner 1978).

4.1.2 The Midfacial Complex Anatomical Concepts

The first signs of the facial mass ossification appear towards seventh week, i.e. a week earlier than those in the vault and before those of the endochondral ossification of the base. Ossification obeys topographical and chronological sites called ossification centers affect

a provision to Nerve correspondence while the growth of the bone piece is governed by predominantly muscular dynamic phenomena (Becker, Drachman and Kirscht 1972).

The appearance of bone seems to correspond to a nervous presence introducing the concept of a neuro-matricial axis whose vomeric model is represented by the internal spheno-palatal axis (Sadler TW 2011). Ossification takes place in two distinct ways:

1) Indirect substitution ossification of a Pre-existing cartilage model. This is chondrocranium intended for form the base of the skull and the nasal septum.

2) Direct membranous modality by direct transformation of the connective tissues. It is the desmocranium intended to form most of the bones of the face and the vault, with the exception of the inferior horn and the lateral masses of ethmoid.

Some bones have a mixed origin of direct and indirect membranous modality substitution of ossification like the sphenoid and vomer bones.

Midfacial complex or the middle of the face between the frontal sinus above, the oral cavity below, and the orbits and maxillary sinuses to the sides compose of the nasal bones which is encased in a pyramidal-shaped Osseo-cartilaginous framework and is divided into two compartments by the nasal septum (Ellis and McNamara 1984; Hitotsumatsu, Rhoton and Albert 2000).

The osseous portion consists of two nasal bones that articulate with the nasal process of the frontal bone superiorly and fuses with the maxilla laterally. Their lower borders are beveled on their inner surfaces where they articulate with the upper lateral nasal cartilages (Dion, Blalock and Gifford 1978).

The nasal cavity is divided by a vertical septum into two similarly paired cavities. Each half has a medial wall (the nasal septum) and a lateral wall that contains ridges called conchae or turbinates. The roof of the nasal cavity consists of the crista galli, the cribriform plate, and the body of the sphenoid containing the sphenoid sinus. The bony floor is made up anteriorly by the palatine process of the maxilla and posteriorly by the horizontal process of the palatine bone (Gardner BG 1982). The nasal septum is a midline bony and cartilaginous structure that is composed of five parts: Cartilage of the nasal septum, Perpendicular plate of ethmoid bone, Crest of the maxillary bone, Crest of the palatine bone, Vomer bone (Sadler TW 2011).

4.1.3 The Vomer Bone Identification and General Considerations

Identification of vomer bone unlikely to misidentify a complete vomer due to its characteristic shape. Fragments, however, are likely to be indistinguishable from other delicate nasal and facial fragments. It composed of two laminae that are fused inferiorly, but separated superiorly. The space between laminae is greater posteriorly than anteriorly (Le Diascorn H 1972).

The primitively double vomer develops from two centers of ossification that appear in the second month in the submucous connective tissue Which covers the lateral faces of the nasal septum issuing from the nasal capsule. The two bone blades (Vomerous wings) are gradually bottom up at the same time as the septal cartilage is reduced from back to front. The vomer then takes the form of a Y shape (Le Diascorn H 1972).

The perpendicular blade reaches the vomer between the 4th and 7th year (Hillenbrandt S 2014). its ossification continues until overlapping with it (Verwoerd, Verhoef and Meeuwis 1989). The vomer can therefore be divided into two parts:

1-An upper part corresponding to the fusion of the two wings.

2-A lower part in relation to the palate.

4.1.4 The Development of The Vomer Bone

The vomer is a latin meaning (ploughshare) or (vomere) latin meaning to (vomit ,throw up) because, the ploughshare threw up the earth on either side in fanciful resemblance to vomitig. Anatomically, it is a thin, trapezoid-shaped plate of bone that lies in the midline and forms part of the nasal septum. It articulates with the sphenoid, ethmoid, and palatine bones, and with the maxilla and septal cartilage. It has two surfaces and four borders as in Figure 4.7 (Arnaud et al. 1997; Sperber, Guttmann and Sperber 2001).
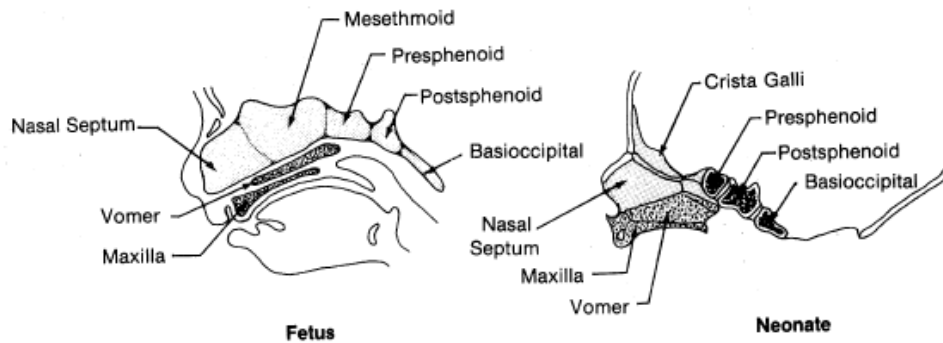
Figure 4.7: Fetus and neonatal appearnce of vomer bone development (Craniofacial Development, Sperber 2001).

The two surfaces, forming part of the medial wall of each half of the nasal cavity, are both covered by mucous membrane and bear grooves for nasopalatine nerves and vessels. The posterior border bears two thickened alae with a deep groove between them into which articulates the underside of the body and the sphenoid. The alae are overlapped by the vaginal processes of the medial Pterygoid plates and the sphenoidal processes of the palatine bones. The long anterosuperior border articulates behind with the perpendicular plate of the ethmoid and in front with the nasal septal cartilage.

There may be a band of cartilage between the ethmoid and vomer even into old age but more usually the two bones fuse in early adult life (Arnaud et al. 1997).

The joint between the vomer and the septal cartilage is unusual in that it is the only freely moveable joint composed of non-cartilage-covered bone on one side and cartilage on the other. The perichondrium of the septum and the bone of the vomer are separated only by a fat pad. This would appear to be a safety device to prevent dislocation of the septum, as pressure on the anterior border causes the cartilage to bend obliquely on itself in its long axis (Atherton J 1967).

The inferior border rests on the median crest formed by the horizontal plates of the palatine bone and the maxilla. The posterior border forms a gently curving, free edge that forms a midline division between the posterior choanae. It is thin below and thickens above as it slopes towards the two alae. Incomplete ossification may lead to perforations in the bone

or to a narrow cavity between the two sides. Most of the variations in the shape of the vomer play a part in the clinical condition of deviated septum (Takahashi M 1987).

The vomer develops from two intramembranous ossification centres that appear in the mucoperichondrium at the lower border of the nasal septum during the ninth week of uterine life (Fawcett E 191l; Macklin CC 1921; Müller and O'Rahilly 1980). Histologically, they appear as two slender strips of bone, widest in the middle and tapering off towards their ends. After about 2 weeks, they fuse at their lower borders beneath the septal cartilage to form a V- or U-shaped bone. Later still, this becomes Y-shaped in coronal section which extends from the sphenoid posteriorly to the premaxilla area, supports the lower edge of the septal cartilage. The posterior part of vomer bone will ossify later as the perpendicular plate of the ethmoid (O'Rahilly and Meyer 1956).

The vomer is visible radiographically at about 11 weeks and in the third trimester of fetal life become a boat-shaped, consisting of two leaves of bone joined inferiorly into a single lamina with a flattened base as seen in (Figure 4.8). Each leaf has a feathery free edge and is pointed and almost vertical anteriorly. Posteriorly, the two leaves open out to form a scoop-shaped end, which develops into the vomerine alae (Sandikcioglu, Mølsted and Kjaer 1994).
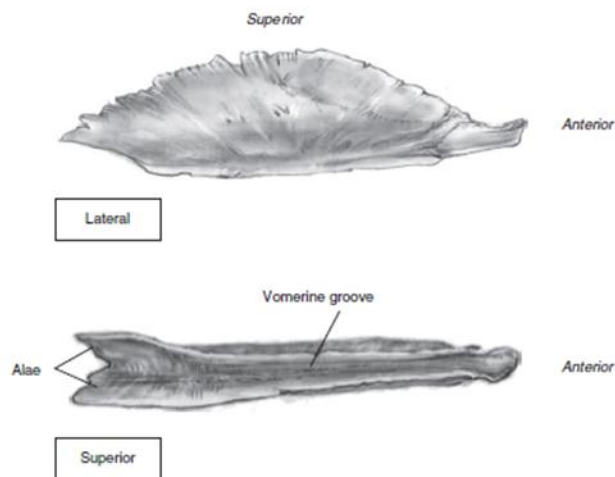
Figure 4.8: The vomer in the third trimester of fetal life is boat-shaped (Schaefer 2009).

Fawcett R (191l), described the vomer bone as the invading and ossifying the posterior end of the anterior paraseptal cartilages, which he believed it was originated from the roof of the nasal capsule.

The postnatal growth of the vomer is intimately connected with the growth of the nasal septum as a whole and the consequent increase in size of the facial skeleton (Scott M 1958).

Takahashi M (1987), in his study of septal deformity, gave a detailed account of the changes in the vomer and distinguished nine phases of development. The downward spread of ossification in the perpendicular plate of the ethmoid reaches the vomer during early childhood and contact between the two structures induces further ossification at the open edges of the vomerine groove.

By the age of 10 years, the height of the posterior edge of the nasal septum is about 85% of its adult size. The superior left and right edges of the vomer fuse, converting the groove into a vomerine canal by the age of puberty. During adult life, the bone undergoes compaction and thinning and also increases in height. In early adult life, there is usually fusion with the perpendicular plate of the ethmoid (Scott M 1958).

4.1.5 Descriptive Anatomy of Vomer Bone

All The faces of the vomer are flat and almost smooth. Quite often there is a deviation of the partition formed by the vomer, as that one of the faces is convex in a greater or lesser part of it's while the other is concave. Sometimes one of the two initial blades forms a projection or a spur. Below there is a breif explain of the vomer bone edges (Figure.8) (Sanakcioglu Mølsted and Kjaer 1994; Sperber, Guttmann and Sperber 2001; Schafer, Black and Scheuer 2009).
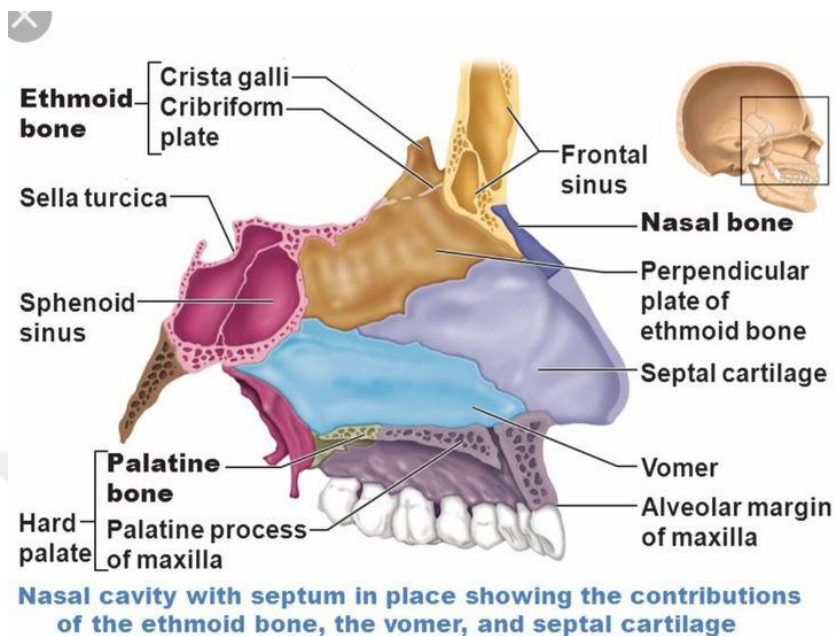
Figure 4.9 Descriptive anatomy of Vomer bone (www.lumenlearning.com, 03rd Feb, 2016).

1)The upper edge

Its length about 2 cm, slightly oblique down and back, the edge of the top is hollowed over its entire length by a groove, of whose lips the leaves of the vomer. The vomeric sulcus responds to the sphenoidal crest. Ridge Sphenoidal does not descend to the bottom of the groove, there is a channel Antero-posterior, the vomero-sphenoid canal (spheno-vomeric canal Median), in which veins run.

The wings of the vomer, narrower and thinner in front than behind, terminate at their posterior extremity by a well-marked spine directed in Back and forth. They are described two faces, upper and lower. The upper face is almost flat, rests against the lower face of the body of the sphenoid bone and extends from each side to the crack between the vaginal process of the Pterygoid process and the lower face of the bone sphenoid (Sandikcioglu, Mølsted and Kjaer 1994; Schafer, Black and Scheuer 2009).

2)The lateral edge

The lateral edge of the Vomerous wing closes this crack, transforming it into Vomorovaginal canal (lateral spheno-vomereal canal) in which Veinlets and a branch of the spheno-palatine artery. The underside of the Vomerous wings, slightly excavated, oblique in base and on the inside, is smooth and free on the 2/3 anterior of its extent. It is in contact with the medial part of the upper surface of the Sphenoidal process of the palatal bone.

3)The front edge

Its length is about 5.5 cm, oblique down and forward and thick, anterior of the vomer is hollowed over its entire length by a furrow well visible in the young subject, trace of the primitive duality of the bone.

The upper 3/4 of this furrow articulate with the perpendicular blade of the ethmoid, its anterior 1/4, with the septal cartilage. The posterior border long about 2.5 cm, thin, oblique down and forward, edge posteriorly is free. It separates one from the other, the posterior orifices of the nasal cavity or choncha.

4)The bottom edge

Its length is about 4.5 cm, horizontal, the lower edge rests on the nasal ridge formed by the union of the palatal processes of the maxilla on the one hand, of the palatal bones on the other hand. Backward, it reaches the spine Posterior nasal fasciitis (PNS) area, forward it abuts against the incisal crest, portion anterior elevation of the nasal ridge (anterior overlapping phenomenon).

When the vomer has an anterior spur, the lower edge of this spur articulation with the incisal ridge: this edge is then higher than that of the Vomerous blade, the notch that they form hooking the incisive crest (ANS) area.

4.1.6 The Biodynamics of Vomer Bone and Midfacial Complex

The vomer bone consists of two small flanges that conform with the underside of the body of the sphenoid. It has important position because of the nasal septum and its attachments to the palatine and maxillary bones through the vomer bone. Aside from serving as a

buttress for the upper jaw to receive shear forces. Also it is an important site of downward growth of the human face as seemed in Figure 4.10, 4.11 and 4.12 (Schafer Black and Scheuer 2009).
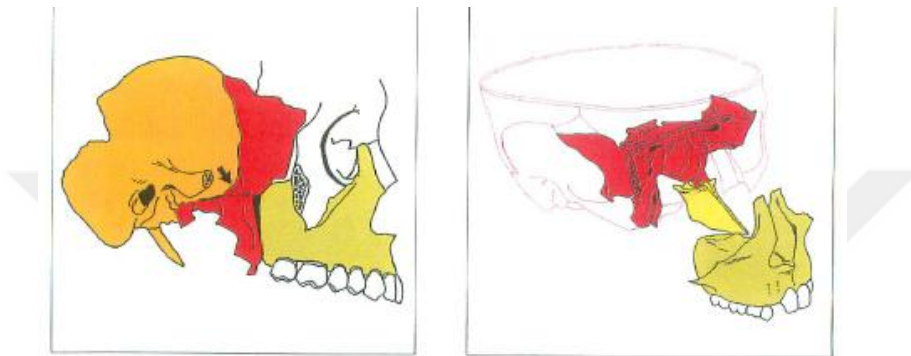
Figure 4.10 Illustration of craniofacial complex compartment biodynamics.
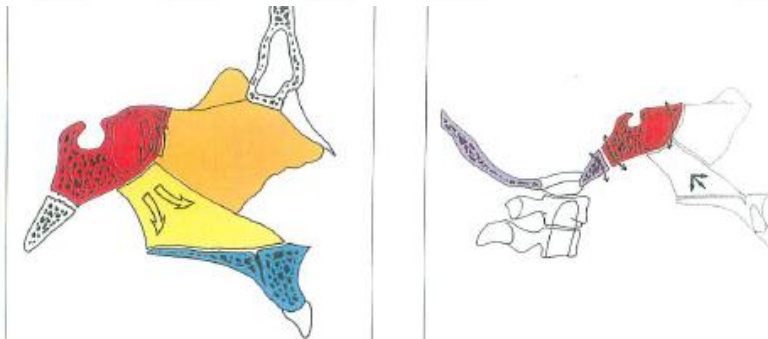
Figure 4.11 Misagittal Biodynamic force flexion and extension through sutural connection.
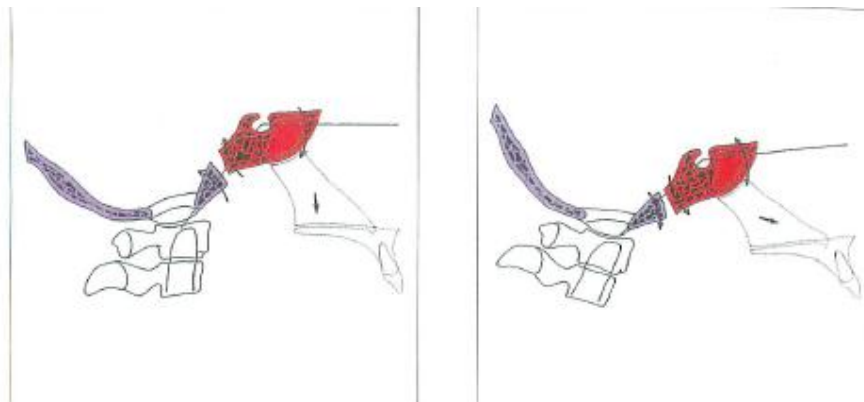
Figure 4.12 Vomeral force transmission in different direction as central stunt.

The midfacial retrognathia in relation with the Class III malocclusions remains unclear. Indeed, the anterior nasal spine (ANS) correlates with the premaxilla-maxillary suture, which may have implications for the midfacial growth (Mooney and Seigel 1986; Markus and Precious 1997).

In the growth of the premaxilla, the nasal septum plays an important direct role and an indirect role in the growth of the maxilla (Delaire and Precious 1986,1987). In accord with the hypothesis of septal-mediated traction of midfacial growth, the developmental process associated with Class III malocclusion could include cartilaginous growth at the septo presphenoidal joint (Sarnat J 1983; Moss-Salentijn and Hendricks-Klyvert 1998).

The nasal septum consists of septal cartilage, the perpendicular plate of the ethmoid (PPE) bone, and the vomer .The nasal capsule and its median nasal septum influence the forward translation of the upper part of the maxilla, the expansion between the lateral walls of the nasal fossae, and the development of the premaxilla (Markus and Precious 1997; Singh, McNamara and Lozanoff 1997a,b and c).

Therefore, Dibbets JMH (1996), reported that the vomero-palatine suture is important for antero-inferior translation of the palatal bones in 20–30% of adult patients with Class III malocclusions. They suggested that the midface is the deciding craniofacial component for classifying the Class III patient, and other recent findings support this notion. The observed Class III malocclusion (midfacial hypoplasia) seen in cleft palate due to

deficiencies or abnormal midfacial growth mechanisms (Siegel, Mooney, Kimes and Todhunter 1991).

Tanne, Matsubara and Sakuda (1995), suggested that the center of rotation of the nasomaxillary complex is located on the poster superior ridge of the pterygomaxillary near (Vomer ala region) fissure registered in the sagittal plane.

Overall, evidence for the importance of the premaxilla region in the morphogenesis of the final maxillary form can be gleaned from studies of the pathoetiology of Orofacial clefting. The use of vomerine flaps results in midline scarring at the inferior border of the vomer at the site of the vomeropalatine suture, fixing the palate to the vomer as shown in Figure 4.13 and 4.14 (Markus and Precious 1997).

This has two effects:

(1) It has an adverse effect on transverse expansion of the maxilla, and

(2) It restricts growth in the sagittal plane; both effects favor the development of a Class III skeletal relationship. As well, the reduction in vertical development of the nasal aperture favors a Class III abnormality (Bergland and Borchgrevink 1974; Delaire and Precious 1985).

On other hand, some authors investigations were emphasized the variability of the midfacial complex in Class III malocclusions due to development deficiency at the transverse palatine suture but that acute angulation of the maxillary incisor may act as a compensatory occlusal mechanism for the shorter maxilla relative to the longer mandible (Friede H 1978; Heidbuchel, kuijpers-Jagtman and Freihofer 1993).
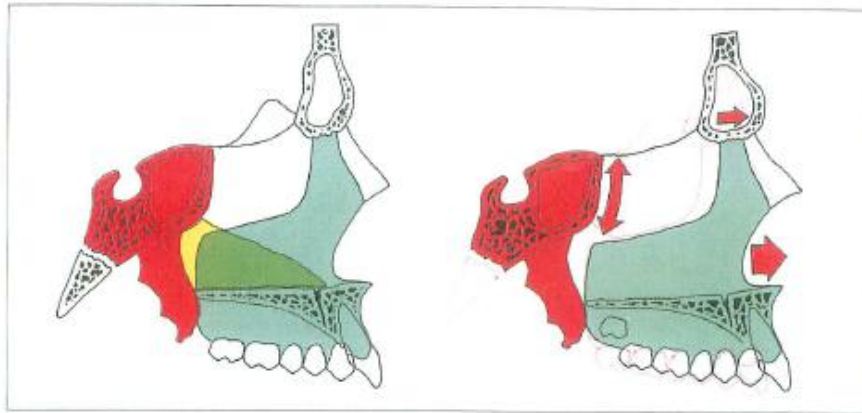
Figure 4.13 Vomeral midfacial force interrelation with anterior maxilla forward movement.
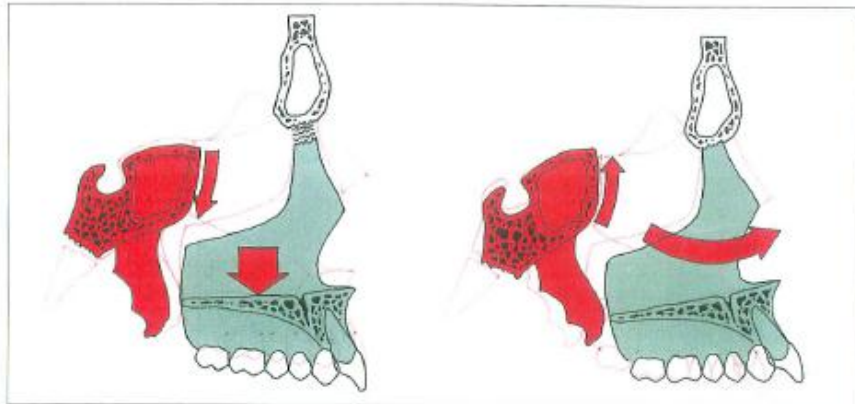
Figure 4.14 Palatal downward movement accompined with dentition.

The vomer bone is only portion has a direct pre-maxillary action, and several observations militate in favor of it as reported by (Bergland and Borchgrevink, 1974; Schafer Black and Scheuer 2009) as follow :

1) The V-shape of the vomer joint with the sphenoid (alar-presphenoidal) is mesethoide at the top with sphenoid and the pre-maxillary at the front is adapted to the incisal crest complementally.

2) Pre-maxillary escapement in the labio-palatine clefts bilateral agreements.

3) The application of the vomer in the total unilateral slits due to the absence of counter-pressure which imbalances the sagittal blade.

4.2 The Class III Malocclusion in terms of major categories

4.2.1 Clinical Consideration of Class III Malocclusion

Class III characterized in both lateral halves of the dental arches by mesial occlusion that is slightly more than one half the width of a single cusp on each side, but in cases that are always progressive as the mesial occlusion becomes greater to the full width of a molar or more. (Angle E 1907)
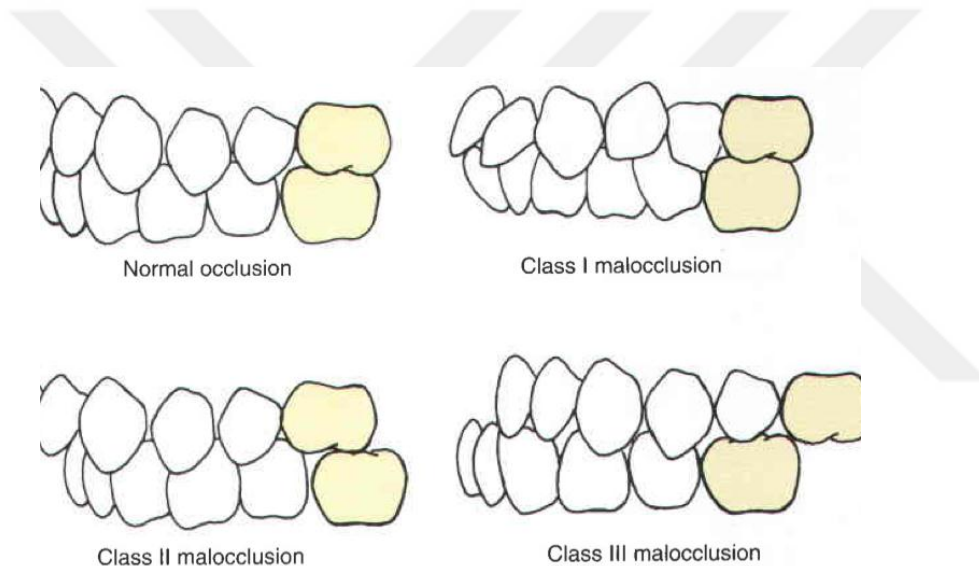
Figure 4.15 Angle classification of different occlusion relationships
(www.dentodontics.com, 29th November, 2015).

Angle's description of Class III malocclusion as seen in Figure 4.15, is known as mesiocclusion. In its symmetrical (division 1) and asymmetric (subdivision) patterns focuses not only on the occlusion between the teeth but also on individual variation (Bishara S 2001).

Angle described that "considerable crowding, especially in the upper arch, and lingual inclination of the lower incisors and canines". Although Angle's classification has been used for over 100 years around the globe, his assumptions on etiology and diagnosis of

the malocclusion is lack of definitive evidences. (Baily, Proffit and White 1995; Brunelle, Bhat and Lipton 1996; Proffit and Fields 2000; Uribe et al. 2013,2014)

Angle's observation on incisor retroclination preceded the age of cephalometric, which demonstrated a corresponding proclination of maxillary incisors, reflecting dentoalveolar compensation by maxillary and mandibular incisors to an underlying skeletal discrepancy is characterized by maxillary retrognathism, mandibular prognathism, or both. Sometimes the incisal compensation is expressed with incisal edge to edge rather than crossbite, yet it is compatible with molar mesiocclusion and an underlying Class III pattern as in Figure 4.16 and 4.17 (Brunelle Bhat and Lipton 1996).

Variations and gradients of severity include the complex differentiation between macrognathism and prognathism and reference comparison between the skeletal bases and alveolar bases. Therefore, the mosaic arrangement of the "parts" requires careful diagnosis under these facts:
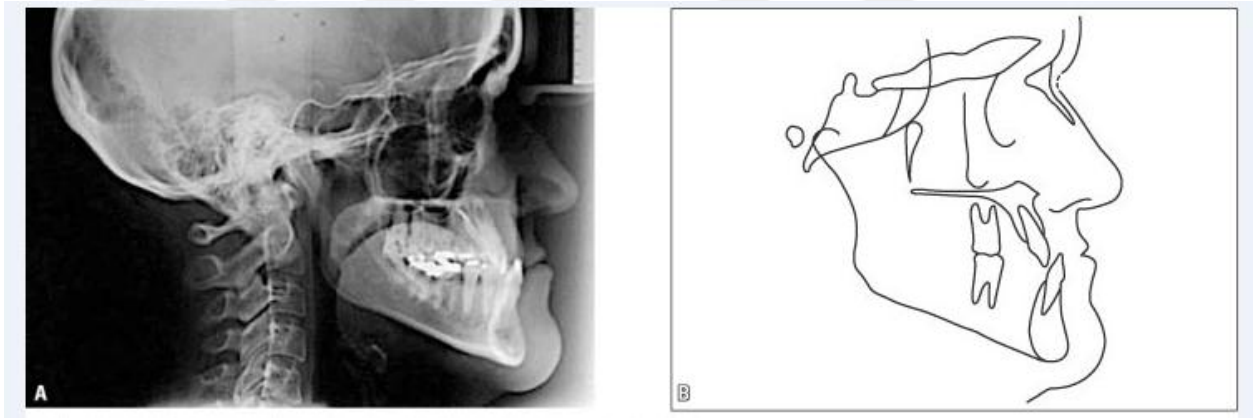
Figure 4.16 A) Lateral cephalometry and B) Tracing (Ricketts 1965).

1. The prevalence of maxillary retrognathism is more than previously thought because its occurrence is more severe (SNA = 78.04 degrees ± 4.04 degrees; norm = 82 degrees ± 2 degrees) than mandibular prognathism (SNB = 81 degrees ± 2 degrees; norm = 80 degrees ± 2 degrees), the angles SNA and SNB yielding differences of 4 degrees and 1 degree from the respective norms.

2. A more cephalic position of the anterior cranial base is underscored by a higher position of sella relative to nasion, concomitant with the previously described decrease in the saddle angle (nasion – sella - basion).

3. A previously unreported superior - posterior tip of the palatal plane.

4. Possibility of environmental induction of mesioclusion: an anterior crossbite, not necessarily related to genetic factors but sustained by mandibular forward positioning caused by occlusal interferences, habits, or to improve breathing, may induce forces that produce maxillary retrognathism that otherwise would not exist and affect the palatal tip through the occlusion (in a manner similar to the action of a headgear (Proffit and Sarver 2000).

5. The thickness of the soft tissue envelope, which may differ from one region to another, can compensate or exacerbate the regional diagnosis.

Three - dimensional imaging of the craniofacial system has not yet generated new knowledge of Class III morphology to enable more accurate diagnosis, the aim of which is to formulate a corresponding individualized treatment approach (Ferro et al. 2003, Anbuselvan and Karthi 2010).
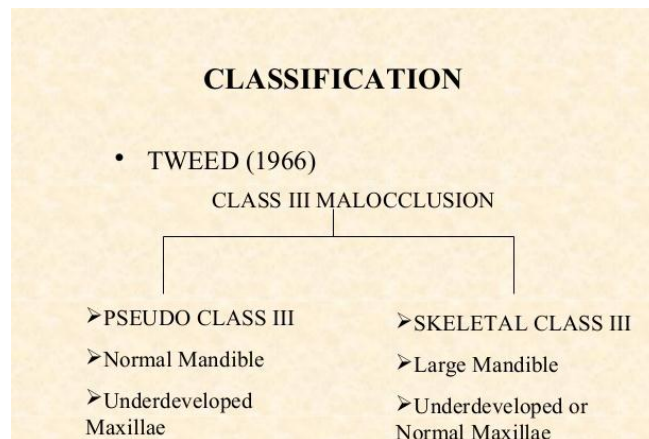
Figure 4.17 Schematic of both Class III malocclusion (Tweed C 1947; Merrifield L 1966).

4.2.1 Genetic etiology of Class III Malocclusion

The association between midfacial hypoplasia and other craniofacial anomalies had been linked by AI trait gene that associated with dental and/or skeletal open bite malocclusions and may be related to craniofacial development (Persson and Sundell 1982; Ravassipour et al. 2005).

Some authors reported cases that involved severe anterior open bite, long face, facial asymmetry with Class III skeletal pattern phenotype. These cases were treated with a multidisciplinary approach and were improved the patient's quality of life (Keles A 2001; Keles, Erverdi and Sezen 2003)

Machicek SL (2007), his findings have been carried out on an achondroplasia mouses model with a phenotype that resembles human achondroplasia. These mouses had a domed skull, hypoplastic midface and nasal bone, anteriorly displaced foramen magnum and a prognathic mandible.

By comparing the study based evidence involved in the etiology of midfacial hypoplasia, further clues into the genetic etiology of Class III malocclusion can be ascertained. Establishing the morphological disharmony related to etiology of skeletal Class III malocclusion may have a direct clinical application in the immediate future, however, detection of the relation spatial analysis of certain compartment such as the vomer bone may provide hope for improvements in the management of such patients (Ngan P 2005, Banabilh et al. 2007).

This information may be used to accurately predict long-term growth changes, and may lead to earlier non-surgical or minor direct surgical interventions. The craniofacial outline of skeletal Class III malocclusion and the development of this disorder must first be considered in the context of the embryology and growth of the craniofacial skeleton (Martin et al. 1998).

The morphological orientation of midfacial complex mechanisms involved in the etiology of Class III malocclusions are an important consideration in the development of this malocclusion (Uribe et al. 2013). Singh GD (1999), inferred that an acute cranial base angle may affect the articulation of the condyles in their glenoid fossae resulting in their

forward displacement, and he also inferred that the reduction in the anterior cranial base size may affect the position of the maxilla.

Currently, the timing of treatment for the Class III patient is difficult, but a greater understanding of the relationship between the morphology of midface complex and development of this disorder may improve the outcome of treatment.

4.2.3 Diagnostic Consideration of Class III Malocclusion

Available evidence on the development of Class III suggests the assessment of references used for more accurate cephalometric diagnosis. Maxillary and mandibular positions are commonly gauged by the angles SNA and SNB. The position of sella can induce misinterpretation of data if not corrected to the natural head position "true" horizontal. A high sella relative to nasion would yield smaller SNA and SNB values when corrected, thus less maxillary and mandibular prognathism and low position of sella would have opposite consequences as in Figure 4.17 (Mouakeh M 2001). Regarding SNB specifically, the deeper the overbite or the more anterior functional positioning of the mandible, the greater the SNB angle, thus the inference of more mandibular prognathism. Accurate appreciation of ANB would require "bite opening" or "rotating" the image of the bimaxillary on the tracing to near normal overbite ($20\% - 30\%$). Such exercise is further rationalized with anterior (functional) maxillary displacement, particularly in the diagnosis of pseudo Class III. These issues are not accounted for in research on Class III malocclusion (Anbuselvan and Karthi 2010).

Skeletal: ANB angle
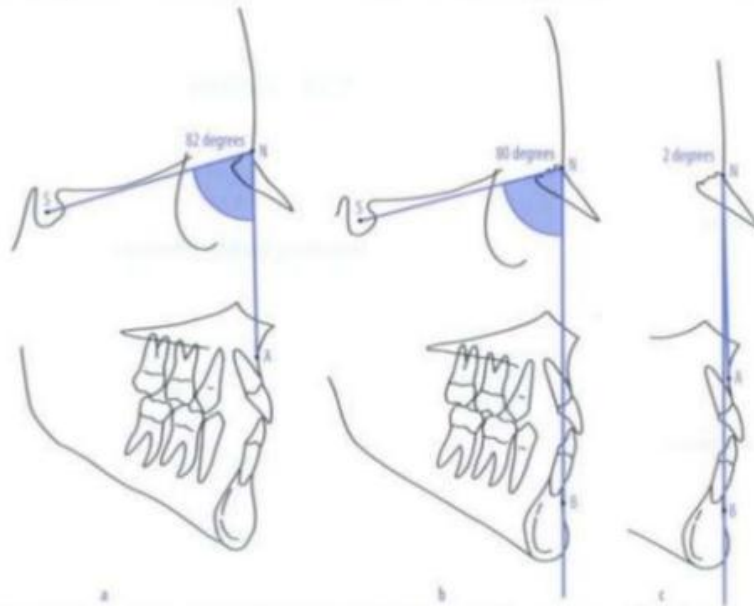
Figure 4.18 Cephalometric analyis of facial profile by analysis ANB angle
(www.slideshare.com, 8th July, 2016).

4.2.4 Variation of Angle Class III Malocclusion Treatment

Angle Class III malocclusions are the worst type of deformities, the orthodontist is called upon to treat with different features as appeard in Figur 4.19. When they have progressed until the age of sixteen or eighteen or after, the jaws have become developed in accordance with the malpositions of the teeth. The deformities have usually passed beyond the boundaries of malocclusion only and the bone deformities. For which with our present knowledge, there is little possibility of affording relief through orthodontic operations (Angle E., 1907, Frazier-Bowers SA, 2015).

Cluster analysis for Class III patients
Five clusters

cluster 1	cluster 2	cluster 3	cluster 4	cluster 5
» Mandibular prognathic (mp) » Long face	» Maxillary deficient (md) » Short face	» Maxillary deficient » Long face	» Mild mand. prognathic » Normal	» combination (mp + md) » Normal
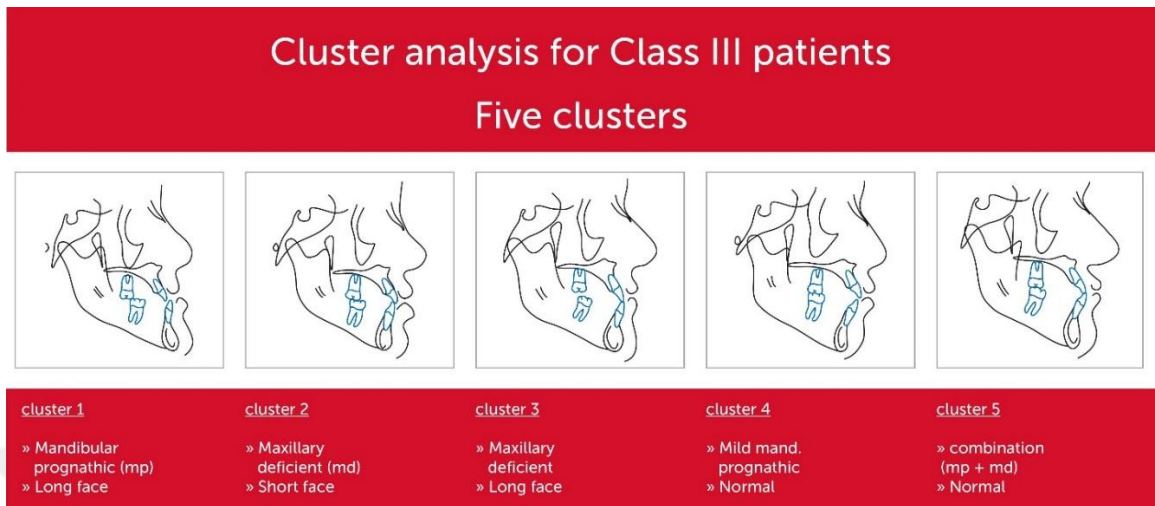
Figure 4.19 Diversity of Angle Class III malocclusion profile (www.scielo.br, 1st September, 2016).

An important clinical observation is forward positioning of the maxillary dentition relative to the mandibular teeth produces an increased maxillary width. Therefore, many practitioners use the phases of Class III malocclusion teatment in relation to severity and age as in Figure 4.20.
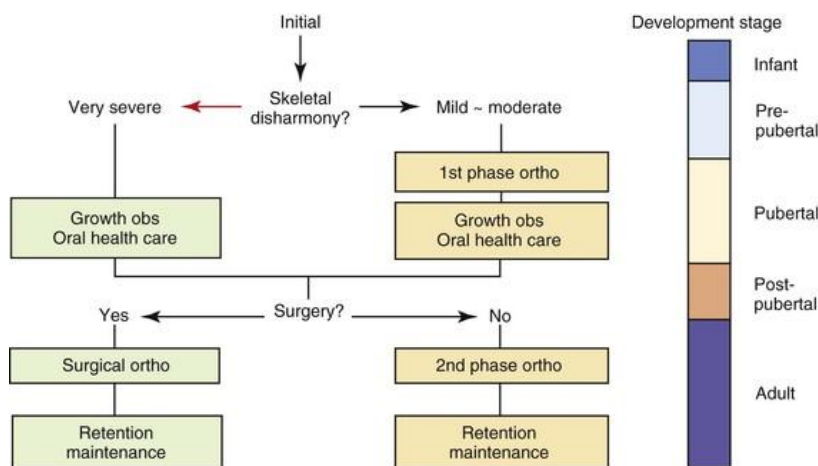
Figure 4.20 Phases of Class III Malocclusion Treatment in relation to Severity and Age (Esthetic and Biomechanics of orthoontics/ Nanda 2014).

Because of the need for long-term evaluation of early treatment and a lower incidence of Class III malocclusion within Caucasian populations. The long-term studies of Class III treatment are limited. Research including the highest level of evidence indicates three related Coclusions:

1)Treatment timing: treat early for more effect.The available evidence emphasizes the efficiency of early treatment because of its potential effect relative to late treatment. Suda et al. (2000), determined "more pronounced" treatment effects in younger children. Kim et al. (1999), concluded that protraction face mask therapy is effective in growing patients but to a lesser degree in those older than age 10 years (Ngan P 2006).

2)Treatment modality: palatal expansion may not be required and chin cup success is questionable. Palatal expansion is often indicated, particularly in the presence of maxillary constriction and crowding. Kim et al. (1999), reported similar protraction with or without expansion, though the average treatment duration was longer without expansion. While protraction combined with an initial period of expansion more significant skeletal effects on the forward movement of point A (Baik HS 1995; Yu et al. 2007). The need for expansion absent in transverse discrepancy (skeletal/dental crossbite) that was not supported by the results of a prospective randomized clinical trial (Yüksel, Üçem and Keykubat 2001; Celikoglu and Oktay 2013).

3)Treatment Timing and Duration: Although the evidence suggests that treatment should start at a younger age in the mixed dentition and the treatment of a severe mesioclusion before the pubertal growth spurt was achievable with sustained compliance. These suggestions were decided that early orthodontic treatment should not be overdone while they dealing with growth changes as in Figure 4.21 (Ghafari, Haddad and Saadeh 2011; Nanda 2014).
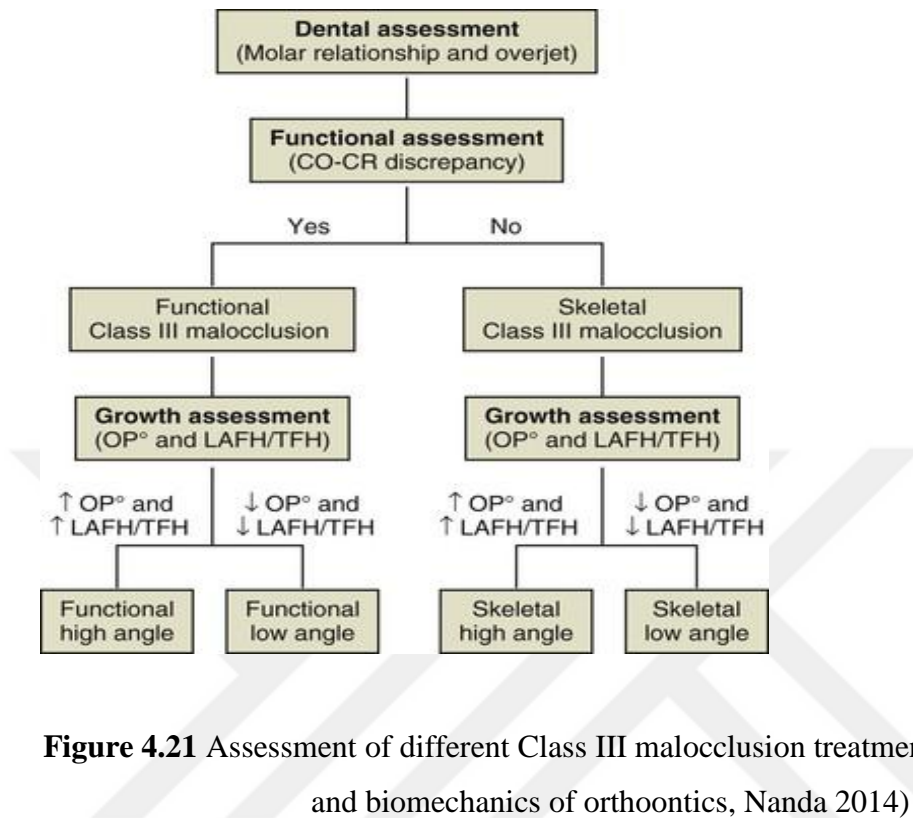
Figure 4.21 Assessment of different Class III malocclusion treatment modality.(Esthetic and biomechanics of orthoontics, Nanda 2014)

4.2.5 Interceptive Orthodontic Treatments

Facial growth modification can be an effective method of resolving skeletal jaw discrepancies in growing children with dentofacial orthopedic appliances including the face mask, maxillary protraction combined with chincup traction and the Frankel functional regulator III appliance (Nanda SK 1988, Bishara S 2001).

Many different functional appliances have proven to be very useful in correcting Class III conditions in the growing patient. Clinically, several studies suggested that more anterior maxillary displacement can be found when treatment begins in the deciduous or early mixed dentition (Turley PK, 2002).

4.2.6 Surgical Treatment

Orthognathic surgery in conjunction with orthodontic treatment is required for the correction of adult skeletal class III malocclusion. The controversy is appeared how to treat underdeveloped maxillary region with midfacial hypoplasia or deficiency and establish a correct treatment plan for correction of disharmony earlier and with no complications (Plooij et al. 2011; Joshi, Hamdan and Fakhouri 2014).

Le Fort II osteotomy is a surgical procedure for the advancement of the entire nasomaxillary complex (the center region of the middle third of the maxillofacial region) to correct midfacial hypoplasia without exophthalmos as appeard in Figure 4.22 (Zuroff et al. 2010). Le Fort II osteotomy and advancement are a recommendable tool to achieve aesthetic harmony in the face while correcting the occlusion.
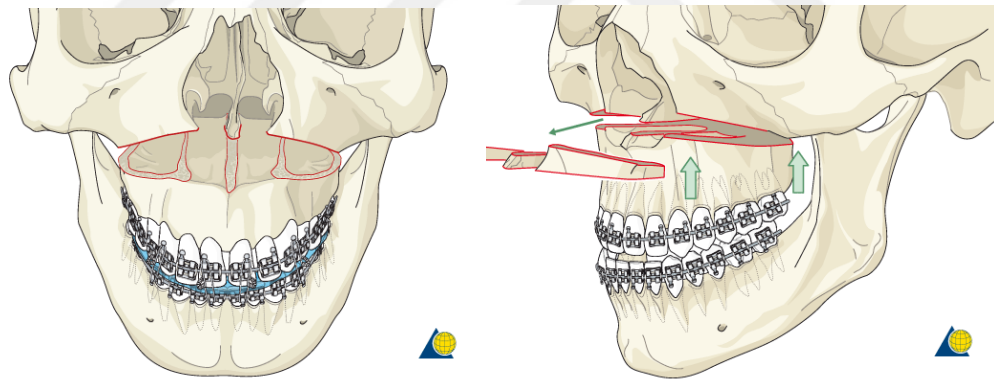
Figure 4.22 Le Forte II procedure A) Lateral and B) Coronal view
(www2.aofoundation.org, 13th May, 2016).

4.3   Fundamental Characteristics of CBCT Image

Cone beam computed tomography refers to CBCT systems in which the beam projected by the X-ray source is in the shape of the cone wide enough to radiate either all or a significant part of the volume of interest. The shape of the beam is controlled by the use of collimators, which block X-rays from being emitted into undesired regions of the scanner field of view as in Figure 4.22. CBCT system of a compact variety suitable for use in small clinics. In the particular system shown in the figure, the gantry rotates in a circular path about the subject firing a beam of X-rays that illuminates the entire desired field of view. This results in a series of two-dimensional (2D) images of the X-ray shadow of the object that is recorded by a 2D array of detector cells. CBCT systems with this particular scan geometry will be the focus of this book, but it is important to realize that in the broader medical imaging industry, CBCT devices can vary considerably both in the shape of the X-ray beam and the trajectory of the source (Sunil K 2014).

The development of compact CBCT for the clinic has made three dimensional imaging widely and quickly accessible. That image fundamentals are mentioned below as in Figure 4.23 (Horner et al. 2009):
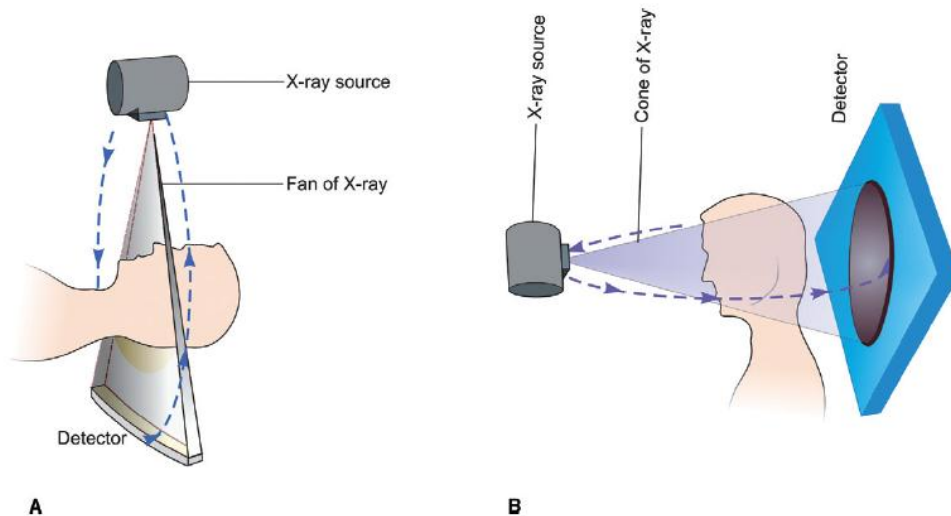
Figure 4.23 Multidetector A) Fan shaped-CT and B) CBCT (Cone Beam Computed Tomography in Orthodontics/ Sunil K 2014).

1. Image Reconstruction

Image reconstruction is the process by which attenuation values for each voxel in the CBCT image are calculated from the X-ray measurements. This process tends to be the most computationally intensive software task performed by a CBCT system. There are tens of millions of voxels in a typical reconstruction grid and each computed voxel value derives information from X-ray measurements taken typically at hundreds of different gantry positions. A complete image reconstruction task may hence require, at minimum, tens of billions of arithmetic and memory transfer operations (Horner et al. 2009). CBCT manufacturers therefore invest considerable development effort in making reconstructions achievable within compute times acceptable in a clinical environment. Because of the computational hurdles associated with image reconstruction, commercial systems have historically resorted to filtered back projection algorithms as in Figure 4.24.

Tube voltage (kVp)	High	Increased energy of the X-ray beam, increased tissue penetration, good signal to noise ratio
	Low	Better contrast resolution, lower signal to noise ratio and lower dose for a given tube current
Tube current (mA)	High	Good signal to noise ratio, thereby increasing the contrast resolution
	Low	Lower patient dose, poor signal to noise ratio
Scan time	Long	Prone to motion related artifacts
	Short	Superior temporal resolution, fewer artifacts
Field of view (FOV)	Large	Larger area is covered, lower spatial resolution
	Small	Better spatial resolution
Slice thickness	Large	Good signal to noise ratio, lower z-axis resolution
	Small	Partial volume effect is reduced, poor signal to noise ratio
Reconstruction algorithm	Smooth	Image appears smother and less noisy, spatial resolution suffers
	High frequency	Better spatial resolution but noisier image

Figure 4.24 CBCT Scan parameters influencing image quality (Cone Beam Computed Tomographyin Orthodontics/ Sunil K 2014).

2. Imaging Performance

Several quantitative measures of image quality that are commonly used to assess the performance of a CBCT device, namely noise performance, low-contrast detectability, and spatial resolution. CBCT manufacturers will typically report such quality measurements in the user manuals issued with their devices. Typically also, manufacturers provide customers equipment to repeat these measurements and specify in the user manual how reproducible the measurements should be (Sunil K 2014).

3. Image Noise

The term measurement noise refers to random variations in CBCT measurements. Image noise refers to the ensuing effect of these variations on the reconstructed image. In CBCT scan, there are several sources of measurement noise that make the measurements not precisely repeatable. When X-rays are fired through a patient along a certain straight-line path, there is randomness in the number of photons that will penetrate through the object to interact with the detector. There is also randomness in the number of photons that, after penetrating the object, will successfully interact with the X-ray detector panel to produce a signal. Finally, there are also elements of random fluctuation in the detector electronics itself, independent of the object and the X-ray source (Horner et al. 2009).

4. Spatial Resolution

Spatial resolution refers to how well small or closely spaced objects are visualized in an image. Spatial resolution in a CBCT system is partly limited by the size of the image voxels used for reconstruction. However, the resolution is further limited by various sources of system blur.

To measure in-plane spatial resolution, it is traditional to report the modulation transfer function (MTF). MTF is a graph showing how the imaged contrast of densely clustered

objects decreases, as a result of system blur, with the clustering density as in Figure 4.25 (Suomalainen et al. 2009).
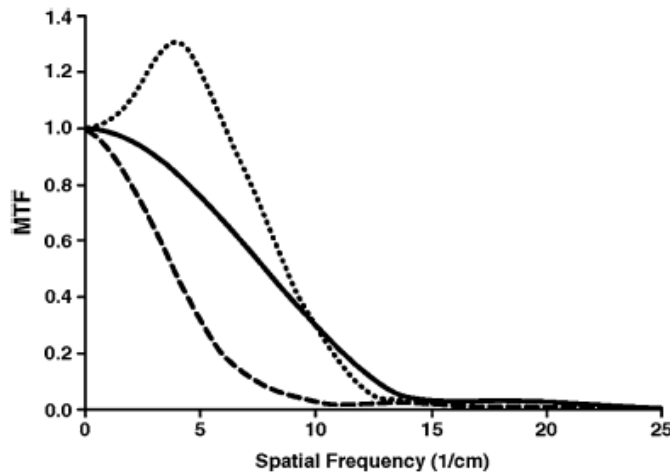
Figure 4.25 Spatial relaion accuracy with MTF value of image (Suomalainen et al. 2009).

As a result of blur effects, the intensity of small or narrow objects is diluted with background material in the image, thereby lowering their apparent contrast. Since objects must be of decreasing size to be clustered more densely, an accompanying decrease in contrast with density is typically observed. This is illustrated a series of progressively denser line pair targets, with the density expressed in line pairs per centimeter (lp/cm). One can see how not only the separation between the more densely spaced line pairs diminishes as a result of blur, but also their percent contrast with the background medium (Roberts et al. 2009).

5. Low-contrast Detectability

Low-contrast detectability is a performance parameter of CT systems that measures its overall ability to resolve small differences in intensity between objects. To test low-contrast detectability in a CT system, phantoms containing low-contrast targets of a range of sizes, are often used. As discussed in the previous section, system blur reduces the

contrast of small objects. However, there are other contrast-limiting effects in a CBCT system that can affect the visibility of large objects as well (Pauwels et al. 2012).

6. Field of View

Many CBCT units allow the operator to restrict the beam size to a predetermined area or field of view. Typically, the field of view is described as small (or limited), medium, or large depending on the extent of anatomic coverage as in Figure 4.26:

The field of view are as below:

a. Small field of view (also referred to as limited or focused fields of view): scan height and width less than 5 cm.

b. Medium field of view (also referred to as dentoalveolar field of view): scan height 5–15 cm.

c. Large field of view (also referred to as craniofacial field of view): scan height greater than 15 cm. It is of utmost importance to select the optimal field of view for a particular diagnostic task (Patel et al. 2009).
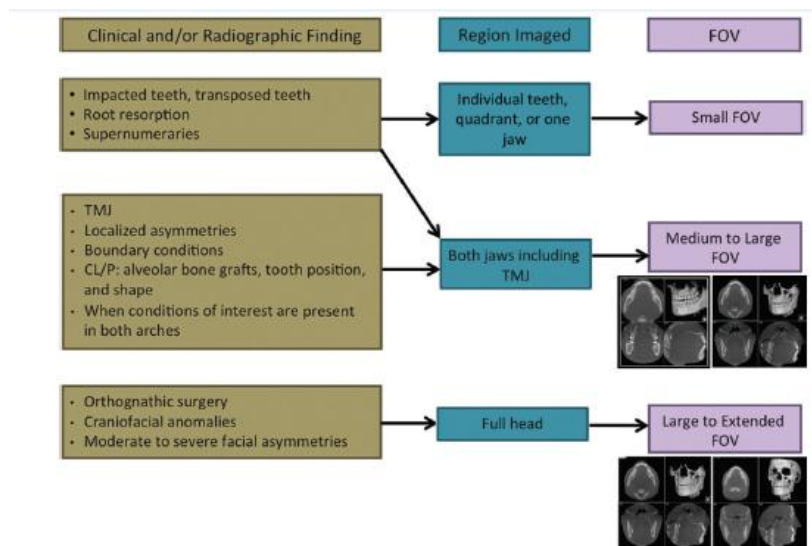
Figure 4.26 Protocol for selection of approperiate CBCT-FOV. (Cone Beam Computed Tomographyin Orthodontics, Sunil K, 2014)

4.3.1 Availability Shifting From 2D To 3D Image Analysis Uses

Technology development has led to scientific advances in diagnosis and treatment planning using three dimensional (3D) assessment of facial morphology at baseline to be more effective and rational for orthodontic and Orthognathic surgery. With the availability of cone beam computed tomography (CBCT), the preparation of the surgical plan is shifting from using 2D radiographic images to 3D images and models. In the past ten years, a number of research centers and commercial companies have strived to provide software environments that allow preparation of the operative plan on 3D models of the skeletal structures extracted from the CBCT (Cevidanes et al. 2005).

As these planning systems begin to be used in clinical practice, it is important to validate the clinical application of these methods. Studies on the 3D bone remodeling and displacements with surgery have helped elucidate clinical questions on variability of outcomes of surgery (Pelinsari et al. 2012). The image analysis tools have been adapted for use with CBCT imaging of the craniofacial complex and have brought significant contribution in clinical needs that broaden the diagnosis and narrow the treatment targets. 3D morphometric approaches like volumetric analysis and landmarks linear and angular analysis are more logical and give a clear preview for topic selected to evaluate by image anlaysis description (Tucker et al. 2010).

4.3.2 Image Analysis Of Dentofacial Anomalies

CBCT imaging offers the ability to analyze facial asymmetry and antero-posterior, vertical, and transverse discrepancies as in Figure 4.27. The virtual treatment simulations can be used for treatment planning in orthopedic corrections and Orthognathic surgery and for printing surgical splints. Computer-aided jaw surgery is increasingly in use clinically due to the possibility of incorporating a high level of precision. In complex cases, CBCT acquisitions for growth observation, treatment progress, and posttreatment observations may be helpful to assess stability of the correction overtime (Aggarwal P 2011; Behnia et al. 2015).

The methods for computer-aided systems follow procedures from the image scanners to the operating room as in Figure 4.27, 4.28 (Ebner et al. 2010; Wilde et al. 2013).

The advantages of those systems, they do not require time or computer expertise for the surgeon.The computer-aided facilities steps include (Dalessandri et al. 2011):

(1) data acquisition: collection of diagnostic data.

(2) Image segmentation: identification of anatomic structures of interest in the image data sets and visualization of 3D display of the anatomic structures.

(3) Diagnosis: extraction of clinical information from the 3D representations of the anatomy, for example, by using mirroring planes.

(4) Planning and simulation: preparation of an operative plan by using the virtual anatomy, and preparation of a simulation of the outcome.

(5) 3D printed surgical guides or individually fabricated synthetic grafts or prosthetic repair.

(6) Intraoperative guidance: assistance for intraoperative realization of the virtual plan.
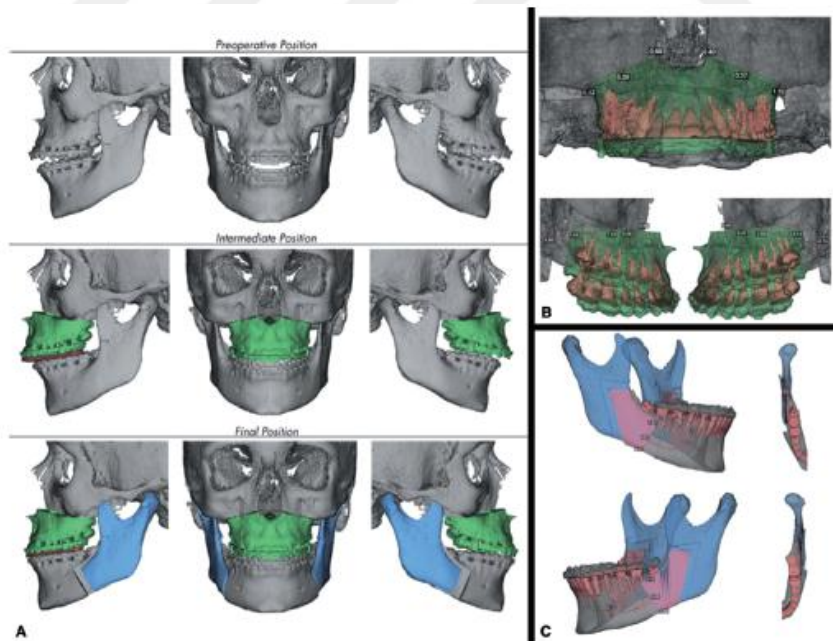
Figure 4.27 3D Virtual planning of orthognathic surgical plane (Cone Beam Computed Tomography/ Sarmant D 2014).
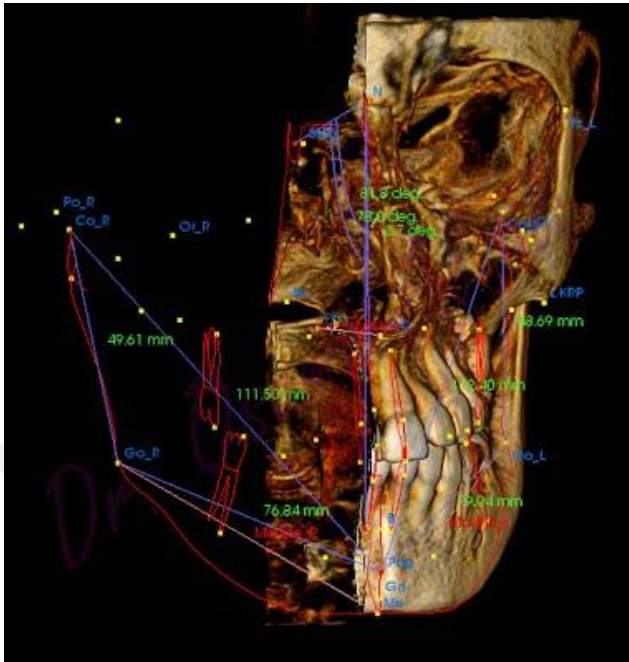
Figure 4.28 3D analysis by liunear and angular references.(www.sciencedirect.com, 19th May, 2016)

4.3.3 Quantitative Image Measurements

Precise quantitative measurement is required to assess the placement of bones in the desired position, the bone remodeling, and the position of surgical cuts and fixation screws and/or plates relative to risk structures. Current quantification methods include the following:

1. Volume measurements

Lepage et al. (2006), reflected the increase or decrease in size, but structural changes at specific locations are not sufficiently reflected real volume measurements. The volume assessment does not reveal location and direction of proliferative or resorptive changes, which would be relevant for assessment clinical results.

2. Landmark-based measurements

Rohr L (2001), presented errors related to landmark identification. Locating of 3D landmarks on complex curving structures is not a trivial problem for representation of components of the craniofacial form (Dean et al., 2005). Bookstein D (1997), noted, there is a lack of literature about suitable operational definitions for the landmarks in the three planes of space (coronal, sagittal, and axial). Gunz et al. (2004), proposed the use of semi-landmarks, that is, landmarks plus vectors and tangent planes that define their location, but information from the whole curves and surfaces must also be included. The studies of Subsol et al. (1998) and Andresen et al. (2000), provided clear advances toward studies of curves or surfaces in 3D, referring to tens of thousands of 3D points to define geometry as shown in Figure 4.28, 4.29.
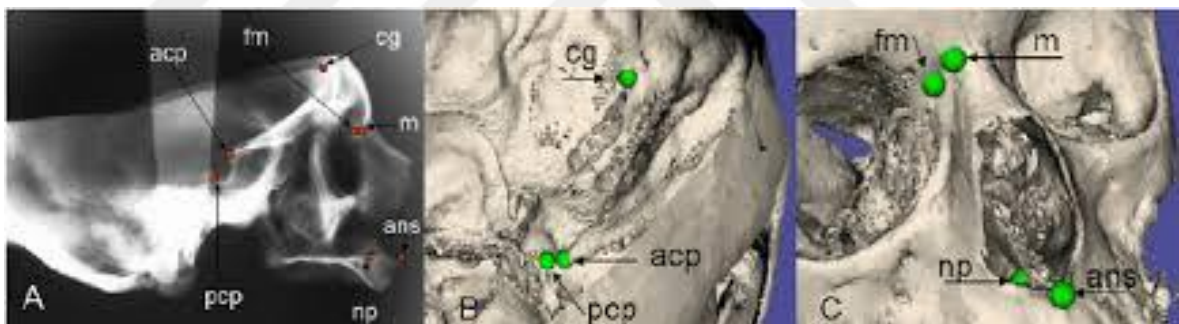
Figure 4.29 Landmark-base measurment analysis.(www.researchgate.com)

4.3.4 Three-Dimensional Imaging Technical Information

Two-dimensional photographs or radiographs have two axes, horizontal and vertical. In a three-dimensional image, there are three axes: X-axis (transversal), Y-axis (vertical) and Z-axis (anterioposterior depth). In medical imaging, both axes form a plane or section. The plane "sagittal plane" in front of the front is called the "coronal plane" from right to left or left to right, and the lower "axial plane" from above or above. The fourth sections used are shown in Figure 4.30 (Katsoulis et al. 2009).

Computer-generated three-dimensional image, photorealistic by using some algorithms to generate images. To display a three-dimensional object on a two-dimensional computer screen there are orthographic projection (four sectional screen), size and shape, in terms of perspective it is more suitable to evaluate the object geometry.
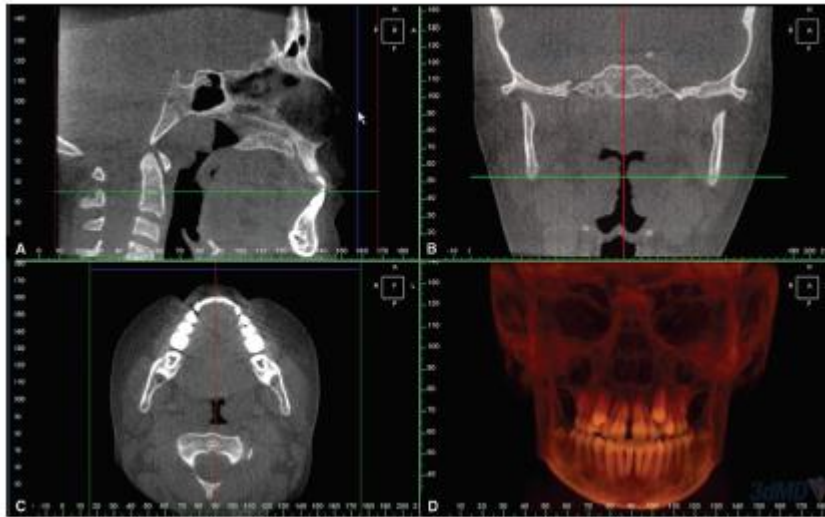
Figure 4.30 Orthographic projection view of CBCT analysis.(www.InTechOpen.com)

The smallest structural element of a two-dimensional digital image is called a "pixel". A pixel is a small quadratic image element that creates rows and columns in two dimensions. Each pixel contains information such as color, brightness, density. Resolution is related to the number of pixels in the image (pixels / mm), the rate of gray falling to the pixel head (bits), and the distribution of gray layers. Radiographic images use gray color with a density value between 8 bits (28 = 256 gray shades) and 12 bits (212 = 4069 gray shades). The smallest structural element of a three-dimensional view is called "voxel". They are small jugs arranged side by side. As in the pixels, each voxel contains information about the related anatomical structure. The size of the data size is the most important barrier to the clinical use of volumetric images (Freeland 2012).

4.3.5 Efficacious Use Of CBCT And Limitations

CBCT and 3D imaging in orthodontic diagnosis and treatment planning accurate imaging is an essential requirement in orthodontics for deriving an appropriate diagnosis, formulating an optimal treatment plan, and monitoring and documenting treatment progress and outcome. The information needed to arrive at a diagnosis and treatment plan has relied on a combination of 2D data obtained from photographs and conventional radiographs and 3D visualization derived through clinical examination of the patient and analysis of plaster casts. Digital technology have evaluated study models, facial and dental morphology using CBCT in three-dimenssions.

Despite the increasing popularity of CBCT, there is a range of opinions among clinicians from those who advocate routinely use for all orthodontic patients to those who recommend its use in specific cases that conventional radiography cannot supply satisfactory diagnostic information and treatment plans (Isaacson et al. 1977; Horner et al. 2009; Sedentexct Project Consortium 2011). This implies that the justification for using CBCT in orthodontics is linked to its diagnostic and therapeutic efficacies of clinical problems that include impacted teeth, facial descripancy. Thus, determining the efficacy of CBCT in enhancing orthodontic diagnosis and therapeutic decisions is a key not only to validate the utility of the technology in specific situations, but also to define clinical protocols that will generate optimal information with minimal radiation exposure (Figure 4.28).
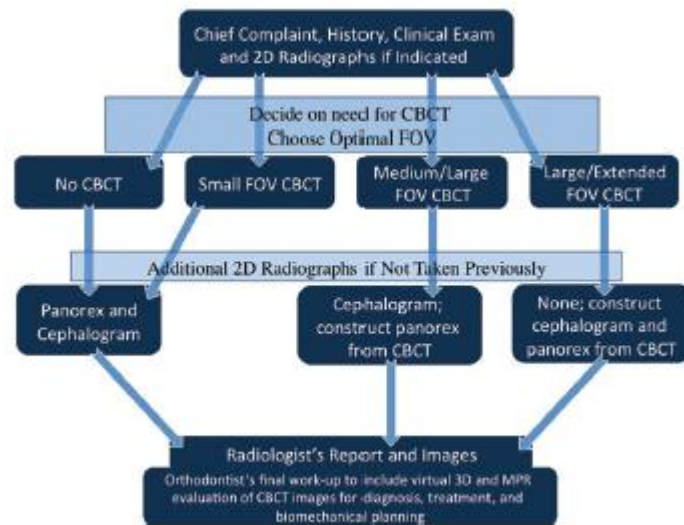
Figure 4.31 Efficacy of using CBCT in Orthoontics (Cone Beam Computed Tomographyin Orthodontics, Sunil K, 2014)

CBCT likely provide information that could result in one or more of the following outcomes:

(1) Enhance diagnosis by localizing the site of aberration as for impacted and transposed teeth,

(2) quantify the magnitude of defect or deformity as for Clefts patients,

(3) help to provide a differential diagnosis on whether the defect is skeletal, dental, or both,

(4) Identify the jaw(s) involved and determine whether the aberration is bilateral or unilateral as in Orthognathic surgery, asymmetry, craniofacial anomaly (Feichtinger et al. 2007).

A potential positive decision to undertake a CBCT examination should be made only after the clinician has carefully evaluated the patient history and chief complaint. Thus decision performed a clinical examination, and, where indicated, taken traditional 2D radiographs not benificial. Such a careful selection of patients for CBCT imaging will ensure maximum benefit while avoiding unnecessary risks to patients who do not need this diagnostic imaging (Frush et al. 2012).

4.3.6 Virtual Reality With 3D Imaging Combinations

Recent advances in technology and computer software have brought together excellent data and methods that facilitate biomedical modeling and simulation research. For the segmentation of three-dimensional volume data, this process is performed automatically in current software without the need for user intervention. Software such as 3D Slicer (MIT, Massachusetts Institute of Technology, USA), Mimics® (Materialize, Leuven, Belgium), Amira (Mercury Computer Systems Inc., Massachusetts, USA), V-works (CyberMed, Seoul, Korea) Image segmentation and modeling based on semi-automatic image processing. These programs use a generalized walking cubic algorithm to construct a segmented wireframe mesh, and form a model in the STL (Standard Triangulation Language) format or in other formats (Enciso et al., 2003). Models created:

1- Merging of different images that US , MRI ,CT origin and others.

2- Analysis and manipulation using computer tools.

Different three-dimensional images segmented by image processing programs which can be combined using the same programs. Uechi et al. (2006), performed the registration of images with skeletal reference to creat a virtual model allows precise planning for aesthetic and function for different treatment alternatives. Realistic simulation of the complex of facial soft tissues consisting of skin, muscles, connective tissue, sebaceous glands, nerves and veins is a very complicated and difficult operation (Jansen et al. 2001). The data obtained from the CBCT images were formatted can not be realistic and deformable. So the studies indicate that the actual outcome does not clearly coincide with real-time simulation of the soft tissue response (Peterlík et al. 2010).

4.3.6 MIMICS Software

It is a medical imaging and control system software developed by Mimics® (Materialise's Interactive Medical Image Control System, Materialise, Leuven, Belgium). It is an interactive computer program can display the finest details, transfering two-dimensional CBCT data to the three-dimensional. The most important feature of Mimics® is that it is segmented using Hounsfield values. The only limit is the physical memory of the working computer. The software allows physicians and radiologists to control CBCT in full detail and segment all tissues. Mimics® has a several modular structures. These modules are:

- Basic module,

- Simulation module,

- STL + module,

- Finite element analysis (FEA) module,

- RP Slice module for rapid prototyping,

- MEDCAD module

- IMPORT module

Physicians and researchers can create a modular structure that is appropriate for the application or operation to be performed. In addition, The two-dimensional CBCT is converted directly into the Mimics® image format, providing ease of use with the import module, and the necessary information is provided for the implementation of future procedures (Santler et al. 1998).

Mimics® uses a flexible interface to quickly obtain a three-dimensional image of the area of interest, parameters for resolution and filtering can be given. For each three-dimensional model height, width, volume, surface and similar information can be obtained. The image data is displayed in various ways, each of which provides unique information. Mimics® split screen; Original axial image and cross-sectional image of "coronal and sagittal". It has the ability to move, zoom, rotate and adjust the contrast of the three-dimensional image. Point-to-point measurements can be made both in two-dimensional sections and in three-dimensional reconstructions. The Mimics® simulation module includes functions of cutting, separating, merging, mirroring, distractor

positioning, determining nerves. The simulation module contains points, planes and measurement lists. It is possible to add to these lists. The angle between three points or between two lines can be measured with this module. Inside the module is a library of distractors (Kim et al. 2010; Manmadhachary et al. 2017).

The Mimics® STL + module interfaces format can be used from an image, from a three-dimensional object can be output from the file. Mimics® makes it easy to understand the problem by creating a three-dimensional model of the problematic area of the patient. In addition, another model that will be created by coloring for problematic regions in a complex structure will help achieve a more efficient solution. This application reduce both the risk and the surgeon's time. In the three-dimensional modeling provide a rapid recovery of the patient problem by covering the anatomical characteristics of the patient (Swennen et al. 2009).

4.4.9 Morphometric Analysis With MIMICS Program

Mimics® program main screen create orthographic view of sagittal, coronal, axial and 3D reconstruction model of the original image as in Figure 4.30. The Mimics® program allows Hounsfield values to be used to separate images from different textures. The desired structure can be separated from other tissues by selecting the existing values of different tissues in the program. This process is performed with the program's thresholding function (Manmadhachary et al. 2017).

The vertebra, mandibula, and cranium can be obtained separately three-dimensionally after bone tissue has been separated from other structures. This process is performed by the user, not automatically by the program. Each structure that is desired to be separated is referred to as adjacent structures (Santler et al. 1998; Swennen et al. 2009).

Within the Mimics® simulation module for cephalometric analysis there are different analyzes where angular and linear measurements can be made: Downs analysis, Steiner analysis, Tweed analysis, Ricketts analysis, Mc Namara analysis, Ortognatic surgery analysis (Le Fort I, II, III and Genioplasty), Soft tissue analysis. In addition, a different analysis can be defined by taking advantage of the points and planes used in existing

analyzes or by specifying new points and planes. After the preferred or later generated cephalometric analysis is selected, the display can be marked on the three-dimensional surface model or on the sectional views (Fishman et al. 1991; De Oliveira et al. 2009; Cevidanes et al. 2010).

5. MATERIALS AND METHODS

5.1. Patient selection

This retrospective study was approved by Clinical Researchs Ethic Comittee of Marmara University, Faculty of Dentistry, with a protocol number: 2016-36. CBCT images of 150 patients were selected and examined from the patient archives of the Departments of Orthodontics, Faculty of Dentistry, Marmara University. Due to image distortion and artifacts, 54 images were excluded and the remaining 96 patients aged from 16 to 30 years old were matched for the present study.

Of the patients, 36 were Angle class I normal occlusion and 60 were Angle class III malocclusion. In total 44 (45.8%) were female and 52 (54.2%) were male. The mean age was 23.23 ± 3.92 year-old. Patients were divied into three groups: normal type (A) group of 37.5% (n = 36), mild type (B) group with edge to edge occlusion of class III malocclusion of 18.8% (n = 18) and severe type (C) group with reverse (negative) occlusion of class III malocclusion of 43.8% (n = 42) as in Figure 5.1.
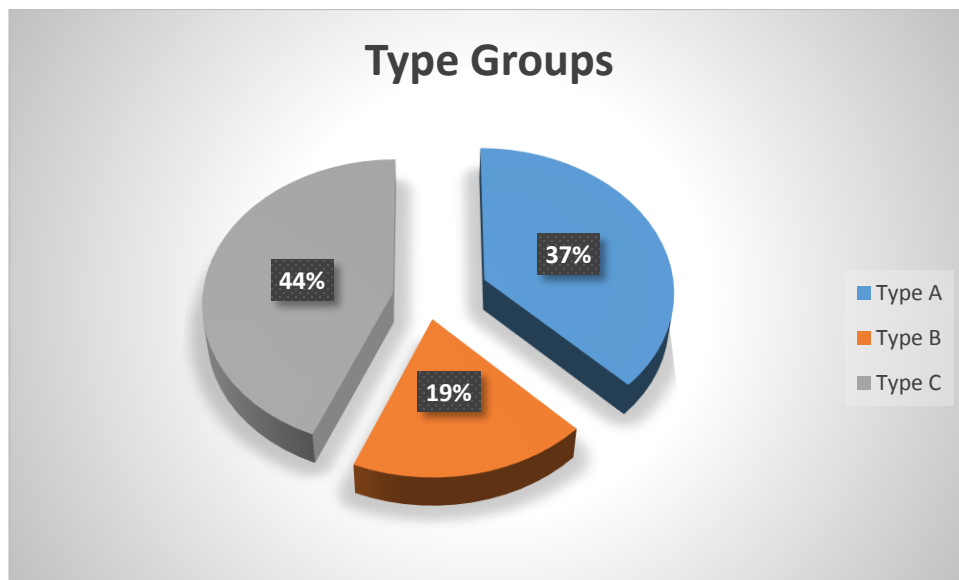
Figure 5.1: Percentage of patients in each groups (Excel MS, 2013).

5.2 The study Inclusion and Exclusion Criteria

1. Inclusion criteria

All patients were caucasian Turkish patient with:

1. Class I skeletal relationship as control (A) group with:

  a. Balanced facial profile appearance.

  b. Full set of permanent dentition.

  c. Normal curve of Spee (0-2) mm.

2. Class III skeletal relationship as study cases for both (B, C) groups with:

  a. Accepted rate of symmetry and midline of coincidence without shifting or deviation.

  b. No previous orthodontic or Orthognathic treatment.

  c. No acute or previous temporomandibular disorder like hyperplasia or ankylosis.

3. Age of patients between (15-30) years old.

2. Exclusion criteria

1. Traumatic facial discrepancy or incompatibility parafunctional habits.

2. Post-operative surgical facial discrepancy.

3. Post orthodontic or through orthodontic treatment or under corrective interventional or protective device applied.

4. No craniofacial dysostosis anomaly, like Crouzon or Apert syndrome.

5. Post Orthognathic surgical treatment or past history of surgical bimaxillary correction.

6. Past history of CNS disease or treatment.

7. Past history of rheumatologic disease or treatment.

8. Midfacial alveolar related pathology (Dentofacial cyst or tumor).

9. Osteogenic related Systemic diseases like (Diabetic milletiuts, kidney related disease).

10. Angle class II skeletal malocclusion with increased overjet value.

All the patients were subjected to Steiner's analysis of interocclusal (ANB) angular value and classified into the following groups as shown in Figure 5.2.
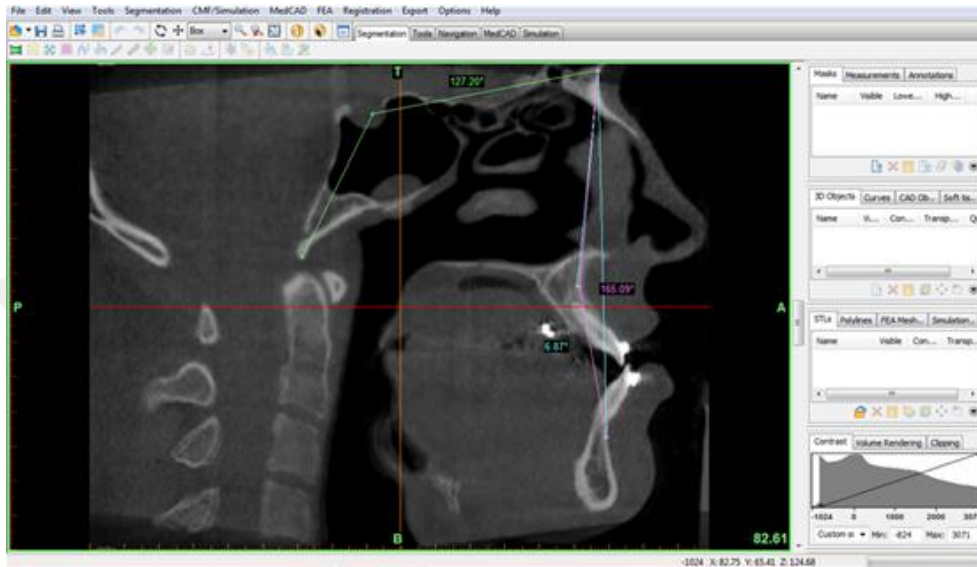
Figure 5.2 Stenier's analysis ANB angular value.

1. The "type A" of Angle Cl I normal occlusion with a maximum interocclusal (ANB) angular relation value above (4°< ANB >1°).

2. The "type B" of Angle Cl III malocclusion with an edge to edge interocclusal (ANB) angular relation value (1°< ANB >-1°).

3. The "type C" of Angle Cl III malocclusion with an inverse interocclusal (ANB) angular relation value (< -1°).

5.3 Collection of Data

All records of CBCT images had been taken for the pre-orthodontic treatment or orthognathic surgery. The CBCT images were taken with the ILUMA CBCT scan for all patients which acquired with technical properties of the CBCT (Iluma Imtec, 3M, St Paul, Minn). The Scans were acquired while the patient was sitting upright with the Frankfort

Horizontal plane (FHP) parallel to the floor, at maximum intercuspation. The patient's head position was adjusted with the help of two laser beams, one parallel to the floor, coinciding with the Frankfort Horizontal plane, and one vertical beam passing through the patient's facial midline. The patients were not asked to swallow and move to their heads or tongues during exposure.

5.4 The Scan Machine and Mimics Software

Technical properties of the machine used:

- Brand Name: Iluma Imtec imaging by 3M Company
- Focal Spot: 0.3 mm x 0.3 mm
- X-ray tube applied: 120 KV
- X-ray tube current: 1-4 mA
- Detector size: 19.5 x 24.5 cm
- Scanning with 360 degrees rotation
- Radiation: 58 micro Sieverts maximum
- Scanning time 7.8- 40 seconds (180 rotation angle)
- Field of View (Imaging area) : 14.2 Cm x 21.1 cm
- Voxel Size: 0.0936 mm
- Gray Scale: 14 bit

In capture mode, the STLs module data was exported in DICOM (Digital Imaging and Communications in Medicine) format. The DICOM image-data obtained from CBCT module were transferred to a network computer workstation, where analysis of linear, angular variables and 3D volumetric analysis were processed in orthographic view using Mimics 19.0 software (Materialise Europe, World Headquarters, Leuven, Belgium).

5.5 Linear and Angular Referance (Shape) Analysis

All CBCT data were examined and analyzed by the same examiner (Dr.Ammar MOHI) under the revision of two orthodontist-examiners in order to estimate proper orthodontic principal for this study.The method for converting CBCT data to DICOM image in orthographic sectional views and segmentation was manually done by the thresholds scale. Firstly, initial orientation (top, bottom, left, right, anterior, posterior) was verified. After verifying the orientation, a predefined threshold representing the bone Hounsfield Units (HU) was chosen with a minimum limit of (-1024) Hounsfield Units (HU) and a maximum of (1650) HU.The threshold (bone scale threshold) is important to create first separation of the involved anatomical structures landmarks. A mask was generated for each patient's study parameters made it seperatly proceed within work flow. The mask can be edited by using aforementioned tool bar for adding removal and cropping function.
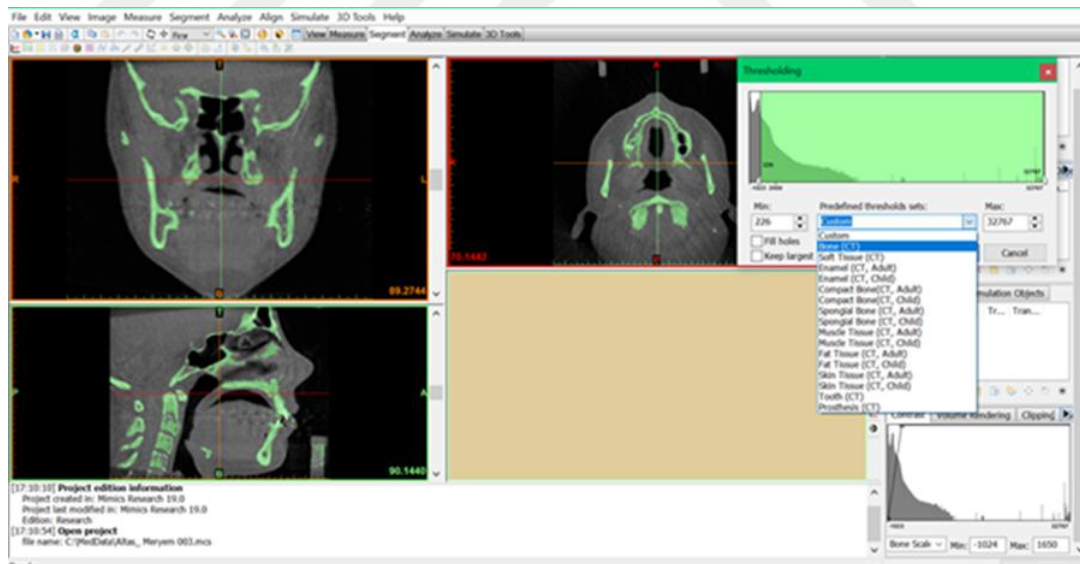
Figure 5.3: Screen view of Mimics software

After the mask was created, using the "segment" tool "region growing" option for the target skeleton (green) was selected and a refine mask created. So any existing irrelevant interferences like metal bar or artifacts were excluded.

Figure 5.4: Region growing segmentation tool

After this refined mask was created, a new mask with different color (yellow) was initiated with high quality and smooth 3D bone model. The 3D tracing of cephalometric analysis was predefined already to estimate the linear and angular measurement on four sectional screen using measurement tool bar of Mimics 19.0 (Materialise, Leuven, Belgium).

Figure 5.5 Three Dimenssional Cranial bone model reconstruction

This skeletal linear and angular reference planes measurements based on landmarks were detected, connected and traced on the 3D models. The definition of the skeletal landmarks, the skeletal planes and the angular references used in this study are presented in Tables 5.2, 5.3 and 5.4.

Before the construction of the planes above, the Frankfurt Horizontal plane was defined to overcome head tilting movement by the plane passing through left and right Porion and right Orbitale. Also the midsagital plane of anterior cranial base through Nasion to Sella turcica central point was detected. If the tracing of any landmark would be disturbed by the presence of artifacts, the threshold of the hard-tissue or the soft-tissue mask would be readjusted or excluded as in Figure 5.5, 5.6, 5.7 and 5.8.

In cases where any point was out of the field of view of the CBCT or distorted, the image was not included in the assessment.
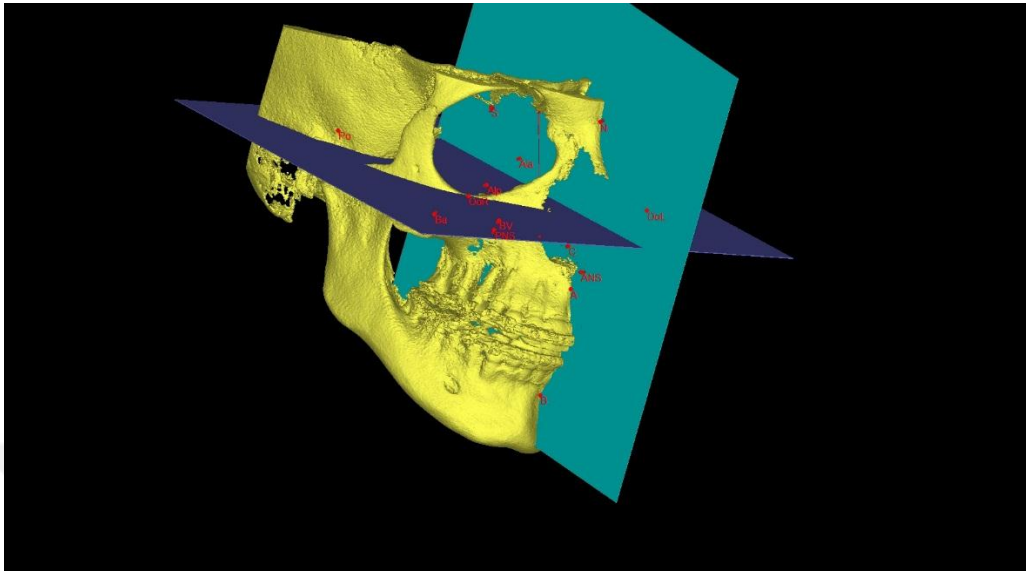
Figure 5.6: 3D Midsagital coordination with Frankfurt plane (Fr-plane) lateral view.
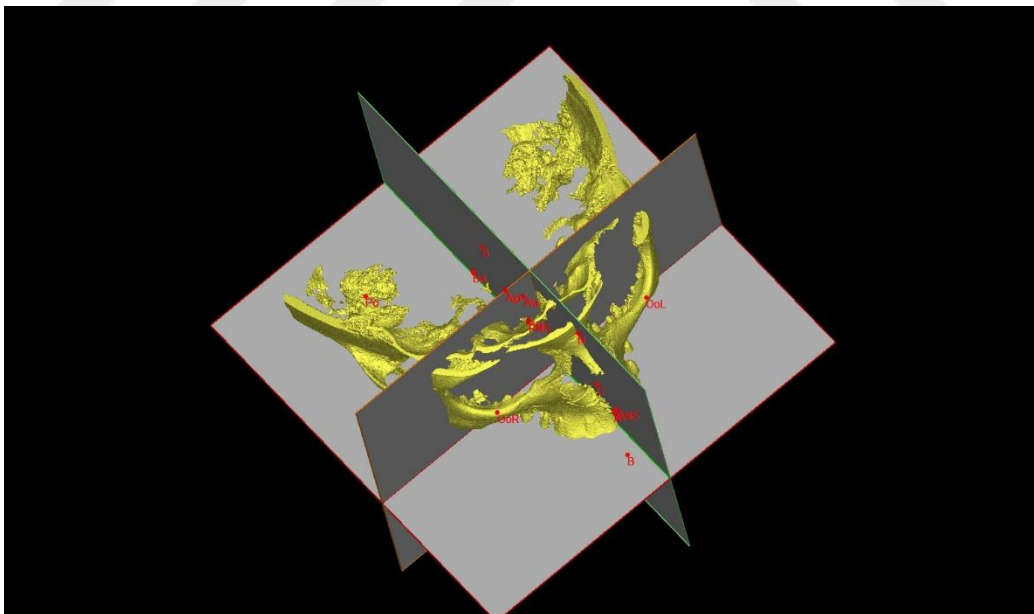
Figure 5.7: Midsagital coordination with Frankfurt plane(Fr-plane) upper view.
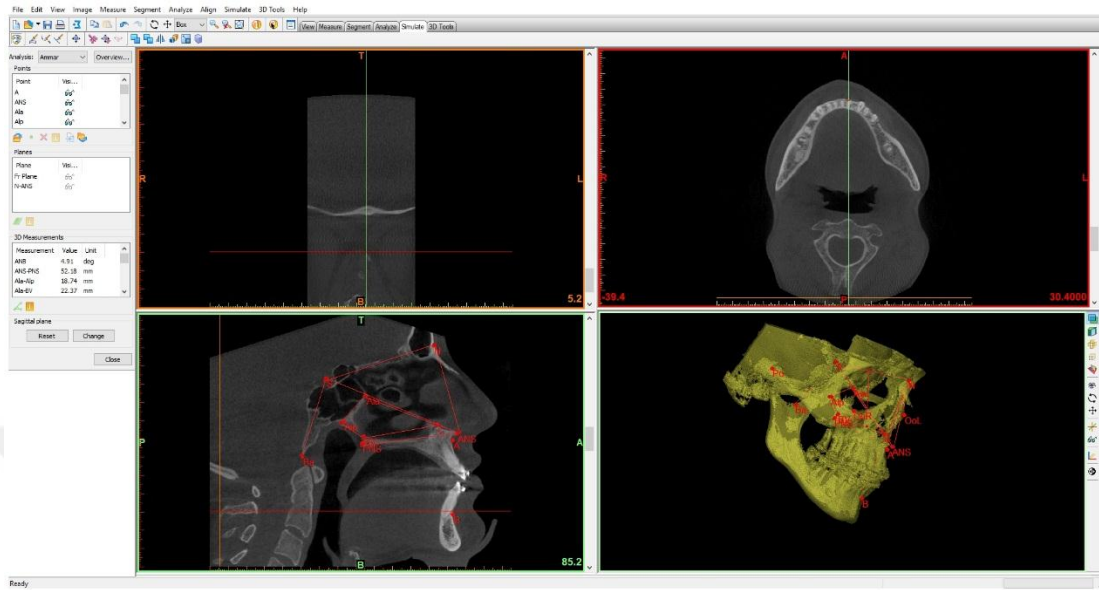
Figure 5.8: Orthgraphic view in 2D and 3D image reconstruction.
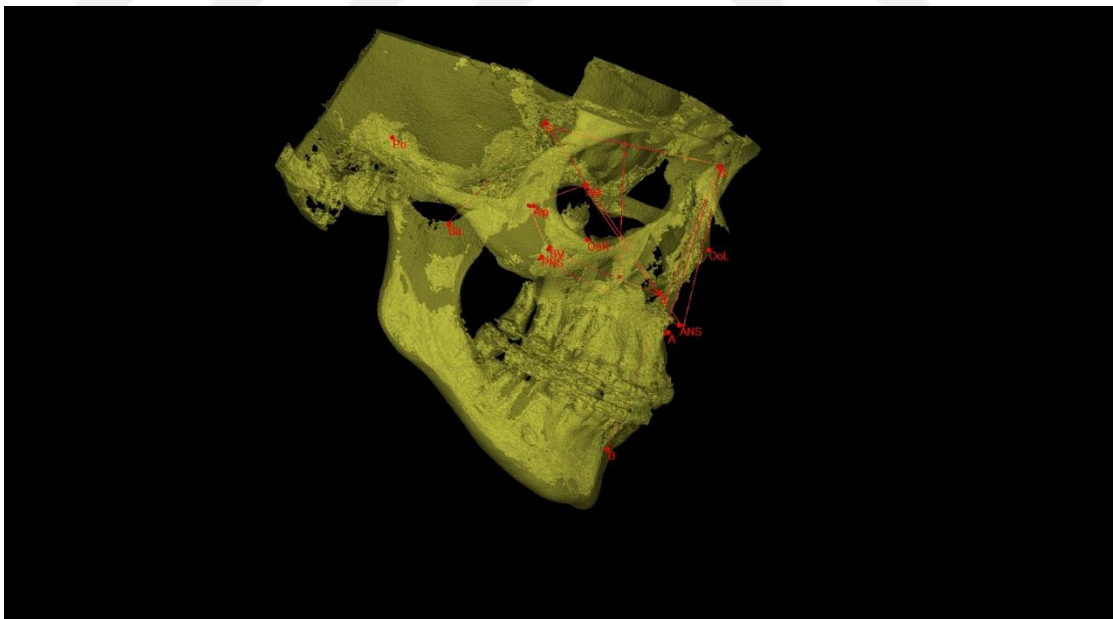
Figure 5.9: Lanmarks with Dimenssional Analysis in 3D Reconstruction view.

Table 5.1: Study Skeletal Landmarks with brief definition.

Landmark	Definition
Nasion (N)	The junction between the nasal and frontonasal sutures
Sella (S)	The center of the sella turcica on the midsagittal plane
Basion (Ba)	The most anterior curve of foramen magnum
Porion (Po)	The most superior point on the upper rim of the external auditory meatus
Orbitale (Or)	The most inferior point on the lower rim of the orbit
Anterior nasal spine (ANS)	The most anterior point on the floor of nose
Posterior nasal spine (PNS)	The most posterior point on the floor of nose
A point (A)	The deepest point between ANS and prosthion at the midsagittal plane of upper alveolus of upper incisors
Canine eminence (Ce)	The point on the surface of the maxilla corresponding to the canine root apex and symmetrical to vomer apex C medially
B point (B)	The deepest point between pogonion and the alveolus of the lower incisors on the midsagittal plane
Vomer apex (C)	The most anterior and medial point at upmost opening of nasopalatine canal corresponding to canine eminence point CE bilaterally
Vomer base(BV)	The most posterior and medial point of maxilla at lowermost opening of sphenopalatine fissure opening corresponding to point PNS medially
Vomer ala anterior (Ala)	The most superior and medial point at uppermost level of anterior sphenoid body.
Vomer ala posterior (Alp)	The most posterior and medial point at lowermost level of anterior sphenoid body.

Table 5.2: Study Linear variable with breif description.

Reference plane	Definition
N-S Cranial base plane	Line plane between points N and S
S-Ba posterior facial plane	Line plane between points S and Ba
Oo-Po Frankfort plane	Line between points Oo, and Po
ANS-PNS midfacial lower occlusal plane	Line between points PNS and ANS
N-ANS anterior vertical facial plane height of midfacial area (anterior depth of midfacial area)	Line between points N and ANS
S-PNS posterior vertical facial plane height of midfacial area (posterior depth of midfacial area)	Line between points S and PNS
N-A anterior premaxilla plane upper facial height plane	Line between points N and A
N-B full facial height plane	Line between points N and B
ANS-C anterior horizontal maxilla impaction plane	Line between points ANS and C
N-C posterior premaxilla plane	Line between points N and C
A-C anterior vertical maxilla impaction plane	Line between points A and C
Ala-Alp horizontal ala plane of vomer	Line between points Ala and Alp
Ala-C transverse roof plane of vomer	Line between points Ala and C
Alp-C sagittal full length of vomer	Line between Alp and C
Alp-BV sagittal posterior plane of vomer	Line between Alp and BV
C-BV sagittal base plane of vomer	Line between C and BV

Table 5.3: Study Angular variables with brief description.

Measurement	Definition
Cranial base angle NSBa (°)	The angle between points: N, S and Ba on the midsagittal plane
Facial intermaxillary angle ANB (°)	The angle between points: A, N, and B on the midsagittal plane
Cephalic impaction angle (°)	The angle formed by intersection between the S-ANS line and ANS-PNS plane projected on the midsagittal plane
Cephalic displacement angle (°)	The angle formed by intersection between the N-S line and S-PNS plane projected on the midsagittal plane
Facial impaction angle (°)	The angle formed by intersection between the N-ANS line and ANS-PNS plane projected on the midsagittal plane
Facial profile angle (°)	The angle between points: N, A and B on the midsagittal plane
Cephalic vomer displacement angle (°)	The angle between points: S, C and PNS on the midsagittal plane
Vomer vertical impaction angle (°)	The angle between points: C, N and ANS on the midsagittal plane
Vomer horizental impaction angle (°)	The angle between points: Ala, C and BV on the midsagittal plane
Vomer backward occlusal angle (°)	The angle between points: ANS, C and PNS on the midsagittal plane
Vomer backward inclination angle (°)	The angle between points: C, BV and ANS on the midsagittal plane
Vomer roof posterior inclination angle (°)	The angle between points: Ala, BV and Alp on the midsagittal plane
Vomer basal posterior inclination angle (°)	The angle between points: Alp, Ala and BV on the midsagittal plane
Vomer midfacial posterior inclination angle (°)	The angle between points : C, BV and Alp on midsagittal plane
Vomer roof midfacial displacing angle (°)	The angle between points : C, Ala and BV on midsagittal plane

5.6 Size Analysis of Reconstructed 3D Vomer Bone Model

After initial shape analysis of linear and angular measurements were finished, The vomer bone size changes represented by different volumetric pattern of 3D reconstructed vomer bone model in three study groups. The "crop mask" and "edit mask" options control the area of interest (AOI) is the vomer bone area that should be isolated from the surrounding as shown in Figure 5.9.
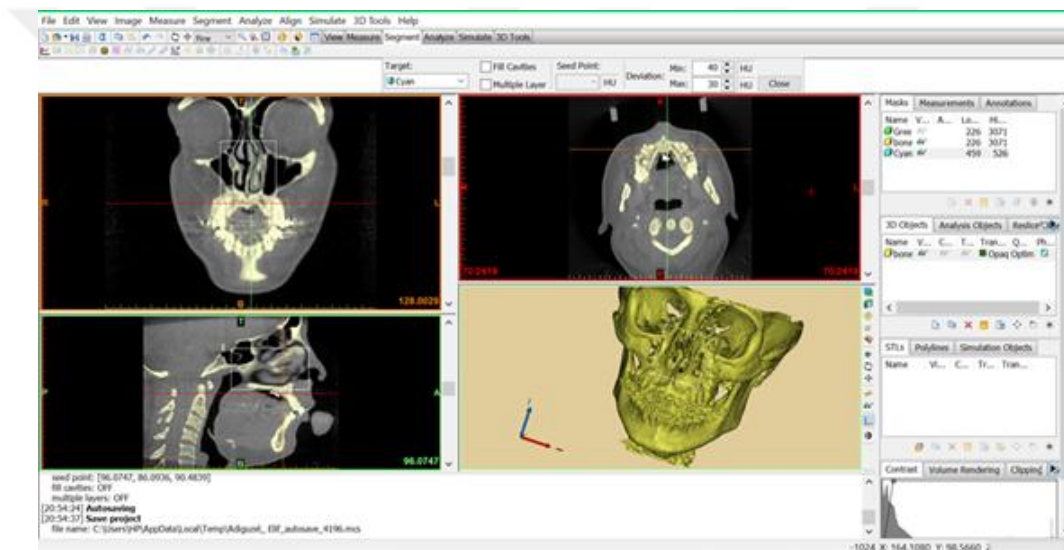
Figure 5.10: The area of interest AOI isolation by crop mask and edit mask tools

The segment tool "split mask "feature was isolated the same skeletal threshold with definitly two different masks boundries by drawing outline area of interest follow lanmarks. With an identified mask color, the vomer bone mask (region A) was isolated from surrounding midfacial mask (region B) of same threshold scale preparing for final steps of 3D reconstruction of vomer bone size pattern measurements as shown Figure 5.10.
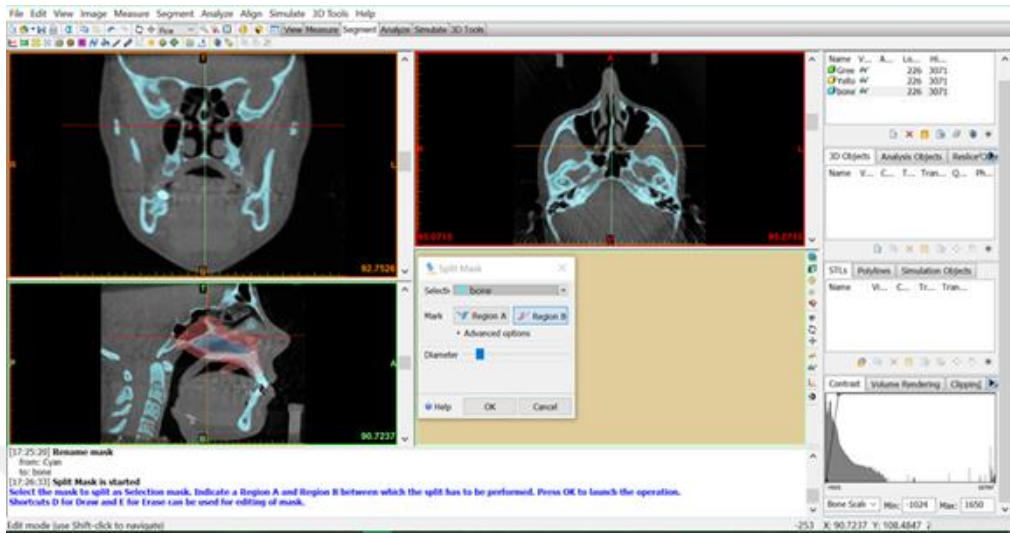
Figure 5.11: Split mask of Vomer bone from surrounding structures

As a result, the images of the isolated vomer bone with a different mask colors within the same AOI appeared in Figure 5.11.
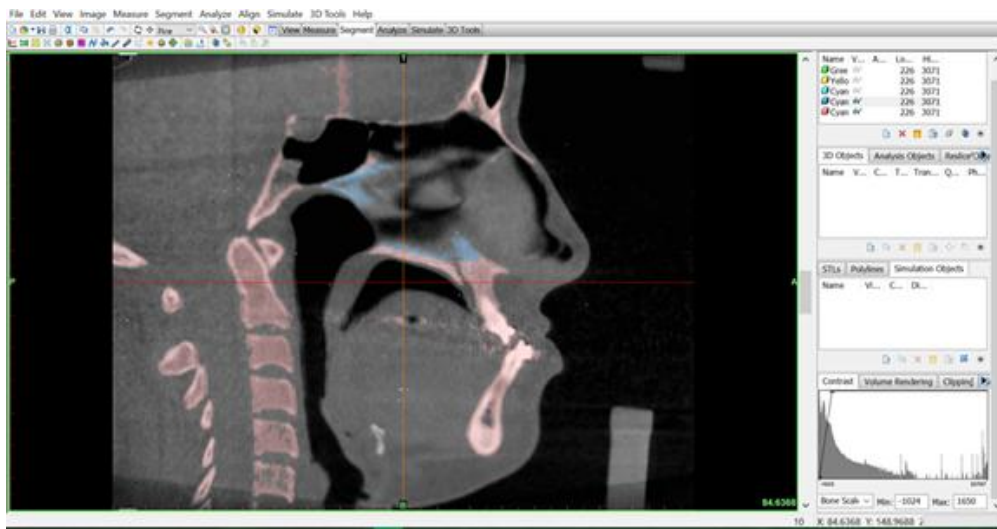
Figure 5.12: The vomer bone with a different mask color within the same AOI

After separation of vomer bone mask by split tool from surrouning AOI, The 3D recostruction of both mask of facial an vomer bone were calculated as in Figure 5.12.
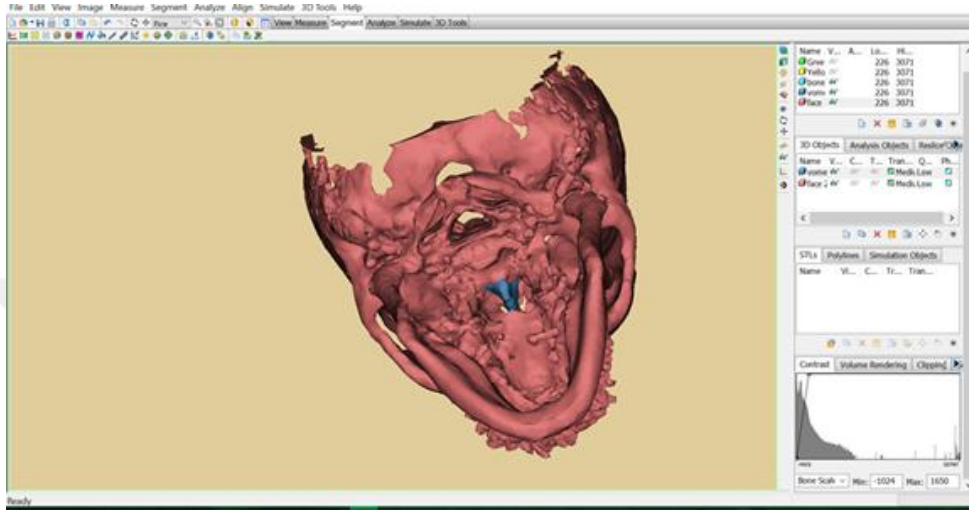
Figure 5.13: The 3D model of reconstructed cranial bone with Vomer identification.

The 3D vomer bone size (volumetric value) in mm3 was calculated separately for each patient in different group for evaluation an comparison as shown in Figure 5.13.

The manipulation of vomer bone or other midfacial bone masks could be formulated as shown in (Figure 5.13) for different purposes with various modification but it required certain knowledge about user manual instructions and training skills to provide an accurate and clear image with definitive craniofacial profile details.
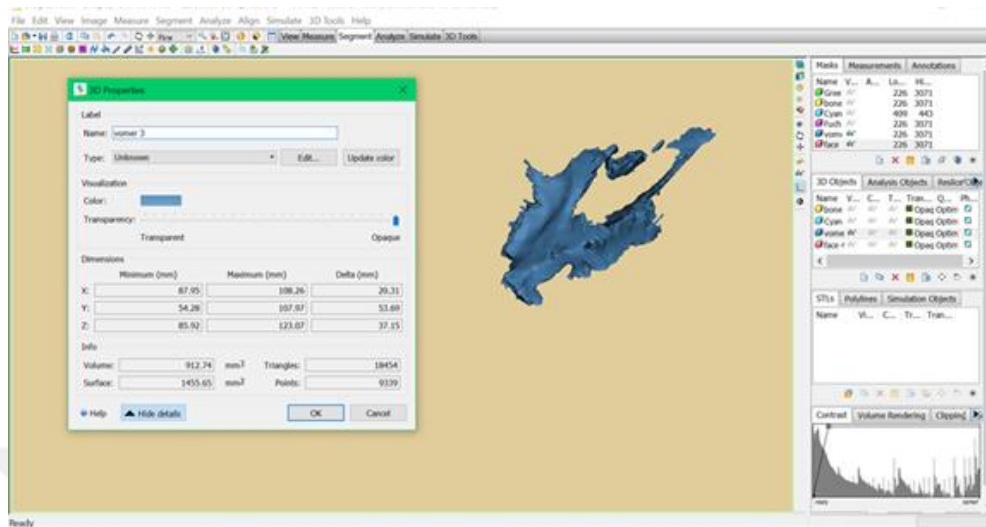
Figure 5.14: The 3D reconstruction model of vomer bone.

5.7 Statistical analysis

Statistical processing and analysis of the data was performed using SPSS statistics program for Windows (version 22.0, SPSS, Chicago, IL, USA). Also Statistical Investigations NCSS 2007 (Kaysville, Utah, USA) program was used for statistical analysis. Student t test was used in two group comparisons of the variables that showed normal distribution in comparison of descriptive statistical methods (mean, standard deviation, median, frequency, ratio, minimum, maximum) as well as quantitative data. Mann Whitney U test was used in two group comparisons of non-paired variables that were used. The Kruskal Wallis test and the Mann Whitney U test were used in the comparison of the three groups without normal distribution. Spearman's Correlation Analysis was used to evaluate the inter-variable relationships. The Fisher-Freeman-Halton Test was used for the comparison of qualitative variables. Statistical Significance was established at $p < 0.05$.

6. RESULTS

6.1 Study Type Age and Gender Desicription

In total of 96 patient images were (45.8%, n = 44) of female and 54.2% (n = 52) male.
The ages of the cases ranged from 15 to 30, with an average of 23.23 ± 3.92 years.
According to the three study groups 37.5% (n = 36) were type A, 18.8% (n = 18) were
type B and 43.8% (n = 42) were type C as shown in Table 6.1.

Table 6.1: Descriptive Analysis of study Type, Age and Gender.

Age (year)	*Min-Max (Median)*	16-30 (23)
	Mean±SDs	23,23±3,92
Gender; *n (%)*	**Female**	44 (45,8)
	Male	52 (54,2)
Type; *n (%)*	**Normal (A)**	36 (37,5)
	Mild (B)	18 (18,8)
	Severe (C)	42 (43,8)

There was no statistically significant difference between the mean ages of cases according
to study groups (p> 0.05). Whereas; there was a statistically significant difference between
male and female (p<0.01). The incidence of C type group in males is significantly higher
as shown in Table 6.2.

Table 6.2: Descreptive Analysis of study Type Groups with Age and Gender.

		Type			
		Normal (A) **(n=36)**	**Mild (B)** **(n=18)**	**Sever (C)** **(n=42)**	**p**
Age (year)	*Min-Max (Median)*	16-30 (22,5)	18-30 (21)	18-30 (23)	[a]**0,644**
	Mean±SDs	23,28±4,25	22,55±4,67	23,47±3,43	
Gender; *n*	**Female**	18 (40,9)	18 (40,9)	8 (18,2)	[b]**0,001****
(%)	**Male**	18 (34,6)	0 (0)	34 (65,4)	

[a]*Kruskal Wallis Test*　　　　[b]*Fisher-Freeman-Halton Test*　　　　***p<0,01*

6.2 Evaluation of the method error

To determined the random error, all measurements of 15 randomly selected CBCTs (20% of the sample, 5 from each group) were repeated 2 weeks after the initial examination by the same examiner. Interclass correlation coefficients (ICCs) test was used to assess the reliability of the measurements as shown in Tables 6.3, 6.4, 6.5 and 6.6.

For each measurement's method error, upper and lower of 95% confidence interval CI was determined. Consistency level between first and second measurements for all parameters was above 95%.

Results of ICC analysis showed that repetition of measurements does not affect the error rate.

Table 6.3: Interclass Correlation Coefficient for Linear parameters.

Variables	ICC	Correlation 95% CI	P
N-S	0.975	0.898-0.994	0.001**
S-Ba	0.950	0.798-0.988	0.001**
Oo-Po	0.984	0.939-0.996	0.001**
ANS-PNS	0.990	0.960-0.998	0.001**
N-ANS	0.986	0.948-0.997	0.001**
S-PNS	0.994	0.976-0.998	0.001**
N-A	0.999	0.998-1.000	0.001**
N-B	0.999	0.994-1.000	0.001**
ANS-C	0.997	0.986-0.999	0.001**
A-C	0.998	0.955-0.997	0.001**
Ala-Alp	0.998	0.994-1.000	0.001**
Ala-C	0.996	0.986-0.999	0.001**
Alp-C	0.956	0.834-0.989	0.001**
Alp-BV	0.999	0.997-1.000	0.001**
C-BV	0.987	0.943-0.996	0.001**

**p<0,001

Table 6.4: Interclass Correlation Coefficient for Angular parameters.

Variables	ICC	Correlation 95% CI	P
NSBa (°)	0.997	0.986-0.999	0.001**
ANB (°)	0.998	0.955-0.997	0.001**
S-ANSPNS (°)	0.994	0.976-0.998	0.001**
NS-PNS (°)	0.999	0.998-1.000	0.001**
N-ANSPNS (°)	0.999	0.994-1.000	0.001**
NAB (°)	0.950	0.798-0.988	0.001**
S-SPNS (°)	0.984	0.939-0.996	0.001**
Ala-CBV (°)	0.990	0.960-0.998	0.001**
CBV-ANS (°)	0.986	0.948-0.997	0.001**
AlpAla-BV (°)	0.998	0.994-1.000	0.001**
CBV-Alp (°)	0.996	0.986-0.999	0.001**
CAla-BV (°)	0.975	0.898-0.994	0.001**

**p<0,001

Table 6.5: Interclass Correlation Coefficient for Volume Size parameters.

Variables	ICC	Correlation 95% CI	P
Face Volume	0.997	0.986-0.999	0.001**
Vomer Volume	0.999	0.994-1.000	0.001**

**p<0,001

Table 6.6: Interclass Correlation Coefficient for Study 2D and 3D parameters.

Measurement	Units	2D	3D	ICC	P
ANB	deg	4,09	4,23	0.966	0.001**
ANS-PNS	mm	49,45	49,46	0.999	0.001**
Ala-Alp	mm	19,02	19,05	0.998	0.001**
Ala-BV	mm	19,90	19,94	0.997	0.001**
Ala-C	mm	41,78	41,82	0.999	0.001**
Ala-CBV	deg	27,38	27,42	0.998	0.001**
Alp-BV	mm	16,06	16,09	0.998	0.001**
Alp-C	mm	55,30	55,31	0.999	0.001**
AlpAla-BV	deg	48,55	48,62	0.998	0.001**
C-A	mm	9,50	9,54	0.995	0.001**
C-ANS	mm	5,16	5,29	0.975	0.001**
C-BV	mm	42,42	42,43	0.999	0.001**
CBV-ANS	deg	4,01	4,24	0.945	0.001**
CBV-Alp	deg	137,10	137,18	0.999	0.001**
N-A	mm	54,22	54,26	0.999	0.001**
N-ANS	mm	48,43	48,44	0.999	0.001**
N-ANSPNS	deg	88,24	88,26	0.999	0.001**
N-B	mm	93,08	93,09	0.999	0.001**
N-S	mm	62,02	62,04	0.999	0.001**
NAB	deg	170,25	170,73	0.997	0.001**
NSBa	deg	122,78	122,86	0.999	0.001**
OoR-OoL	mm	70,15	70,21	0.999	0.001**
OoR-Po	mm	72,46	72,58	0.998	0.001**
OrL-Po	mm	106,05	106,18	0.998	0.001**
S-ANSPNS	deg	33,56	33,62	0.998	0.001**
S-Ba	mm	44,90	44,94	0.999	0.001**
S-PNS	mm	44,07	44,12	0.998	0.001**
SC-PNS	deg	37,27	37,30	0.999	0.001**

**p<0,001

6.3 Assessment of Linear References measurements
6.3.1 Cranial Linear Reference parameters

There was a highly significant difference between the cranial parameters and study groups in cranial upper border variable (SN, SBa, RPo, NBa, SC) and lower border (ANS-PNS) variables. No significant difference was noted with (NA,NB,Opo) variables as shown in Table 6.7.

Table 6.7: Cranial Linear parameters.

Cranial		Type			p	
		Normal (A) (n=36)	Mild (B) (n=18)	Sever (C) (n=42)		
SN	Min-Max (Median)	59,97-71,43 (66,7)	59,67-65,47 (63)	61,23-70,45 (67,2)	0,021*	A=C>B
	Mean±SDs	66,04±3,81	62,53±2,23	66,40±2,92		
SBa	Min-Max (Median)	36,23-49,87 (42,4)	34,67-40,38 (39,9)	31,85-47,21 (43,9)	0,001**	A=C>B
	Mean±SDs	43,07±4,09	38,85±1,88	43,42±3,05		
R-Po	Min-Max (Median)	83,32-103,02(92,3)	88,9-93,61 (92,2)	92,69-102,33(98,9)	0,001**	C>A=B
	Mean±SDs	92,87±5,87	91,79±1,55	98,34±1,98		
SC	Min-Max (Median)	68-80,21 (73,7)	69,34-75,14 (72,4)	66,32-78,98 (76,7)	0,047*	C>B
	Mean±SDs	74,19±3,95	72,31±1,82	75,45±3,31		
Opo	Min-Max (Median)	58,81-75,65 (68,8)	62,97-70,91 (65,4)	63,33-73,33 (68,2)	0,357	-
	Mean±SDs	66,77±5,16	66,81±2,90	68,81±2,50		
ANS-PNS	Min-Max (Median)	45,42-58,79 (54,3)	43,88-50,26 (46,2)	41,71-71,33 (48,4)	0,001**	A>B=C
	Mean±SDs	53,17±4,41	46,15±1,89	48,96±6,41		
NA	Min-Max (Median)	51,38-64 (59)	54,11-59,86 (57,2)	46,41-67,57 (57,3)	0,486	-
	Mean±SDs	58,67±3,99	57,22±2,65	58,07±4,74		
NB	Min-Max (Median)	82,43-113,21(97,6)	91,94-99,61 (94,3)	66,26-109,4 (95,5)	0,880	-
	Mean±SDs	96,58±10,12	94,93±2,66	94,32±8,95		
NBa	Min-Max (Median)	90,32-107,52(98,7)	93,85-99,17 (94,8)	94,31-112,97(99,1)	0,011*	A=C>B
	Mean±SDs	98,99±5,13	95,28±1,65	100,31±4,96		
Kruskal Wallis Test		*p<0,05*		**p<0,01*		

	Type		
	A-B	**A-C**	**B-C**
SN	*0,035**	*0,955*	*0,004***
SBa	*0,010**	*0,517*	*0,001***
R-Po	*0,643*	*0,004***	*0,001***
SC	*0,217*	*0,382*	*0,006***
Opo	*0,837*	*0,499*	*0,060*
ANS-PNS	*0,001***	*0,005***	*0,197*
NA	*0,258*	*0,438*	*0,556*
NB	*0,719*	*0,725*	*0,683*
NBa	*0,035**	*0,583*	*0,002***

Mann Whitney U Test **p<0,05* ***p<0,01*

6.3.2 Midfacial Linear Reference parameters

There was a highly significant difference between the midface parameters and study groups in midface anterior border variables (AC, N-ANS, C-ANS, NC) and posterior border (S-PNS) variable. At the same time, no significant difference was noted with (BV-PNS, N-Ala) variables as in Table 6.8.

Table 6.8: Midfacial Linear parameters

Midfacial		Type				
		Normal (A) (n=36)	**Mild (B) (n=18)**	**Sever (C) (n=42)**	***p***	
AC	*Min-Max (Median)*	6,37-15,11 (10,1)	11,42-14,85 (13,9)	9,9-30,21 (14,3)	***0,001*****	B=C>A
	Mean±SDs	10,50±2,85	13,60±1,24	15,84±4,72		
N-ANS	*Min-Max (Median)*	48,94-59,45 (53,8)	47,65-53,76 (51,4)	48,9-60,65 (57,7)	***0,002*****	C>A=B
	Mean±SDs	53,65±3,36	51,12±1,81	56,46±3,65		
S-PNS	*Min-Max (Median)*	40-51,71 (47,1)	43,33-47,22 (45,5)	40,12-55,31 (50,2)	***0,003*****	C>A=B
	Mean±SDs	46,09±3,78	45,40±1,18	49,35±4,04		
BV-PNS	*Min-Max (Median)*	4,11-6,65 (5,1)	4,21-5,66 (5,5)	4,21-19,43 (5,5)	***0,259***	-
	Mean±SDs	5,25±0,72	5,38±0,45	6,03±3,10		
C-ANS	*Min-Max (Median)*	7,22-15,6 (11)	9,82-14,12 (13,7)	5,53-20,13 (14,6)	***0,002*****	B=C>A
	Mean±SDs	11,13±2,48	12,93±1,5	14,17±3,00		
N-Ala	*Min-Max (Median)*	48,93-62,03 (53,6)	48,97-51,87 (50,9)	20,14-55,57 (51,3)	***0,049****	B=C>A
	Mean±SDs	53,55±3,61	50,64±0,91	49,31±7,51		
NC	*Min-Max (Median)*	42,72-54,96 (49,4)	41,27-47,36 (44,7)	42,72-53,31 (49,2)	***0,005*****	A=C>B
	Mean±SDs	49,53±3,07	44,95±2,05	48,35±3,16		

Kruskal Wallis Test **p<0,05* ***p<0,01*

	Type		
	A-B	**A-C**	**B-C**
AC	*0,009***	*0,001***	*0,390*
N-ANS	*0,072*	*0,020**	*0,001***
S-PNS	*0,471*	*0,003***	*0,009***
BV-PNS	*0,198*	*0,143*	*0,946*
C-ANS	*0,045**	*0,001***	*0,070*
N-Ala	*0,033**	*0,042**	*0,874*
NC	*0,001***	*0,360*	*0,016**

Mann Whitney U Test   **p<0,05*   ***p<0,01*

6.3.3 Vomer Linear Reference parameters

There was a highly significant difference between all study groups and vomer bone (Ala-Alp, CBV, C-Alp, Ala-BV, C-Ala) linear variables. At the same time, no significant difference was noted with variables as in Table 6.9.

Table 6.9: Vomer Linear parameters.

		Type				
Vomer		**Normal (A)** **(n=36)**	**Mild (B)** **(n=18)**	**Sever (C)** **(n=42)**	***p***	
Ala-Alp	*Min-Max (Median)*	14,36-21,15 (18,6)	12,5-18,92 (15,5)	12,5-49,27 (20,2)	*0,006***	A=C>B
	Mean±SDs	18,20±2,27	15,74±1,87	20,54±7,23		
Ala-BV	*Min-Max (Median)*	15,24-27,66 (21,7)	15,31-22,46 (21,8)	18,11-29,72 (23,7)	*0,049**	C>A
	Mean±SDs	21,20±3,40	20,73±2,41	23,65±3,18		
CBV	*Min-Max (Median)*	34,33-46,03 (41,7)	29,17-37,72 (34,4)	25,91-41,58 (34,8)	*0,001***	A>B=C
	Mean±SDs	41,27±3,54	33,35±2,81	35,22±4,45		
C-Alp	*Min-Max (Median)*	52,24-67,54 (60,7)	44,2-57,41 (49)	33,21-60,98 (55,1)	*0,001***	A>C>B
	Mean±SDs	60,50±5,52	50,06±4,46	53,81±5,90		
C-Ala	*Min-Max (Median)*	41,23-54,58 (46,4)	33,32-51,33 (42,1)	26,16-51,04 (43,7)	*0,025**	A>B=C
	Mean±SDs	47,01±4,23	41,32±6,60	42,94±5,92		
Alp-BV	*Min-Max (Median)*	18,74-27,75 (24,3)	16-23,59 (18)	15,71-42,33 (24,1)	*0,002***	A=C>B
	Mean±SDs	23,59±3,25	18,73±2,37	23,69±5,26		

Kruskal Wallis Test   **p<0,05*   ***p<0,01*

	Type		
	A-B	**A-C**	**B-C**
Ala-Alp	*0,016**	*0,128*	*0,004***
Ala-BV	*0,537*	*0,040**	*0,054*
CBV	*0,001***	*0,001***	*0,258*
C-Alp	*0,001***	*0,001***	*0,021**
C-Ala	*0,027**	*0,022**	*0,483*
Alp-BV	*0,001***	*0,499*	*0,002***

Mann Whitney U Test   *p<0,05   **p<0,01

6.3.4 Correlation between Vomer and Cranial Linear parameters

There was a significant positive correlation between the vomer bone linear parameters and cranial linear variable for all study groups in cranial base upper border (SN,SBa,NBa,SC) variables and (Alp-Ala, C-BV, C-Alp) variables as in Table 6.10.

Table 6.10: Correlation between Vomer and Cranial Linear parameters

Vomer	Cranial	TypeA		TypeB		TypeC	
		r	*p*	r	*p*	r	*p*
Ala-Alp	**SN**	0,783	*0,001***	-0,312	*0,413*	0,514	*0,017**
	SBa	0,486	*0,041**	-0,075	*0,847*	0,461	*0,036**
	SC	0,739	*0,001***	-0,218	*0,574*	0,370	*0,098*
	ANS-PNS	0,711	*0,001***	-0,444	*0,232*	-0,121	*0,602*
	NA	0,845	*0,001***	-0,156	*0,688*	-0,087	*0,709*
	NB	0,742	*0,001***	-0,043	*0,913*	-0,105	*0,649*
Ala-BV	**SN**	0,536	*0,022**	0,270	*0,482*	0,402	*0,071*
	SBa	0,053	*0,836*	-0,092	*0,814*	-0,052	*0,824*
	SC	0,374	*0,127*	0,385	*0,306*	0,135	*0,559*
	ANS-PNS	0,701	*0,001***	0,142	*0,715*	0,066	*0,775*
	NA	0,562	*0,015**	0,063	*0,871*	0,042	*0,855*
	NB	0,717	*0,001***	-0,077	*0,844*	0,315	*0,165*
CBV	**SN**	0,608	*0,007***	0,118	*0,762*	0,432	*0,048**
	SBa	0,432	*0,073*	-0,059	*0,881*	0,411	*0,064*
	SC	0,640	*0,004***	-0,084	*0,831*	-0,023	*0,920*
	ANS-PNS	0,695	*0,001***	0,527	*0,145*	-0,082	*0,724*
	NA	0,548	*0,019**	0,063	*0,871*	0,297	*0,191*
	NB	0,490	*0,039**	0,248	*0,520*	0,238	*0,298*
C-Alp	**SN**	0,765	*0,001***	0,084	*0,830*	0,635	*0,002***
	SBa	0,490	*0,039**	-0,300	*0,433*	0,313	*0,166*
	SC	0,785	*0,001***	0,283	*0,460*	0,087	*0,707*
	ANS-PNS	0,917	*0,001***	0,317	*0,406*	0,092	*0,693*
	NA	0,703	*0,001***	-0,311	*0,415*	0,468	*0,033**
	NB	0,738	*0,001***	0,094	*0,811*	0,402	*0,071*
C-Ala	**SN**	0,649	*0,004***	0,412	*0,271*	0,179	*0,437*
	SBa	0,201	*0,423*	-0,117	*0,765*	0,186	*0,420*
	SC	0,654	*0,003***	0,283	*0,460*	0,261	*0,254*
	ANS-PNS	0,858	*0,001***	0,400	*0,286*	0,346	*0,124*
	NA	0,610	*0,007***	-0,185	*0,634*	-0,393	*0,078*
	NB	0,641	*0,004***	0,230	*0,552*	0,206	*0,371*
Alp-BV	**SN**	0,548	*0,019**	-0,169	*0,664*	0,325	*0,151*
	SBa	0,313	*0,206*	-0,661	*0,053*	-0,028	*0,903*
	SC	0,463	*0,053*	0,351	*0,354*	0,536	*0,012**
	ANS-PNS	0,360	*0,142*	0,109	*0,781*	0,251	*0,272*
	NA	0,513	*0,030**	-0,055	*0,889*	-0,310	*0,171*
	NB	0,589	*0,010**	-0,274	*0,476*	0,100	*0,665*

r:Spearman's coorelation coefficient   **p<0,05*   ***p<0,01*

6.3.5 Corelation between Vomer Bone and Midfacial Linear parameters

There was a significant positive correlation between the vomer bone linear parameters and midface linear variable for all study groups in anterior midface (AC, N-ANS, N-Ala) and posterior variables (S-PNS, BV-PNS) variables with all vomer bone parameters as in Table 6.11.

Table 6.11 Correlation between Vomer and Midfacial Linear parameters

| | | TYPE | | | | | |
| | | TypeA | | TypeB | | TypeC | |
Vomer	*Midfacial*	r	*p*	r	*p*	r	*p*
Ala-Alp	**AC**	0,618	*0,006**	0,118	*0,762*	0,452	*0,040**
	N-ANS	0,746	*0,001***	0,402	*0,284*	0,389	*0,081*
	S-PNS	0,806	*0,001***	-0,343	*0,366*	0,197	*0,393*
	BV-PNS	0,272	*0,276*	-0,387	*0,303*	0,357	*0,112*
	C-ANS	0,251	*0,316*	-0,101	*0,796*	0,052	*0,823*
	N-Ala	0,505	*0,033**	-0,357	*0,345*	0,002	*0,993*
	NC	0,507	*0,032**	-0,268	*0,486*	0,336	*0,137*
Ala-BV	**AC**	0,457	*0,056*	-0,169	*0,664*	0,125	*0,589*
	N-ANS	0,492	*0,038**	-0,335	*0,379*	0,296	*0,193*
	S-PNS	0,688	*0,002***	0,226	*0,559*	0,534	*0,013**
	BV-PNS	0,298	*0,229*	0,378	*0,315*	0,376	*0,093*
	C-ANS	0,492	*0,038**	-0,151	*0,698*	0,137	*0,553*
	N-Ala	0,356	*0,147*	-0,340	*0,370*	0,179	*0,438*
	NC	0,432	*0,073*	0,100	*0,797*	-0,004	*0,987*
CBV	**AC**	0,067	*0,791*	0,177	*0,648*	0,165	*0,474*
	N-ANS	0,606	*0,008***	-0,167	*0,667*	0,350	*0,119*
	S-PNS	0,451	*0,060*	0,008	*0,983*	0,441	*0,045**
	BV-PNS	0,264	*0,289*	0,318	*0,405*	-0,025	*0,914*
	C-ANS	0,061	*0,810*	0,479	*0,192*	0,274	*0,229*
	N-Ala	0,761	*0,001***	0,038	*0,923*	0,141	*0,542*
	NC	0,664	*0,003***	0,184	*0,635*	0,072	*0,758*
C-Alp	**AC**	0,259	*0,299*	0,244	*0,527*	0,131	*0,571*
	N-ANS	0,746	*0,001***	-0,567	*0,112*	0,500	*0,021**
	S-PNS	0,740	*0,001***	-0,133	*0,732*	0,734	*0,001***
	BV-PNS	0,235	*0,347*	0,061	*0,877*	0,303	*0,182*
	C-ANS	0,059	*0,817*	0,226	*0,559*	0,328	*0,147*
	N-Ala	0,713	*0,001***	0,075	*0,847*	0,061	*0,792*
	NC	0,664	*0,003***	-0,117	*0,765*	0,057	*0,805*
C-Ala	**AC**	0,129	*0,610*	0,034	*0,932*	0,504	*0,020**
	N-ANS	0,754	*0,001***	-0,417	*0,265*	0,157	*0,498*
	S-PNS	0,684	*0,002***	0,317	*0,406*	0,169	*0,465*
	BV-PNS	0,094	*0,711*	-0,269	*0,485*	0,227	*0,323*
	C-ANS	0,065	*0,798*	0,142	*0,715*	0,106	*0,648*
	N-Ala	0,633	*0,005***	-0,092	*0,814*	-0,487	*0,025**
	NC	0,540	*0,021**	-0,100	*0,798*	-0,353	*0,116*
Alp-BV	**AC**	0,763	*0,001***	-0,203	*0,601*	0,371	*0,098*
	N-ANS	0,354	*0,150*	-0,586	*0,097*	0,428	*0,053*
	S-PNS	0,498	*0,035**	-0,192	*0,620*	0,284	*0,211*
	BV-PNS	0,279	*0,263*	-0,309	*0,419*	0,704	*0,001***
	C-ANS	0,653	*0,003***	0,176	*0,650*	0,072	*0,756*
	N-Ala	0,585	*0,011**	0,458	*0,215*	-0,222	*0,334*
	NC	0,278	*0,265*	0,067	*0,864*	0,092	*0,692*

r:Spearman's coorelation coefficient   **p<0,05*   ***p<0,01*

6.4 Assessment of Angular References measurements

6.4.1 Cranial angular Reference parameters

There was a highly significant difference between the cranial angular parameters and study groups in interocclusal angle (ANB). Also the cranial base angle (NSBa) and anterior impaction angle (ANC) variables were highly significant differences within study groups. No significant difference was noted with facial plane angle (NAB) variable as in Table 6.12.

Table 6.12 Cranial Angular parameters

Cranial		Type			p	
		A (n=36)	B (n=18)	C (n=42)		
NSBa	Min-Max (Median)	117,8 / 2361,43 (131,6)	117,23 / 1133,13 (124,7)	113,98 / 2649,24 (127,2)	0,036*	A>C
	Mean±SDs	131,19±6,15	125,90±6,12	126,15±6,90		
ANB	Min-Max (Median)	0,25 / 67,53 (3,7)	-3,38 / -0,96 (-1,4)	-7,83 / -64,1 (-3)	0,001**	A>B>C
	Mean±SDs	3,75±2,2	-0,11±3,68	-3,05±1,96		
NAB	Min-Max (Median)	160,21 / 3087,42 (173,8)	165,55 / 1551,04 (173,2)	163,91 / 3648,31 (175,1)	0,522	-
	Mean±SDs	171,52±5,81	172,34±4,16	173,73±4,30		
ANC	Min-Max (Median)	3,82 / 127,23 (6,4)	6,32 / 100,17 (9,4)	1,79 / 181,59 (7,2)	0,036*	B>A
	Mean±SDs	7,07±2,39	11,13±4,39	8,65±4,35		
Kruskal Wallis Test		*p<0,05	**p<0,01			

	Type		
	A-B	A-C	B-C
NSBa	0,057	0,018*	0,874
ANB	0,012*	0,001**	0,049*
NAB	0,837	0,310	0,402
ANC	0,009**	0,185	0,154
Mann Whitney U Test	*p<0,05	**p<0,01	

6.4.2 Midfacial angular Reference parameters

There was a highly significant difference between the midfacial angular parameters and study groups in (AAla-C, BV-CA, AC-ANS) variables. At the same time, no significance difference was noted with (NANS-PNS, CBV-ANS) variables as in Table 6.13.

Table 6.13 Midfacial Angular parameters

Midfacial		Type			p	
		A (n=36)	B (n=18)	C (n=42)		
AAla-C	Min-Max (Median)	2,66 / 118,05 (6,7)	1,92 / 26,73 (2,9)	0,9 / 151,24 (6,3)	0,001**	A=C>B
	Mean±SDs	6,56±1,95	2,97±1,02	7,20±2,78		
NANS-PNS	Min-Max (Median)	71,58 / 1480,66 (82,5)	81,86 / 754,48 (84,1)	76,53 / 1753,68 (82,5)	0,546	-
	Mean±SDs	82,26±4,35	83,83±1,64	83,51±3,91		
CBV-ANS	Min-Max (Median)	0,03 / 101,04 (6,1)	1,08 / 64,97 (7,2)	1,02 / 165,08 (9,5)	0,166	-
	Mean±SDs	5,61±3,29	7,22±3,21	7,86±4,17		
BV-CA	Min-Max (Median)	106,1 / 2212,91 (124,2)	109,21 / 1142,85 (125,4)	89,92 / 2430,17 (116,3)	0,022*	A=B>C
	Mean±SDs	122,94±9,33	126,98±10,73	115,72±12,13		
AC-ANS	Min-Max (Median)	24,78 / 685,95 (38,5)	12,26 / 250,05 (24,4)	23,15 / 832,78 (34,5)	0,034*	A=C>B
	Mean±SDs	38,11±6,91	27,78±11,51	39,66±13,37		

Kruskal Wallis Test   *p<0,05   **p<0,01

	Type		
	A-B	A-C	B-C
CAla-N	0,758	0,367	0,982
AAla-C	0,001**	0,447	0,001**
NANS-PNS	0,328	0,481	0,512
CBV-ANS	0,258	0,071	0,541
BV-CA	0,471	0,032*	0,017*
AC-ANS	0,014*	0,693	0,025*

Mann Whitney U Test   *p<0,05   **p<0,01

6.4.3 Vomer angular Reference parameters

There was a highly significant difference between the midfacial angular parameters and study groups in (AAla-C, BV-CA, AC-ANS) variables. At the same time, no significance difference was noted with (NANS-PNS, CBV-ANS) variables as in Table 6.14.

Table 6.14: Vomer Angular parameters

Vomer		**Type** A (n=36)	B (n=18)	C (n=42)	*p*	
AlaCBV	*Min-Max (Median)*	22,29 / 491,11 (25,5)	26,65 / 312,41 (36,2)	22,24 / 727,52 (36,2)	*0,001**	B=C>A
	Mean±SDs	27,28±4,36	34,71±4,61	34,64±7,57		
CAla-BV	*Min-Max (Median)*	50,87 / 1205,74 (66,1)	38,97 / 456,67 (53)	42,13 / 1220,24 (58,2)	*0,001**	A>B=C
	Mean±SDs	66,99±10,39	50,74±7,36	58,11±9,87		
Ala-BVAlp	*Min-Max (Median)*	37,04 / 984,95 (55,1)	29,41 / 387,11 (39,4)	27,74 / 969,56 (50)	*0,019**	A>B=C
	Mean±SDs	54,72±10,19	43,01±10,81	46,17±9,94		
CAlaAlp	*Min-Max (Median)*	121,72 / 2456,53 (135,1)	109,66 / 1092,4 (118,4)	104,33 / 2554,51 (123,9)	*0,004**	A>B=C
	Mean±SDs	136,47±9,9	121,38±12,04	121,64±13,8		
SANS-PNS	*Min-Max (Median)*	25,17 / 526,94 (29)	28,27 / 281,37 (31,5)	8,01 / 626,29 (30)	*0,048**	B>A
	Mean±SDs	29,27±2,49	31,26±1,87	29,82±5,49		
SC-BV	*Min-Max (Median)*	30,69 / 660,86 (35,9)	38,06 / 378,65 (42,3)	34,22 / 872,58 (41,9)	*0,001**	B=C>A
	Mean±SDs	36,71±2,79	42,07±2,88	41,55±4,13		
CN-ANS	*Min-Max (Median)*	7,98 / 250,59 (14,2)	13,21 / 152,1 (15,6)	11,15 / 311,05 (15,2)	*0,310*	-
	Mean±SDs	13,92±3,37	16,9±4,23	14,81±2,56		

Kruskal Wallis Test　　　**p<0,05*　　　***p<0,01*

	Type A-B	A-C	B-C
AlaCBV	*0,002***	*0,001***	*0,946*
CAla-BV	*0,001***	*0,017**	*0,077*
Ala-BVAlp	*0,012**	*0,030**	*0,377*
CAlaAlp	*0,007***	*0,003***	*0,839*
SANS-PNS	*0,015**	*0,086*	*0,512*
SC-BV	*0,001***	*0,001***	*0,803*
CN-ANS	*0,150*	*0,490*	*0,267*

Mann Whitney U Test　　　**p<0,05*　　　***p<0,01*

6.4.4 Correlation of vomer and cranial angular planes parameters

There was a significant correlation between the vomer bone angular parameters and cranial angluar variable for all study groups in interocclusal angular (ANB) with almost vomer bone angular variables in positive and negative direction. No significant corelation was appeard with vomer bone variable (AlaBV-Alp) as in Table 6.15.

Table 6.15: Correlation between Vomer and Cranial Angular parameters

Vomer	Cranial	TypeA r	TypeA p	TypeB r	TypeB p	TypeC r	TypeC p
AlaCBV	NSBa	-0,082	0,747	-0,550	0,125	-0,392	0,079
	ANB	0,210	0,403	0,326	0,391	0,697	0,001**
	NAB	-0,136	0,589	0,533	0,139	0,720	0,001**
	ANC	-0,029	0,909	0,350	0,356	0,163	0,480
CAla-BV	NSBa	0,287	0,248	0,467	0,205	0,531	0,013*
	ANB	0,155	0,539	-0,444	0,232	-0,432	0,049*
	NAB	-0,134	0,595	0,083	0,831	-0,366	0,103
	ANC	-0,027	0,916	0,067	0,865	-0,272	0,233
Ala-BVAlp	NSBa	0,035	0,890	0,450	0,224	0,309	0,173
	ANB	0,060	0,813	-0,033	0,932	-0,261	0,253
	NAB	-0,045	0,858	0,183	0,637	-0,183	0,428
	ANC	0,209	0,406	-0,200	0,606	-0,243	0,288
CAlaAlp	NSBa	0,669	0,002**	-0,067	0,865	0,745	0,001**
	ANB	-0,159	0,528	0,527	0,145	-0,681	0,001**
	NAB	0,145	0,567	0,083	0,831	-0,666	0,001**
	ANC	-0,091	0,720	0,200	0,606	-0,079	0,735
SANS-PNS	NSBa	0,100	0,694	-0,100	0,798	-0,543	0,011*
	ANB	-0,212	0,399	0,243	0,529	0,743	0,001**
	NAB	0,251	0,315	-0,250	0,516	0,740	0,001**
	ANC	-0,427	0,077	0,633	0,067	0,176	0,446
SC-BV	NSBa	0,246	0,325	-0,217	0,576	-0,698	0,001**
	ANB	-0,043	0,864	0,126	0,748	0,573	0,007**
	NAB	0,072	0,776	0,250	0,516	0,598	0,004**
	ANC	0,114	0,653	0,683	0,042*	0,539	0,012*
CN-ANS	NSBa	0,405	0,096	0,000	1,000	0,058	0,803
	ANB	-0,248	0,321	0,393	0,295	-0,431	0,049*
	NAB	0,151	0,550	0,300	0,433	-0,435	0,049*
	ANC	0,607	0,008**	0,833	0,005**	0,661	0,001**

r:Spearman's coorelation coefficient   **p<0,05*   ***p<0,0*

6.4.5 Correlation of vomer and midfacial angular planes parameters

There was a significant positive correlation between the vomer bone angular parameters and midface angluar variable for all study groups in occlusal backward inclination (CBV-ANS) and premaxilla inclination (AC-ANS) variable with almost vomer bone angular variables. No specific significant corelation was appeard between vomer bone variables and other midface variable as in Table 6.16.

Table 6.16: Correlation between Vomer and Midfacial Angular parameters

		TYPE					
		TypA		**TypB**		**TypC**	
Vomer	*Midfacal*	**r**	*p*	**r**	*p*	**r**	*p*
AlaCBV	**CAla-N**	0,356	*0,147*	0,117	*0,765*	0,057	*0,805*
	AAla-C	-0,105	*0,677*	0,183	*0,637*	0,289	*0,205*
	NANS-PNS	0,472	*0,048**	-0,600	*0,088*	0,043	*0,854*
	CBV-ANS	-0,037	*0,883*	0,717	*0,030**	0,682	*0,001***
	BV-CA	-0,492	*0,038**	-0,017	*0,966*	-0,117	*0,614*
	AC-ANS	0,113	*0,656*	-0,750	*0,020**	-0,440	*0,046**
CAla-BV	**CAla-N**	0,171	*0,499*	-0,267	*0,488*	0,003	*0,991*
	AAla-C	0,328	*0,184*	-0,450	*0,224*	0,334	*0,140*
	NANS-PNS	0,020	*0,938*	-0,017	*0,966*	0,235	*0,306*
	CBV-ANS	0,280	*0,260*	-0,233	*0,546*	-0,313	*0,167*
	BV-CA	-0,104	*0,680*	0,300	*0,433*	-0,404	*0,069*
	AC-ANS	-0,109	*0,668*	0,417	*0,265*	0,689	*0,001***
Ala-BVAlp	**CAla-N**	0,305	*0,219*	0,500	*0,170*	-0,049	*0,832*
	AAla-C	0,249	*0,319*	0,517	*0,154*	0,327	*0,148*
	NANS-PNS	-0,175	*0,488*	0,000	*1,000*	0,042	*0,856*
	CBV-ANS	0,208	*0,408*	0,483	*0,187*	-0,254	*0,266*
	BV-CA	-0,026	*0,919*	0,067	*0,865*	-0,302	*0,183*
	AC-ANS	-0,169	*0,504*	-0,050	*0,898*	0,517	*0,016**
CAlaAlp	**CAla-N**	0,034	*0,893*	-0,400	*0,286*	0,036	*0,878*
	AAla-C	0,173	*0,493*	-0,050	*0,898*	0,109	*0,640*
	NANS-PNS	-0,057	*0,823*	0,183	*0,637*	0,141	*0,542*
	CBV-ANS	-0,001	*0,997*	-0,467	*0,205*	-0,329	*0,145*
	BV-CA	0,164	*0,514*	0,300	*0,433*	-0,160	*0,487*
	AC-ANS	-0,030	*0,906*	-0,017	*0,966*	0,554	*0,009***
SANS-PNS	**CAla-N**	0,254	*0,309*	-0,100	*0,798*	-0,237	*0,301*
	AAla-C	-0,134	*0,596*	-0,417	*0,265*	0,246	*0,283*
	NANS-PNS	0,551	*0,018**	0,333	*0,381*	0,086	*0,712*
	CBV-ANS	-0,229	*0,360*	-0,250	*0,516*	0,557	*0,009***
	BV-CA	-0,184	*0,465*	0,617	*0,077*	-0,357	*0,112*
	AC-ANS	0,151	*0,551*	-0,050	*0,898*	-0,237	*0,302*
SC-BV	**CAla-N**	0,189	*0,452*	-0,033	*0,932*	-0,040	*0,864*
	AAla-C	0,117	*0,644*	-0,300	*0,433*	0,174	*0,450*
	NANS-PNS	0,282	*0,256*	0,033	*0,932*	0,171	*0,459*
	CBV-ANS	0,078	*0,760*	0,267	*0,488*	0,705	*0,001***
	BV-CA	-0,204	*0,417*	0,417	*0,265*	0,096	*0,680*
	AC-ANS	-0,260	*0,298*	-0,467	*0,205*	-0,585	*0,005***
CN-ANS	**CAla-N**	-0,011	*0,964*	-0,417	*0,265*	-0,133	*0,565*
	AAla-C	-0,020	*0,938*	-0,467	*0,205*	-0,267	*0,242*
	NANS-PNS	-0,243	*0,331*	0,100	*0,798*	0,045	*0,847*
	CBV-ANS	-0,022	*0,932*	-0,333	*0,381*	-0,098	*0,672*
	BV-CA	0,460	*0,055*	0,600	*0,088*	0,626	*0,002***
	AC-ANS	0,121	*0,632*	-0,117	*0,765*	-0,266	*0,243*

r:Spearman's coorelation coefficient   *p<0,05   **p<0,01

6.5 Assessment of 3D Model of Reconstructed Vomer Bone

The vomer volume measurements of all study cases showed a statistically significant difference (p <0.01). According to the bilateral statistical comparisons; Vomer bone size measurement of C groups was (2249,77±457,69) mm3 significantly higher than A group (1253,64±263,46) and B group (1656,64±477,78) measurments were shown with a high significant differences (p <0.001) as in Table 6.17.

Table 6.17: Assessment of 3D Model of Reconstructed Vomer Bone

Volume		Type			*p*	
		A (n=36)	**B (n=18)**	**C (n=42)**		
Face vol	*Min-Max (Median)*	313310,6-568871,2 (359786,3)	307725,2-465322,3 (421677,7)	307725,2-568111,4 (493231,8)	*0,001***	C>A=B
	Mean±SDs	411827,53±94680,17	395089,79±54770,1	482389,16±74392,88		
Vomer vol	*Min-Max (Median)*	888,1-1784,3 (1208,6)	993,6-2119,7 (1889,5)	1073,6-2843,3 (2090,3)	*0,001***	C>B>A
	Mean±SDs	1253,64±263,46	1656,64±477,78	2249,77±457,69		

Kruskal Wallis Test   **p<0,05*   ***p<0,01*

	Type		
	A-B	**A-C**	**B-C**
Face vol	*0,941*	*0,004***	*0,001***
Vomer vol	*0,005***	*0,001***	*0,001***

Mann Whitney U Test   **p<0,05*   ***p<0,01*

7. DISCUSSION

Midfacial deficiency or hypoplasia has become an important concept for orthodontists and maxillofacial surgeons due to wide range of facial discrepancy. The Class III incisal relationship is more likely a skeletal deformity than a dental problem (Iwasaki et al.,2009, 2011 and 2014).

The vomer morphometry represents a central key of midfacial growth and has a significant morphogenic influence on the etiology of controversial clinical concept (Latham RA 1969; Jerolimov, Keros, Bagić and Lazić 1999; Komar 1986; Wealthall and Herring 2006; Holton, Yokley and Figueroa 2012, Hur et al. 2016).

Several clinical manifestations of dentofacial malformation patients demonstrated the vomer bone biodynemic interstitial forces as a functional growth modulation and a compensation detector. These normal forces are direct for better facial integrity and preserve the craniofacial compartment in acceptable outline to some extent (Sato SA 2001). There were many inaccuracies perpetuated to its identification, location, size, morphology and function (Kjaer and Fischer 1996; Sadler TW 2011).

Some researchers have partially described the role of the vomer bone in the development of the maxillary complex. That has a possible influencing factor in the lowering of the hard palate or in the distribution of masticatory forces to the cranial base (Friede H 1978; Kimes et al. 1992; Hansen et al. 2004, Lilja et al. 2006). However, its influence on the morphology of the craniofacial architecture still remains unclear (Barteczko K 2004; Hilloowala and Kanth 2007). Most of the information from previous studies about craniofacial interrelations was obtained from 2D cephalometric images which has a limitation in the identification of this structure. Nowadays, the development of the Cone beam computed tomography systems and its applications in craniofacial diagnosis provide new alternatives to evaluate the morphology of the craniofacial skeleton in a three-dimensional way with great accuracy (Adam et al. 2004; Korbmacher, Kahl-Nieke, Schöllchen and Heiland 2007; Lagravere et al. 2008; Muramatsu et al. 2008, Periago et al. 2008; Van Vlijmen, Berge and Swennen 2009).

Recently, cone beam computed tomography (CBCT) systems have been developed specifically for the maxillofacial region evaluation. Many devices are capable of imaging most skull anthropometric landmarks used in cephalometric analysis. Time and dose requirements have been suggested to be the same as other dental radiographic modalities. High dimensional accuracy an reality have been reported for maxillofacial CBCT in measurement of facial structures that assissted the CBCT imaging shifting from 2D cephalometry to 3D visualization of craniofacial morphology (Adam et al., 2004; Periago et al. 2008).

Three dimensional image analysis is being used for diagnosis, treatment planning and evaluation of treatment outcomes (Lagravere et al. 2008; Muramatsu et al. 2008). The main objective of the evaluation and measurements on the obtained images is to clearly identify the size, shape outline and relationship of the craniofacial structures to each other and to determine the degree of deviation from normal toward anomaly or dysmorphology (Olszewski and Reychler 2011; De Jong and Breugem 2013; Ren et al. 2014,2015).

 For this purpose, 3D CBCT images were analyzed between the dates of April 2016 to November 2017 in Marmara University, Faculty of Dentistry, Department of Oral and Dento-Maxillofacial Radiology. A total of 96 patients (45.8%, n = 44) were female and 54.2% (n = 52) were male. The ages of the cases ranged from 15 to 30 with an average of 23.23 ± 3.92 years. When the types into three groups were classified according to purpose of this study. There were type (A) 37.5% (n = 36), type (B) 18.8% (n = 18) and type (C) 43.8% (n = 42). All study subjects were white, Caucasian Turkish population and patients were selected respectively. 3D CBCT data obtained from the analysis relation between the vomer bone and different structures are described with a significant difference and correlation at a different level of assessment (cranial, midfacial and vomer bone) using definite variable parameters using Standard anatomical points references (Basili et al. 2009; Ren et al. 2015).

Firstly, cephalometric landmarks were determined then the linear references and angular inclination variable were measured at different level using Mimics19.0 tools for the description of shape outline of vomer bone in a comparison among three different study groups.

Secondly, 3D model of the reconstructed vomer bone for the recognition of size differences among study groups using volumetric mask tools of Mimics 19.0.

According to the statistical analysis of this study parameters by significant difference and correlation, our parameters variables of vomer bone give a clear image description toward relevant relation of vomer bone with midface hypoplasia in class III Malocclusion.

Cephalometric analysis methods of measuring linear and angular skeletal parameters of vomer bone and their relations with each other (Dhopatkar, Bhatia and Rock 2002; Van Vlijmen, Berge and Swennen 2009).

In this study, 21 linear and 16 angular palnes of 13 skeletal landmarks in three level analysis were used. Attention is drawn to the fact that all cases with Class III malocclusion have same angle malocclusion profile within anterioposterior diminished and retrusion maxilla with long face skeletal relationships range from mild (edge to edge relation) to sever midface hypoplasia (retrusion) (Ngan P 2005,2006).

Formerly, in order the cephalometric analysis to be used in a realistic diagnosis and treatment planning, the individual values must be compared with the average face pattern standars and the differences should be interpreted (Periago et al. 2008, Lagravere et al. 2008).

For this reason, Class I normal occlusion from the first time was used as inclusion standard normal group orthopedic analysis. In order to determine the size and location of the craniofacial structures in different cephalometric analysis methods, the reference cephalometric points of this structure, which are preferably highly reproducible and high in detection are used. While cephalometric points may sometimes be directly marked points, they can sometimes be superposition points seen in the cuts of the lines formed between the points or in the lateral cephalograms (Korbmacher, Kahl-Nieke, Schöllchen and Heiland 2007). The choice of cephalometric points used in this study has not been based on superposition and sagittal points that occur in the lateral cephalogram but must be detected accurately in the three-dimensional image (Adam et al. 2004).

Cephalometric analysis is three-dimensional object with two-dimensional projection images. In this study cephalometrics were measured without magnification correction; the shapes of the anatomical structures in the regions most affected by magnitude and the

magnitude of the influence of the angular and linear measurements have been tried to be more clearly defined formerly by operators (Van Vlijmen Berge and Swennen 2009).

Conventional cephalometrics tow dimenssional analysis can give a general idea of the problem in most cases. However, unambiguous craniofacial deformities are not clearly diagnosed and treatment planning alone suffices. Especially in Orthognathic surgery planning, the position, size and relationships of craniofacial structures need to be determined more precisely. In order to solve this problem, although many investigators try to make three-dimensional reconstructions using two-dimensional posteroanterior and lateral cephalograms, the reproducibility of measurements and sensitization has not been adequately used (Muramatsu et al. 2008).

In this study, unlike a conventional cephalograms, CBCT images without errors, such as superposition of anatomical structures or different magnifications in different regions, have been used frequently for the purpose of examining craniofacial structures (Halazonetis DJ 2007).

In the initial image visualization with CBCT, using three sectional view of coronal, sagittal and axial section data with three-dimensional reconstruction, and the investigators evaluated these images in terms of using orthodontic points (Materialise 2009; Li et al. 2016).

In studies where cephalometric CBCT 3D images are compared with between the two-dimensional cephalometric radiography technique; More accurate results were obtained from three-dimensional CT images (Park et al., 2012,2013; Scolozzi and Herzog 2017).

Togashi et al 2005 also studied the effects of linear measurements on three-dimensional CT images on whether they were affected by the head position, as well as the effects of two-dimensional cephalograms. CT images of a skull taken at 1 mm, 3 mm, 5 mm and 7 mm slice thicknesses and different angled head positions were examined in three dimensions. Changes in the head position do not affect linear measurements on three-dimensional CT images. However, as the slice thickness increases, it is indicated that some measurement errors have occurred in some linear measurements (Hajeer et al. 2004).

CBCT images linear and angular measurements made in the lateral cephalograms are reported to be influenced by the unfavorable head position (Trpkova et al. 1997; Kau et

al. 2009). The choice of that on CT images quality, the linear and angular measurement values, are sensitive, considering the cases head (N-ANS) plane perpendicular to the Frankfurt plane ground plane without initial rotation) as a midsagittal plane in our study, although the studies were conducted that slight head movement not affected the initial position and rotation of the CT images because of stabilization of natural head posture with ear rods were controlled (Schatz et al. 2010).

The definition of the reconstructed vomer bone slightly differs from that defined by Basili et al. (2009), that a constructed vomer bone extended forward to the ANS point. The reason for this was to obtain a clear landmark and excellent reproducibility in positioning them, but in that way, the reconstructed vomer bone apex (C) point was extended more than its real normal anatomical border. So in this study we adjust apex point (C) over incisal crest of maxilla in sagittal view and to be over nasopalatine orifice superiorly that anatomically well-defined than that of before to be prevent superimposition of ANS and C points anteriorly and reveal outline of vomer bone clear. This must be considered in the interpretation of the results (Fawcett E 1911; Farkas LG 1994; Sperber G 2001).

On the other hand, new studies using 3D facial bone CT scanning provides sagittal images routinely and can be demonstrate an excellent view of the nasal septum outline by distinguishing the border of the bony structure at minimal cost (Moore et al. 2005).

Basili et al. (2009), Foster and Holton (2015) and Hur et al. (2016), have shown the vomer bone more highlighted and interesting interrelations within craniofacial architecture using 3D CBCT analyis. This bone usually remains hidden from our cephalometric analysis, because of the difficulties in identifying it in a two-dimensional X-ray.

The application of the three-dimensional Computerized Tomography, and the possibility of creating 3D volumetric digital skull reconstruction provided the opportunity to analyze the skull, with great accuracy and reproducibility by applying a different computer based software, like the one used in this study. The analysis of the structures was developed by defining landmarks and planes (Muramatsu et al. 2008).

These were extracted initially from the traditional 2D cephalometric analysis, allowing us to compare the data with other study results; and some of them redefined to a three-dimensional environment, in order to be able to correlate anatomical structures. To

emphasize the role of vomer bone as a midfacial strut or force modulator for compensating the collapse of the midfacial complex (Adam et al. 2004; Lagravere et al. 2008; Periago et al. 2008; Van Vlijmen Berge and Swennen 2009).

Traditional two-dimensional radiograph (2D) refers to lateral cephalic radiography, panoramic radiography, and posteroanterior cephalic radiography analyses are used to measure the shape, size, position, and orientation of the different facial units are projected onto a single sagittal plane. Nonetheless, the information that can be gathered from them is limited. In determining position, the information is limited to the anterioposterior and vertical dimensions. In determining size, the parameters are limited to length and height. However three-dimensional (3D) images taken from computed tomography (CBCT) can be a solution and be effective in diagnosing and treating maxillofacial deformities.

A clear visualization of the vomer bone role was determined by two categories:

1) Shape outline changes by linear and angular measured values changes (landmarks analysis):

For all study groups, all linear measurements were shown a statistically significant at three different levels (cranial , midface, vomer) for of 21 linear parameters.

For all study groups ; all angular measurements almost shown a statistically significant at three different levels (cranial , midface, vomer) for almost of 16 angular parameters were used.

The result of this study was parallel with study of (Dibbets JH 1996; Polat and Kaya 2007; Lee and Liao 2013; Panainte, Suciu and Mártha 2017), that they has been shown that the role of the cranial base in the aetiology of class III malocclusion resulting in midfacial deficiency but they did not overlook completely and there were some doubt has been cast on the association between the Angle's classes difference and facial morphology correlation. Therefore, a rigorous quantitative analysis of the spatial organisation of size and shape change during class III morphogenesis is warranted.

As well as there were a high significant differences of occlusal plane (ANS-PNS) and interocclusal base angle (ANB) with linear parmeters of vomer bone and its angular inclination for all study groups. That finding was emphasized the result reported by (Dhopatkar, Bhatia and Rock 2002; Periago et al.2008; Tanaka and Sato 2008). They have

been emphasized there were a significant differences clinically between (ANB) measurements and midface or occlusal maxilla plane length (ANS-PNS) variable of different Class III Angle malocclussion in comparison to norm.

In total of statistically significant differences parameters ; There were some parameters in each level of analysis were no significant differences among study groups.

Among 21 linear parameters; only 11 parameters were highly significant and positively correlation among all study groups. whereas 16 angular parameters; 12 angular measurements were highly significant difference and some negatively correlation with midfacial (C) groups severity.

Within limitation of this study sample size and the retrospectivity, later studies have described the relation between cranial and facial profile of different malocclusions classes with large sample size and prospectivety analysis. However; there were no clear significant differences about the shape outline anlysis of craniofacial skeleton with (ANS-PNS) plane and interocclusal plane angle (ANB) for describing the facial parameters significant differences (Kerr et al.1993; Dhopatkar, Bhatia and Rock 2002; Tanaka and Sato 2008).

Furthermore, there was no significant difference of age mean among the three groups in the vomer bone. Based on the role of the vomer in the maxillary growth of the cleft palate, malocclusion and craniofacial discrepancies.

The age distribution of the study groups varied when the nasomaxillary complex was examined. Some studies have chosen patients with a very broad age range, and some studies have examined patients in certain age groups and some other not mentioned absolutely.

The age analysis of this study related litreature review, Basili et al (2009), examined patient in the adulthood; Botti et al (2017); in the childhood, Kim et al (2010), in an average age of 42 years; Foster and Holton (2015), examined mices of the age between (9-15) weeks; Singh et al (1998), examined sample age between 5-11 years old; Peter et al (2010), examine the cases of 16 years old; Olszewski et al (2011); determined the cases of 7 years old; Langford et al (2002), examined children between 1 month and 15 years of age; Mayer et al (2009), examined samples between ages 18 and 86 of ages; Agrawal et

al (2012), examined cases under the age of 2 years; Van loon et al (2010), examined within the age over 12 years; Teke et al (2007), examined cases between 20-50 years of age; Chovalopoulou et al (2013), examined patient in the adulthood age; Mayordomo et al (2013), examined between 15-40 years of age; Ren et al. (2014) and (2015), examined between 3-25 years of age; Uygun et al (2016), examined between 21-50 years of age; Yang et al. (2016), age of mixed and primary permanent dentitions children; De Menzes et al. (2011), reported that the ages of twin 10 years old were examined; Sandikcioglu (2009), reported the age of examined fetus after spontaneous ablation; Suri et al. (2008), examined within the mean age of 11.59 ± 1.34 years; Liao et al. (2013), examined patients at 20 years old; Choi et al (2012), examined between 19-43 years old; De Jong et al. (2013) examined within the mean age of 4 month; Pelo et al. (2009), examined the age between 18-43 years old; Schneiderman et al. (2009) examined the age over 15 years old of female and 17 years old of male.

In this study, considering the completion of growth development of the midface complex and the vomer bone inclusively. These consieration took in regard to determine the outline alteration away from anatomical variation or incomplete growth confessional concepts. So the patients over 15 years of age were preferred and Included. The mean value of age was 23,23±3,92 years for this study patients. When considering that, There were no significant differences between age groups as this study was parallel and conducted by Choi et al. (2012), Schneiderman et al. (2009), Mayordomo et al. (2013), Teke et al. (2007), Hur et al. (2016), Basili et al. (2009), Uygun et al. (2016) Holton et al. (2015), Suri et al. (2008), Pelo et al. (2009), Olszewski et al. (2011).

Liao et al. (2013), stated that there was a positive correlation between the age groups and the vomer bone dimensional changes in relation to midface components. They evaluated separately in specific age groups at 20 years old, they found no relationship between them. Sandikcioglu et al. (2009), concluded that the maxillary growth and the vomer bone volume with an increase of fetus age; there was an association between them.

Hur et al. (2016), observed that when the age increases, the vomer bone proportion had no significant relation among three different study group like this present study. This is

thought to be due to the fact that the study Hur et al. groups consisted of children and adult individuals with an upmost level of age intervals (13-105) years used a dry skull cadavers. Basili et al. (2009), Foster and Holton (2015), Uygun et al. (2016), Ren et al. (2014 and 2015), Singh et al. (1998), reached the conclusion that the vomer bone proportion varies in different groups with different sex but there were no age related changes.

In this study, in accordance to the findings of De Jong et al. (2013), Uygun et al. (2016), Ren et al. (2015), Hur et al. (2016) results. No statistically significant relationship between age and different study type groups (p> 0.05) were found.

When the gender was evaluated in this study, There were parrell result to study of Liao et al. (2013), Uygun et al. (2016), De Jong et al. (2013), Botti et al. (2017), Kim et al. (2010), Schneiderman et al. (2009), Pelo et al. (2009), Langford et al. (2002), Teke et al. (2007), Suri et al. (2008) and Choi et al. (2012).

It was thought that the reasons for this difference in age and gender distribution were due to the retrospective nature of these studies and concept of manner to focus the surgical outcome of clefts accompanied with/without malocclusion.

This study is a retrospective and a careful attention has been paid to the balanced distribution of the male to female ratio when the patient were selected. The study group consisted of 96 patients 44 female (45,8%) and 52 male (54,2%)

Wendl et al. (2017), Chovalopoular et al. (2013), Mayordomo et al. (2013) found the anterior maxilla part had a significant volume differences evaluated in the males with more deep and elongated anteriorly than the females.

Basili et al. (2009), Agrawal et al. (2012), Hur et al. (2016) reported the same result by evaluating the nasal septum components in relation to the vomer bone proportions.

In this study accordance to the findings of Wendl et al. (2017), Mayordomo et al. (2013), Basili et al. (2009), Agrawal et al. (2012), Hur et al. (2016), represented that the total maxillary variable in relation to the vomer bone dimensional changes of males significantly higher than females (p<0.01) were found.

In recent studies evaluated the vomer bone relation with the palatal deficiency of the healthy maxilla bone. Agrawal et al. (2012), Foster and Holton (2015), Hur et al. (2016), compared the maxilla bone of the control group with clefts pediatric of sex-matched

patients. As a result with long-standing cleft defects, The vomero-maxillary volumes were found to be affect the midface deformity. They also found that cleft caused an increase in bone thickness posteriorly, which in turn caused anterior bending and deviation of the posterior nasal border.

Ren et al. (2014, 2015), assessed the relationship of the palate-vomeral development of 19 female and 11 male patients in centric occlusion before the surgeries with submucosal clefts. Also Murthy et al. (2016), measured the Pre-maxillary complex morphology in bilateral cleft and deviated pre-maxilla features. Both of them as a retrospective cross-sectional study reported the morphology of midface complex and the vomer bone. They determined that there was a significant relationship between the vomer bone anterior deviation and the premaxilla bone. On this highlighting, this study revealed parallelism to these studies by highly significant differences between the vomer angular inclinations (CBV-ANS, Ala-CBV, C-Ala BV) and backward retardation.

Botti et al. (2017), measured the degree of the anteroinferior impaction angle of the vomer bone at the incisive canal using CT scans. As this study measured the impaction angle of anterior vomeral area (Ala-CBV) in relation to the midface defecincy rather than that in Botti's study focused on the differences of vomeral outline in healthy individuals.

For this reason, inclusion criteria of the present study were being with no craniofacial anomalies, no pathological changes such as fractures, inflammation, cysts, and tumors in the midface area, no surgical treatment in the nasal region were included in the study. It was taken into account the close relation of the nasomaxillary complex with the teeth, attention has been paid to ensure that all teeth except the 3rd molar teeth are present and missing teeth are missing. Since the teeth and jaws changed their relationships with each other, the cases were selected from those who had not received any orthodontic treatment. Patients with systemic records and radiographic review of nasal treatments were not included in the study group, thus ensuring that all individuals in the study group consisted healthy individuals and patient with orthodontic and orthognathic demand.

Numerous methods have been used to measure the volume of nasomaxillary compartments. Palatine process, Septal cartilage, Ethmoid, Sphenoid and the vomer bone measuring methods used in conjunction with advancing technology have been developed.

Initial studies were done using dry heads or by injecting various materials into the cadaver. The major disadvantages of dry head measurements are; Age and gender are unknown and there is destruction of vomer border.

In cadaver measurements, because of the invasive nature of the materials used, they are not applicable to living organisms, and some midfacial complex anatomical structures not appear clearly and the difficulty of its reproducibility (Foster and Holton 2015).

Wendl et al. (2017), performed his study using a conventional 2D imaging system (ProMax 2D) in 38 Class III patients treated with a chincup were retrospectively analyzed. A greater skeletal discrepancy between maxilla and mandible and anterio-posterior midface dysplasia was appeard.

The deficiency of conventional radiographs in nasomaxillary complex imaging have been tried to be solved by using of three dimensional imaging methods (such as CT, MRI, CBCT). With these imaging methods, anatomical structures can be evaluated in different planes (coronal, axial, sagittal, cross-sectional). In addition, one of the greatest advantages of three-dimensional imaging methods is that the measurements made on acquired images are reproducible without harming the living organism according to other invasive methods (Adam et al. 2004).

Many studies have been carried out on the volume measurement of midface units in CBCT, considered as the gold standard for surgical, anthropological and dentoalveolar evaluation. Some of these studies obtained information about the volumes of the midface area skeletal units using various formulas on the images and some computer software's on some parts (Langford et al. 2002; Ren et al. 2014, 2015; Botti et al. 2017).

Ren et al. (2014) measured the volume of was to visualize bony defects of the palate and vomer in submucous cleft palate patients (SMCP) by three-dimensional (3D) computed tomography (CT) reconstruction and to classify the range of bony defects. The images were taken by using spiral CT. 3D reconstruction models of the palate and vomer bones were created. The sagittal extent of the bony cleft in SMCP was classified into four types. The extent of the vomer defect was classified into three shape types that significant differences highly in sever type of hard palate defects in SMCP. The association of clefts insufficiency with anatomical malformations of vomer may be complex but it is appear

obviously by 3 reconstructed model that resemble our findings of vomer bone size variation among different study groups in relation to malocclusion severity.

As a retrospective study, Botti et al. (2017), measured the vomer-palatal junction of anterior maxilla to evaluate the degree of impaction of the vomer in the incisive canal (IC) by using CT scans. Thirty-two out of a series of 506 nasal sinus CT scans were used. As a result, 31 of the 32 vomer images were impacted in the IC. In the case of a Y-shaped vomer, the length of the vomer was impacted in 41% of the length of the IC. In the case of I-shaped vomers, the length of the vomer was impacted in 41% of the length of the IC. The only vomer that did not impact into the IC was Y-shaped. In regard they confirmed that the vomer is deeply impacted in the incisive canal.

Langford et al. (2002) firstly reported the volumetric maxillary deficiency in form, position, and development of children with prominent features of craniosynostosis. Maxillary volumes were larger in boys at all ages. However, the pattern of nasomaxillary growth in boys and girls was not similar in volume (boys: mean maxillary volume = 56.55 cm", girls: mean maxillary volume = 40.68, p< 0.001). These findings were in parallel with this study result that volume size of the vomer bone model was larger in male than female in different groups.

The first study has been used CBCT computer software for volume evaluation of maxillary compartments was conducted by Agarwal et al. (2012). They determined the analysis of the maxilla in unilateral cleft lip and palate. The contribution of maxillary hypoplasia to the etiology of this deformity has often been implicated for surgical treatment. They assessed the relevant maxillary parameters of length, width, height, depth, and volume in patients with UCLP and compare the parameters of the cleft and noncleft sides. The volume of each maxilla was calculated on 3D reconstructions using the technique of manual segmentation, which allowed complete reconstruction of the right and left maxilla individually. They emphasized that anatomy of the maxillary asymmetry existing in UCLP and underlines the importance of correcting the bony deficiency by appropriate techniques to harmonize the results of rhinoplasty.

Mayordomo et al. (2013), aimed to use CBCT to analyze the available bone volume in the palatine process of the maxilla (PPM), which is a potential source of bone grafts. The

study comprised 6 women and 14 men (mean age 39.4 ± 11.5 years). Calculated bone volume averaged as 2.41± 0.785 cm3. The palatine process of the maxilla contains a considerable bone volume (2.41 ± 0.785 cm3). As a result, they regarded the anterior maxilla palatine as powerful area for the regeneration of maxillary atrophy.

Pelo et al. (2009), Langford et al. (2002), Teke et al. (2007), Agrawal et al. (2012), Oliveira et al. (2016), as anatomical outline morphometry studies, were used Multiplanar CT scan of helical C-arm and MRI device. In almost of a volumetric analysis of hard tissues accompanied with special consideration to surgical and esthetic demand.

Schneider et al. (2009), De Menzes et al. (2011), Choi et al. (2012), Mayordomo et al. (2013), Yang et al. (2016) emphasized the differences of volumetric measurements using proper image acquisition and segmentation by certain software.

Schneider et al. (2009), their measurements were made with i-CAT scan, version 1.0.3.4 or higher (Imaging Sciences International). De Menzes et al. (2011), Images were acquired using i-CAT scanner (Imaging Sciences International, Hatfield, PA, USA).

The available bone volume in the palatine process of the maxilla (PPM), which is a potential source of bone grafts. 20 CBCT scans were evaluated from the most caudal axial slice of the PPM and the bony surface was calculated cranially up to the nasal floor (Mayordomo et al. 2013).

Teke et al. (2007), Chovalopoular et al. (2013), examined healthy Greek /Turkish population in a forensic scope of view for the sexual dimorphism determination using CBCT and MRI images. All other studies almost represented the volumetric analysis of certain bony compartment that subjected on clefts patient and in less on Class III malocclusion with maxillary deficiency.

The three dimenssional analysis of the vomer bone shape and size were not definitely evaluated in different skeletal patterns up to this present study time. However a lot of studies determined the vomer bone outline inclusively by measuring the widest dimensions (width, length, height) of the maxilla, nasal and palatine bone compartements in all three dimenssion but not the concentrated the vomer bone breifely.

Langford et al. (2002), used the MRI for the maxillary volumetric analysis of children from 1 month up to 15 years old because its ideal imaging method with no risk of the ionizing radiation and with multiplanar assessment.

Rafferty et al. (2006), argued that the CBCT was developed to acquire multiple projections in the rotation about a subject. Initial imaging used to investigate the system's spatial resolution in 3D image reconstruction. Subsequently bone dissection was performed on five cadaver heads using the modified C-arm as an image guidance system. They concluded CBCT provided submillimeter accuracy at high speed with low radiation dosage to offer utility of intraoperative imaging system.

In recent years, CBCT has been able to achieve high-resolution images with low doses, and the end result can be preferred to CT.

A significant reduction in radiation dose using CBCT has been shown by Mayordomo et al. (2013). They considering the incisive canal to the points of the posterior bone boundary. A three-dimensional (3D) image of the delimited zone was constructed and analyzed using 3D imaging software. The study calculated bone volume averaged of the palatine process of the maxilla and regarded as a potential donor site for the regeneration of maxillary atrophy.

The reasons for choosing CBCT instead of CT in both studies were; CBCT is described having less radiation dose than CT, less artifacts and less cost. At the same time, the fact that patients are in a sitting position during shooting is very important in airway assessments. Supine position led to morphological changes in the airway indicating that gravity affects the soft tissue surrounding the oropharyngeal cavity and contribution of the midfacial complex (Adam et al. 2004).

Various software programs such as MIMICS, Simplant pro-crystal, Dolphin, Viterea console, ProMax Planmeca, Amira 5.3.3, Vision FMC, GVCM and ITK-snap which can be used of some with 3D/2D imaging methods such as CT and MRI before, are also compatible with CBCT images. These software provide a great advantage especially for treatment planning and preoperative-postoperative evaluation of orthodontic and surgical treatment patients (Kim et al. 2013; Hur et al. 2015; Ren et al. 2016).

Kim et al (2010), Liao et al (2013) used 2D image analysis cephalometrics to determine the maxilla growth in relation with particular component of vomer and palatine process of anterior maxilla by using different software ProMax Planmeca, or commercial program like Vision FMC with variant results according to linear references estimation and algorithmic relationship of parameters used. Wendl et al (2017), recently stated that it was possible to evaluate the maxillary complex with segmentation via 2D CBCT analysis by using ProMax Planmeca software.

However; the 3D image analysis was used by Botti et al. (2017); Olszewski et al. (2011); Ren et al. (2014,2015); Fakhry et al. (2013); Agrawal et al., (2012); Oliveira et al. (2016); Mayordomo et al. (2013), to evaluated the volumetric changes of maxilla components totally or partially like the palatine process or the vomer-palatine area in clefts patients using different software like Simplant pro-crystal, Viterea console, Amira 5.3.3, Vision FMC, GVCM and ITK-snap rather than using a MIMICS software.

Olszewski et al. (2011), Hur et al. (2016), Yang et al. (2016), have used MIMICS software to evaluate the morphometric pattern alteration and volumetric change of particular bone like the nasal septum, ethmoid, maxilla, palatine process in relation to craniofacial discrepancy mostly in clefts patients. As in those study, the thresholds have chosen with a minimum value of (-1024) HU and a maximum of (1064) HU in the software to subtract the hard tissue from surrounding.

This study was suggested that the evaluation of the dimensional or volumetric size change of the midfacial complex under the highlight of all literature. Hur et al. (2016) and Ren et al. (2014,2015), were estimated some of this study principal like points definition and compartements segmentation but they were more concentrated toward clefts rather than malocclusion patients.

The volumetric measurements of the vomer bone were designed in parallel with the study of Basili et al. (2009), Ren et al. (2014), Hur et al. (2016) that performed by using MIMICS 19.0 with the same values range of thresholds. The midfacial compartment preliminary cropped from other facial compartment preparing to subtract the vomer bone from other midface bones like ethmoid, palatine, sphenoid, and maxilla absolutely using the tools of splitting with color identification. The borders of the vomer bone outline were determined

using defining anatomical landmarks themselves used in linear and angular evaluations. Thus, the separation of the vomer bone from neighboring structures was ensured.

Because of the anatomical position of the vomer bone and their association with the maxillary dentofacial area relation, a lot of studies were investigated the obvious relationship with dental and skeletal malocclusion that have been performed by Singh et al. (2001), Basili et al (2009) and Foster and Holton et al. (2015).

According to the central position of the vomer bone within midface complex, the classification of malocclusions made by taking the vomer bone inclusively to be evaluated more accurately. Basilli et al. (2009), stated that the skeletal evaluation made only according to the cranial base angle guidelines does not give a clear information about the situation of the final facial esthetic. Because the grouping of cluster appear with different features of Angle class III malocclusion. For example, class III patient's maxilla are retruded lead to the class III malocclusion with midface hypoplasia but with different pattern or clustering.

Finally, a virtual 3D CBCT reconstructed models of both full skull and vomer bone can be used instead of 2D conventional cephalometric radiography (Muramatsu et al. 2008).

Although; There was a statistically significant differences between the type groups and the volumetric sizes (p<0.01), also with the retrusion sagittal position of the midface in relation to the vomer bone. The ANS-PNS value gives the information only about the 2D two dimensional antero-posterior length of the maxilla and related compartements but not give real 3D accuarte image of dentofacial anaomalies. It is thought that this may be due to the fact that the vomer bone size of those with low ANS-PNS values are more sever midfacial deficiency. Also the impaction angle of the vomer bone (Ala-CBV) and anterior vomer-palatal base backward inclination (CBV-ANS) in relation to ANB angle of malocclusion emphasize a high interrelation of midface compartement with the vomer bone. However, the vomer bone 3D reconstructed model shown a high significant in males with more elongations than females. That response of the elongation and extension has a real evidence about the compensating role of the vomer bone that modulate the dimensional changes of the facial profile in midface area accompned Angle class III malocclusion.

8. CONCLUSIONS

Within the limits of this study, the vomer bone was considered to be directly related to maxillary complex and midface compartements totally because of its spatial anatomical interrelation. Three-dimensional analysis of the vomer bone changes in relation to the midfacial hypoplasia pattern in a class III malocclusion groups proved the hypothesis of functional compensation of this study. The vomer bone dimensional shape changes and size derangement varied in different skeletal discrepancy.

There was no relationship between age and different study groups parameters.

There were significant differences of the vomer bone dimensional outline (shape) and volumes (size) in different skeletal facial pattern and it was found highly severe in males than in females.

Based on the findings of this study, it can be concluded that:

1. The exact morphometry of the hard facial tissue was accompanied the dentofacial discrepancy accurately analysed by using 3D analysis software like Mimics.

2. The dimensional changes of the vomer bone in relation to Class III malocclusion were correlated with the midface skeletal changes. This changes were presented not only in the orientation of the vomer bone to be displaced and diminished but also they were in volumetric size changes to compensate and preserve the midface contour.

3. The effect of the vomer bone spatial variation on the midface complex was clear in accordance with the occlusal midsagittal plane and interocclusal angle.

4. The dimensional changes of vomer bone could not be evaluated as an isolated manner but they should be determined in relation to different parts of the face. Thus, different malocclusion patterns could have an effect on distinct area represent by (C) point anteriorly and backward inclination of vomer bone.

5. Morphological changes of the vomer bone in relation to the midfacial deficicency were observed using multiple 3D analysis of skeletal landmarks (C, BV, Ala and Alp) and should be considered for a detailed diagnosis of dentofacial malocclusion.

6. In class III malocclusion patients, volume or size measurement differences related to the different dentofacial units were more frequently identified in males with severe midfacial hypoplasia and less often in females.

7. Subjects classified as sever hypoplasia dentofacial pattern seemed to have skeletal changes more than mild dentofacial pattern for compensation by surface modulations and bone remodeling of the vomer bone response. .

8. Although class III malocclusion patients have different morphometric patterns for different populations and gender, size and shape outline measurements of the vomer bone region with the absolute mean ages showed no significant differences.

9. At the occlusal anterior levels; hypoplasia was apparent with meaningful changes. In the vomer anterior apex of C point area in relation to both A, ANS points revealed the inclination backward with severe pattern of midfacial hypoplasia.

10. The comparison of different skeletal dentofacial pattern type group's size and shape measurements of the vomer bone segments provided evidence of midface hypoplasia pattern severity in the craniofacial region. To create an ideal treatment plan in malocclusion patients, not only the angle classification in general concept but also the morphometric analysis for subgroups with different dentofacial pattern should be evaluated.

In conclusion, the multifactorial nature of the vomer bone on the surrounding dentofacial parameters needs to be evaluated in well designed future prospective studies for better understanding of the contribution of each factor to the final result.

9. REFERENCES

Ackerman JL, Proffit WR, Sarver DM. The emerging soft tissue paradigm in orthodontic diagnosis and treatment planning. Clinical orthodontics and research, 1999, 2.2: 49-52.

Adams GL, Gansky SA, Miller AJ, Harrell WE, Hatcher DC. Comparison between traditional 2-dimensional cephalometry and a 3-dimensional approach on human dry skulls. American journal of orthodontics and dentofacial orthopedics. 2004; 126(4), 397-409.

Agarwal RR, Parihar A, Mandhani PA, Chandra R. Three-dimensional computed tomographic analysis of the maxilla in unilateral cleft lip and palate: implications for rhinoplasty. Journal of Craniofacial Surgery, 2012, 23.5: 1338-1342.

Agrawal JM, Agrawal MS, Nanjannawar LG, Parushetti AD. CBCT in orthodontics: the wave of future. J Contemp Dent Pract, 2013, 14.1: 153-7.

Aggarwal P and Mehra R. High speed CT image reconstruction using FPGA. IMAGE, 2011, 22.4.

Alam MK, Basri R, Kathiravan P, Sikder MA. Saifuddin, M, Iida J. Cephalometric evaluation for Bangladeshi adult by Steiner analysis. International Medical Journal, 2012, 19.3: 262-265.

Alqerban A, Jacobs R, Fieuws S, Nackaerts O, Willems G, SEDENTEXCT Project Consortium. Comparison of 6 cone-beam computed tomography systems for image quality and detection of simulated canine impaction-induced external root resorption in maxillary lateral incisors. American Journal of Orthodontics and Dentofacial Orthopedics, 2011, 140.3: e129-e139.

Anbuselvan GJ, Karthi M. Judicial Use Of Expansion Screws In Removable Appliance For Anterior Crossbite Correction-Case Report. J Indian Acad Dent Spec, 2010, 1: 38-42.

Andresen B, Elena M. Criteria for assessing the tools of disability outcomes research. Archives of physical medicine and rehabilitation, 2000, 81: S15-S20.

Angle EH. Treatment of Malocclusion of the Teeth. SS White dental manufacturing Company, 1907.

Arnaud EJ, Perrault M, Revol M, Servant JM, Banzet P. Surgical treatment of dermatofibrosarcoma protuberans. Plastic and reconstructive surgery, 1997, 100.4: 884-895.

Arnold WH, Sperber GH, Machin GA. Cranio-facial skeletal development in three human synophthalmic holoprosencephalic fetuses. Annals of Anatomy-Anatomischer Anzeiger, 1998, 180.1: 45-53.

Atherton JD. Morphology of facial bones in skulls with unoperated unilateral cleft palate. Cleft Palate J, 1967, 4.18-30: 1048.

Bacon W, Eiller V, Hildwein M, Dubois G. The cranial base in subjects with dental and skeletal Class II. Eur J Orthod. 1992; 14:224–8.

Baik HS. Clinical results of the maxillary protraction in Korean children. American Journal of Orthodontics and Dentofacial Orthopedics, 1995, 108.6: 583-592.

Bailey LJ, Proffit WR, White RP. 1995. Trends in surgical treatment of Class III skeletal relationships. Int J Adult Orthod 10:108–118.

Banabilh, SM, Suzina AH, Dinsuhaimi S, Singh, GD. Cranial base and airway morphology in adult Malay with obstructive sleep apnoea. Australian orthodontic journal, 2007, 23.2: 89.

Barteczko K, Jacob M. A re-evaluation of the premaxillary bone in humans. Anat Embryol. 2004; 207(6):417–37.

Basili C, Otsuka T, Kubota M, Slavicek R, Sato S. Three-dimensional CT analysis of vomer bone in the architecture of craniofacial structures in caucasic human skulls. International journal of stomatology & occlusion medicine. 2009; 2(4), 191-204.

Baume LJ. The postnatal growth activity of the nasal cartilage septum. Helvet. odont. acta, 1961, 5: 9-13.

Becker MH, Drachman RH, Kirscht JP. Predicting mothers' compliance with pediatric medical regimens. The Journal of pediatrics, 1972, 81.4: 843-854.

Behnia HSR, Kiani MT, Morad G, Khojasteh A. Accuracy and reliability of cone beam computed tomographic measurements of the bone labial and palatal to the maxillary anterior teeth. International Journal of Oral & Maxillofacial Implants, 2015, 30.6.

Bergland O, Borchgrevink H. The role of the nasal septum in midfacial growth in man elucidated by the maxillary development in certain types of facial clefts: A preliminary report. Scandinavian journal of plastic and reconstructive surgery, 1974, 8.1-2: 42-48.

Bernard-Mayordomo R, Guijarro-martínez R, Hernández-alfaro F. Volumetric CBCT analysis of the palatine process of the anterior maxilla: a potential source for bone grafts. International Journal of Oral and Maxillofacial Surgery, 2013, 42.3: 406-410.

Bishara S. Textbook of Orthodontics: Class III malocclusion, 2001,166-168.

Björk A, Skieller V. Growth of the maxilla in three dimensions as revealed radiographically by the implant method. British Journal of Orthodontics, 1977, 4.2: 53-64.

Bookstein FL. Morphometric tools for landmark data: geometry and biology. Cambridge University Press, 1997.

Broadbent BH, Golden WH. Bolton standards of dentofacial developmental growth. CV Mosby, 1975.

Brunelle JA, Bhat M, Lipton JA. Prevalence and distribution of selected occlusal characteristics in the US population, 1988–1991. Journal of Dental Research, 1996, 75.2_suppl: 706-713.

Callender T. The development of The Human Maxilla, Vomer, and Paraseptal Cartilages. By Professor Fawcett, MD, University of Bristol. The usually accepted descriptions of the development of the maxilla of man state that it arises by a number of separate centres— the number varying. The Journal of Anatomy and Physiology, 1911, 45: 378.

Carlos QJ, Trosien A, Hatcher D, Kapila, S. Craniofacial imaging in orthodontics: historical perspective, current status, and future developments. The Angle orthodontist, 1999, 69.6: 491-506.

Celikoglu M, Oktay H. Effects of maxillary protraction for early correction of class III malocclusion. European journal of orthodontics, 2013, 36.1: 86-92.

Cevidanes LHS, Bailey LJ, Tucker JGR, Styner MA, Mol A, Phillips C. et al. Superimposition of 3D cone-beam CT models of orthognathic surgery patients. Dentomaxillofacial Radiology, 2005, 34.6: 369-375.

Cevidanes LHC, Tucker S, Styner M, Kim H, Chapuis J, Reyes M. et al. Three-dimensional surgical simulation. American journal of orthodontics and dentofacial orthopedics, 2010, 138.3: 361-371.

Chang JZC, Chen YJ, Chang FHF, Yao JCC, Lan WH, Liu PH. et al. Morphometric analysis of mandibular growth in skeletal Class III malocclusion. Journal of the Formosan Medical Association, 2006, 105.4: 318-328.

Cheverud JM, Midkiff JE. Effects of fronto-occipital cranial reshaping on mandibular form. American Journal of Physical Anthropology, 1992, 87.2: 167-171.

Cheverud JM, Kohn LA, Konigsberg W, Leigh SR. Effects of fronto-occipital artificial cranial vault modification on the cranial base and face. American Journal of Physical Anthropology, 1992, 88.3: 323-345.

Choi YK, Park SB, Kim YI, Son WS. Three-dimensional evaluation of midfacial asymmetry in patients with non syndromic unilateral cleft lip and palate by cone-beam computed tomography. The Korean Journal of Orthodontics, 2013, 43.3: 113-119.

Chovalopoulou ME, Valakos ED, Manolis SK. Sex determination by three-dimensional geometric morphometrics of the palate and cranial base. Anthropologischer Anzeiger, 2013, 70.4: 407-425.

Dalessandri D, Laffranchi L, Tonni I, Zotti F, Piancino MG. et al. Advantages of cone beam computed tomography (CBCT) in the orthodontic treatment planning of cleidocranial dysplasia patients: a case report. Head & face medicine, 2011, 7.1: 6.

DE Jong JP, Breugem CC. Early hard palate closure using a vomer flap in unilateral cleft lip and palate: effects on cleft width. Clinical oral investigations, 2014, 18.4: 1285-1290.

Delaire J, Precious D. "Influence of the nasal-septum on maxillonasal growth in patients with congenital labiomaxillary cleft." Cleft Palate Journal, 1986, 23(4): 270-277.

Delaire J, Precious D. "Interaction of the development of the nasal-septum, the nasal pyramid and the face." International Journal of Pediatric Otorhinolaryngology, 1987, 12(3): 311-326.

Del Santo B, Valdés R, Mata J, Felipe A, Casado FJ, Pastor-Anglada M. Differential expression and regulation of nucleoside transport systems in rat liver parenchymal and hepatoma cells. Hepatology, 1998, 28.6: 1504-1511.

De Oliveira AEF, Cevidanes LHS, Phillips C, Motta A, Burke B, Tyndall D. Observer reliability of three-dimensional cephalometric landmark identification on cone-beam computerized tomography. Oral Surgery, Oral Medicine, Oral Pathology, Oral Radiology, and Endodontology, 2009, 107.2: 256-265.

Dhopatkar A, Bhatia S, Rock P. An investigation into the relationship between the cranial

base angle and malocclusion. Angle Orthod 2002; 72: 456–63.

Dibbets JH. Morphological associations between the Angle classes. European journal of orthodontics, 1996, 18.2: 111-118.

Dion LD, Blalock JE, Gifford GE. Retinoic acid and the restoration of anchorage dependent growth to transformed mammalian cells. Experimental cell research, 1978, 117.1: 15-22.

Dixon A, Hoyte D, Rönning O. Fundamentals of craniofacial growth. New York: CRC Press; 1997.

Du Raan FJ. Department of Orthodontics. 2017.

Ellis III E, McNamara JR JA. Components of adult Class III malocclusion. J Oral Maxillofac Surg 1984; 42: 295-305.

Enciso R, Nguyen M, Shigeta Y, Ogawa T, Clark GT. Comparison of cone-beam CT parameters and sleep questionnaires in sleep apnea patients and control subjects. Oral Surgery, Oral Medicine, Oral Pathology, Oral Radiology, and Endodontology, 2010, 109.2: 285-293.

Enlow DH, Bang S. Growth and remodeling of the human maxilla. American journal of orthodontics, 1965, 51.6: 446-464.

Enlow DH, Harvold EP, Latham RA, Moffett BC, Christiansen RL. et al. Research on control of craniofacial morphogenesis: an NIDR state-of-the-art workshop. American journal of orthodontics, 1977, 71.5: 509-530.

Enlow DH, Hans MG. Growth of the mandible. Essential of facial growth, 1996, 57-78.

Epker BN, Schendel SA. Total maxillary surgery. International journal of oral surgery, 1980, 9.1: 1-24.

Ebner FH, Kürschner V, Dietz K, Bültmann E, Nägele T, Honegger J. Craniometric changes in patients with acromegaly from a surgical perspective. Neurosurgical focus, 2010, 29.4: E3.

Fakhry N, Puymerail L, Michel J, Santini L, Lebreton-Chakour C. et al. Analysis of hyoid bone using 3D geometric morphometrics: an anatomical study and discussion of potential clinical implications. Dysphagia, 2013, 28.3: 435-445.

Falkner F, Tanner JM. Human Growth, Vol. 2, Postnatal Growth. 1978.

Fawcett E. The development of the human maxilla, vomer and paraseptal cartilage. J Anat Phys. 1911; 45:378–405

Farkas LG. Anthropometry of the Head and Face. Raven Pr, 1994.

Feichtinger M, Mossböck R, Kärcher H. Assessment of bone resorption after secondary alveolar bone grafting using three-dimensional computed tomography: a three-year study. The Cleft Palate-Craniofacial Journal, 2007, 44.2: 142-148.

Ferro A, Nucci LP, Ferro F, Gallo C. Long-term stability of skeletal Class III patients treated with splints, Class III elastics, and chincup. American Journal of Orthodontics and Dentofacial Orthopedics, 2003, 123.4: 423-434.

Fish LC, Epker BN. Surgical-orthodontic cephalometric prediction tracing. Journal of clinical orthodontics: JCO, 1980, 14.1: 36.

Fishman EK, Magid D, Ney DR, Chaney EL, Pizer SM, Rosenman JG. et al. Three-dimensional imaging. Radiology, 1991, 181.2: 321-337.

Freeland TD. Articulators in orthodontics. In: Seminars in Orthodontics. WB Saunders, 2012. p. 51-62.

Frazier-Bowers SA. An interview with Sylvia Frazier-Bowers. Dental Press J.2015; 93(2):134-9.

Freudenthaler J. Comparison of Japanese and European overbite depth indicator and antero-posterior dysplasia indicator values. The European Journal of Orthodontics, 2011, 34.1: 114-118.

Friede H. The vomero-premaxillary suture—a neglected growth site in mid-facial development of unilateral cleft lip and palate patients. Cleft Palate J, 1978, 15.4: 398.

Frush DP, Donnelly LF, Rosen NS. Computed tomography and radiation risks: what pediatric health care providers should know. Pediatrics, 2003, 112.4: 951-957.

Fudalej P, Dragan M, Wedrychowska-Szulc B. Prediction of the outcome of orthodontic treatment of Class III malocclusions—a systematic review. The European Journal of Orthodontics, 2010, 33.2: 190-197.

Galvão Caan. Estudo de algumas medidas cefalométricas da Classe III. Ortodontia 1980; 13: 166-74.

Gange RJ, Johnston LE. The septopremaxillary attachment and midfacial growth: an experimental study on the albino rat. American journal of orthodontics, 1974, 66.1: 71-81.

Gardiner BG. Tetrapod classification. Zoological Journal of the Linnaean Society, 1982, 74.3: 207-232.

Ghafari JG, Haddad RV, Saadeh ME. Class III Malocclusion—the Evidence on Diagnosis and Treatment. Evidence-Based Orthodontics, 2011, 247-280.

Gill IJ, Fisher AN, Hinchcliffe M, Whetstone J, Farraj N, De Ponti R. et al. Cyclodextrins as protection agents against enhancer damage in nasal delivery systems II. Effect on in vivo absorption of insulin and histopathology of nasal membrane. European Journal of Pharmaceutical Sciences, 1994,1.5: 237-248.

Graber T, Vanarsdall R, Vig K. Orthodontics: Current Principles and Techniques. Mosby, St. Louis. 2005,45:378–405.

Graber TM, Vanarsdall RL. Orthodontics currents principles and techniques. 2nd ed. Philadelphia: Mosby-Year Book; 1994.

Guis F, Ville Y, Vincent Y, Doumerc S, Pons JC, Frydman R. Ultrasound evaluation of the length of the fetal nasal bones throughout gestation. Ultrasound in Obstetrics & Gynecology, 1995, 5.5: 304-307.

Gunz P, Mitteroecker P, Bookstein F, Weber GW. Computer-aided reconstruction of incomplete human crania using statistical and geometrical estimation methods. In: Enter the past: the e-way into the four dimensions of cultural heritage; CAA 2003; computer applications and quantitative methods in archaeology; proceedings of the 31st conference, Vienna, Austria, April 2003. Archaeopress, 2004. p. 92-94.

Guyer EC, Ellis III EE, McNamara JJ, Behrents RG. Components of Class III malocclusion in juveniles and adolescents. Angle Orthod 1986; 56: 7-30.

Hall BK, Precious DS. Cleft lip, nose, and palate: the nasal septum as the pacemaker for midfacial growth. Oral surgery, oral medicine, oral pathology and oral radiology. 2013; 115(4), 442-447.

Hajeer MY, Millett DT, Ayoub AF, Siebert JP. Current Products and Practices: Applications of 3D imaging in orthodontics: Part I. Journal of orthodontics, 2004, 31.1: 62-70.

Halazonetis DJ. Morphometric correlation between facial soft-tissue profile shape and skeletal pattern in children and adolescents. American journal of orthodontics and dentofacial orthopedics, 2007, 132.4: 450-457.

Hallgrímsson B, Liu W, Ford-Hutchinson AF, Jirik FR. Epigenetic interactions and the structure of phenotypic variation in the cranium. Evolution & development, 2007, 9.1: 76-91.

Hansen L, Nolting D, Holm G, Hansen B, Kjaer I. Abnormal vomer development in human fetuses with isolated cleft palate. Cleft Palate Craniofac J. 2004; 41(5):470–3.

Hartman CH, Holton NE, Miller SF, Yokley TR, Marshall SD, Srinivasan S, Southard TE. 2016. Nasal septal deviation and facial skeletal asymmetries. Anat Rec 299:295–306.

Heidbuchel WM, Kuijpers-Jagtman AM, Freihofer PM. An orthodontic and cephalometric study on the results of the combined surgical-orthodontic approach of the protruded premaxilla in bilateral clefts. Journal of Cranio-Maxillofacial Surgery, 1993, 21.2: 60-66.

Hildebrandt S. Current status of identification of victims of the National Socialist regime whose bodies were used for anatomical purposes. Clinical Anatomy, 2014, 27.4: 514-536.

Hill DLG, Batchelor PG, Holden M, Hawkes DJ. Medical image registration. Physics in medicine and biology, 2001, 46.3: R1.

Hilloowala R, Kanth H. The transmission of masticatory forces and nasal septum: structural comparison of the human skull and Gothic cathedral. CRANIO®, 2007, 25.3: 166-171.

Hitotsumatsu T, Rhoton JR, Albert L. Unilateral upper and lower subtotal maxillectomy approaches to the cranial base: microsurgical anatomy. Neurosurgery, 2000, 46.6: 1416-1453.

Ho HD, Akimoto S, Sato S. Occlusal plane and mandibular posture in the hyperdivergent type of malocclusion in mixed dentition subjects. Bull Kanagawa Dent Coll. 2002; 30:87–92.

Holton NE, Yokley TR, Figueroa A. Nasal septal and craniofacial form in European-and African-derived populations. Journal of anatomy, 2012, 221.3: 263-274.

Horner K, Islam M, Flygare L, Tsiklakis K, Whaites E. Basic principles for use of dental cone beam computed tomography: consensus guidelines of the European Academy of Dental and

Maxillofacial Radiology. Dentomaxillofacial Radiology, 2009, 38.4: 187-195.

Hur MS, Won HS, Kwak DS, Chung IH and Kim IB. Morphological Patterns and Variations of the Nasal Septum Components and Their Clinical Implications. Journal of Craniofacial Surgery, 2016, 27.8: 2164-2167.

Ishii H, Morita S, Takeuchi Y, Nakamura S. Treatment effect of combined maxillary protraction and chincap appliance in severe skeletal Class III cases. Am J Orthod Dentofacial Orthop 1987; 92: 304-12.

Ishii N, Deguchi T, Hunt NP. Craniofacial differences between Japanese and British Caucasian females with a skeletal Class III malocclusion. The European Journal of Orthodontics, 2002, 24.5: 493-499.

Isaacson RJ, Zapfel RJ, Worms FW, Erdman AG. Effects of rotational jaw growth on the occlusion and profile. American journal of orthodontics, 1977, 72.3: 276-286.

Iwasaki T, Hayasaki H, Takemoto Y, Kanomi R, Yamasaki Y. Oropharyngeal airway in children with Class III malocclusion evaluated by cone-beam computed tomography. American Journal of orthodontics and Dentofacial orthopedics 2009, 136.3: 318. e1-318. e9.

Iwasaki T, Takemoto Y, Inada E, Sato H, Saitoh I, Kakuno E, Yamasaki, Y. Three-dimensional cone-beam computed tomography analysis of enlargement of the pharyngeal

airway by the Herbst appliance. American Journal of Orthodontics and Dentofacial Orthopedics 2014, 146.6: 776-785.

Iwasaki T, Saitoh I, Takemoto Y, Inada E, Kanomi R, Hayasaki H, Yamasaki Y. Evaluation of upper airway obstruction in Class II children with fluid-mechanical simulation. American Journal of Orthodontics and Dentofacial Orthopedics 2011, 139.2: e135-e145.

Jacobson A, Evans WG, Preston CB, Sadowsky PL. Mandibular prognathism. Am J Orthod 1974; 66: 140 71.

Jerolimov V, Keros J, Bagić I, Lazić B, Komar D. Vomer as relevant factor in the mastication forces transmission system. Collegium antropologicum 1999, 23.1: 133-142.

Joshi N, Hamdan A, Fakhouri WD. Skeletal malocclusion: a developmental disorder with a life-long morbidity. Journal of clinical medicine research, 2014, 6.6: 399.

Kapust AJ, Sinclair PM, Turley PK. Cephalometric effects of face mask/expansion therapy in Class III children: a comparison of three age groups. American Journal of Orthodontics and Dentofacial Orthopedics, 1998, 113.2: 204-212.

Katsoulis J, Pazera P, Mericske-Stern R. Prosthetically Driven, Computer-Guided Implant Planning for the Edentulous Maxilla: A Model Study. Clinical implant dentistry and related research, 2009, 11.3: 238-245.

Kau CH, Božič M, English J, Lee R, Bussa H, Ellis R. Cone-beam computed tomography of the maxillofacial region—an update. The International Journal of Medical Robotics and Computer Assisted Surgery, 2009, 5.4: 366-380.

Keles A, Erverdi N, Sezen S. Bodily distalization of molars with absolute anchorage. The Angle orthodontist, 2003, 73.4: 471-482.

Keles A. Maxillary unilateral molar distalization with sliding mechanics: a preliminary investigation. The European Journal of Orthodontics, 2001, 23.5: 507-515.

Kerr WJS, Buchanan IB, Mccoll JH. Use of the PAR index in assessing the effectiveness of removable orthodontic appliances. British Journal of Orthodontics, 1993, 20.4: 351-357.

Kimes KR, Mooney MP, Siegel MI, Todhunter JS. Growth rate of the vomer in normal and cleft lip and palate human fetal specimens. The Cleft Palate-Craniofacial Journal, 1992, 29.1: 38-43.

Kim JH, Viana MA, Graber TM, Omerza FF, BeGole EA. The effectiveness of protraction face mask therapy: a meta-analysis. American Journal of Orthodontics and Dentofacial Orthopedics, 1999, 115.6: 675-685.

Kim TS, Caruso JM, Christensen H, Torabinejad M. A comparison of cone-beam computed tomography and direct measurement in the examination of the mandibular canal and adjacent structures. Journal of endodontics, 2010, 36.7: 1191-1194.

Kim DI, Lee U, Park DK, Kim YS, Han KH, Kim KH, Han SH. Morphometrics of the hyoid bone for human sex determination from digital photographs. Journal of forensic sciences, 2006, 51.5: 979-984.

Kim SH, Kang SM, Choi YS, Kook YA, Chung KR, Huang JC. Cone-beam computed tomography evaluation of mini-implants after placement: is root proximity a major risk factor for failure?. American Journal of Orthodontics and Dentofacial Orthopedics, 2010, 138.3: 264-276.

Kjaer SB, Pedersen JK, Blaabjerg F. A review of single-phase grid-connected inverters for photovoltaic modules. IEEE transactions on industry applications, 2005, 41.5: 1292-1306.

Kjær I, Niebuhr E. Studies of the cranial base in 23 patients with cri-du-chat syndrome suggest a cranial developmental field involved in the condition. American Journal of Medical Genetics Part A, 1999, 82.1: 6-14.

Korbmacher H, Kahl-Nieke B, Schöllchen M, Heiland M. Value of two cone-beam computed tomography systems from an orthodontic point of view. Journal of Orofacial Orthopedics/Fortschritte der Kieferorthopädie, 2007, 68.4: 278-289.

Lagravère M, Carey J, Toogood R, Major PW. Three dimensional accuracy of measurements made with software on cone beam computed tomography images. Am J Orthod Dentofacial Orthop. 2008; 134:112–6.

Langford RJ, Natarajan K, Nishikawa H, Dover SM, Hockley AD. Maxillary volume growth in childhood. Plastic and reconstructive surgery, 2003, 111.5: 1591-1597.

Langford RJ, Sgouros S, Natarajan K, Nishikawa H, Dover SM, Hockley AD. Maxillary volume growth in craniosynostosis. Plastic and reconstructive surgery, 2003, 111.5: 1598-1604.

Latham RA. The pathogenesis of the skeletal deformity associated with unilateral cleft lip and palate. The Cleft palate journal, 1969,6: 404-414.

Lawrence R. Pediatric septoplasty: a review of the literature. Int J Pediatr Otorhinolaryngol 2012,76:1078–1081.

Le Diascorn H. Anatomie et physiologie des sutures de la face. Prélat, 1972.

Lepage K, Thomson DJ, Kraut S, Brady DJ. Multitaper scan-free spectrum estimation using a rotational shear interferometer. Applied optics, 2006, 45.13: 2940-2954.

Lieberman E, Hallgrímsson B, Liu W, Parsons TE, Jamniczky A. Spatial packing, cranial base angulation, and craniofacial shape variation in the mammalian skull: testing a new model using mice. Journal of Anatomy, 2008, 212.6: 720-735.

Lilja J, Mars M, Elander A, Enocson L, Hagberg C, Worrell E, Friede H. Analysis of dental arch relationships in Swedish unilateral cleft lip and palate subjects: 20-year longitudinal consecutive series treated with delayed hard palate closure. The Cleft palate-craniofacial journal, 2006, 43.5: 606-611.

Li X, Xu L, Zhu Y, Egger J, Chen X. A semi-automatic implant design method for cranial defect restoration. Int J CARS, 2016, 11.Suppl 1: S241-S243.

Macklin CC. Preliminary note on the skull of a human fetus of 43 MM. Greatest length. The Anatomical Record, 1921, 22.4: 251-265.

Machicek SL. Mandible Size and Prognathism of MEK1 Transgenic Achondroplastic Mice. In: Presentation at AADR Meeting (March 2007). 2007.

Manmadhachary A, Kumar YR, Krishnanand L. Effect of CT acquisition parameters of spiral CT on image quality and radiation dose. Measurement, 2017, 103: 18-26.

Mao JJ, Nah HD. Growth and development: hereditary and mechanical modulations. American journal of orthodontics and dentofacial orthopedics, 2004, 125.6: 676-689.

Mao JJ. Mechanobiology of craniofacial sutures. J Dent Res 2006,81:810–816.

Markus AF, Smith WP, Delaire J. Facial balance in cleft lip and palate I. Normal development and cleft palate. British Journal of Oral and Maxillofacial Surgery, 1992, 30.5: 287-295.

Markus AF, Precious DS. Effect of primary surgery for cleft lip and palate on mid-facial growth. British Journal of Oral and Maxillofacial Surgery, 1997, 35.1: 6-10.

Martínez-Abadías N, Esparza M, Sjøvold T, González-José R, Santos M, Hernández M. Heritability of human cranial dimensions: comparing the evolvability of different cranial regions. Journal of Anatomy 2009, 214.1: 19-35.

Martin RB, Burr DB, Sharkey NA, Fyhrie DP. Skeletal tissue mechanics 1998.(Vol. 190). New York: Springer.

Materialise NV. Mimic's version 13, 2009.

McBratney BM, Margaryan E, Ma W, Urban Z, Lozanoff S. 2003. Frontonasal dysplasia in 3H1 Br/Br mice. Anat Rec 2001,271:291–302.

McCarthy RC. Anthropoid cranial base architecture and scaling relationships. J Hum E 2001, 40:41–66.

Mcnamara JR, James A. An orthopedic approach to the treatment of Class III malocclusion in young patients. Journal of clinical orthodontics: JCO, 1987, 21.9: 598-608.

Menezes LMD, Azeredo F, Weissheimer A, Rizzato JL, Rizzatto SMD. Cone-Beam computed tomography evaluation of maxillary expansion in twins with cleft lip and palate. Dental Press Journal of Orthodontics, 2012, 17.2: 42. E1-42. e11.

Merrifield LL. The profile line as an aid in critically evaluating facial esthetics. American journal of orthodontics, 1966, 52.11: 804-822.

Merwin D, Ngan P, Hagg U, Yiu C, Wei SH. Timing for effective application of anteriorly directed orthopedic force to the maxilla. American Journal of Orthodontics and Dentofacial Orthopedics, 1997, 112.3: 292-299.

Migale D, Barbato E, Bossù M, Ferro R, Ottolenghi L. Oral health and malocclusion in 10-to-11 years-old children in southern Italy. European Journal of Paediatric Dentistry, 2009, 10.1: 13.

Moon YA, Sug-Joon C, Young I. Cephalometric predictors of long-term stability in the early treatment of Class III malocclusion. The Angle orthodontist, 2005, 75.5: 747-753.

Mooney MP, Siegel MI. 1986. Developmental relationship between premaxillary-maxillary suture patency and anterior nasal spine morphology. Cleft Palate J 23:101–107.

Moore SJ, Fan Y, Bhogal AK, Dicks E, Fernandez BA, Beales PL. Clinical and genetic epidemiology of Bardet–Biedl syndrome in Newfoundland: A 22-year prospective, population-based, cohort study. American Journal of Medical Genetics Part A, 2005, 132.4: 352-360.

Moss ML. The pathogenesis of artificial cranial deformation. American Journal of Physical Anthropology, 1958, 16.3: 269-286.

Moss-Salentijn L, Hendricks-Klyvert M. Dental and Oral Tissues. Lea & Febiger edition, Philadelphia, 1990.

Mossey PA. The heritability of malocclusion: part 2. The influence of genetics in malocclusion. British journal of orthodontics, 1999.

Mouakeh M. Cephalometric evaluation of craniofacial pattern of Syrian children with Class III malocclusion. Am J Orthod Dentofacial Orthop 2001; 119: 640-9.

Muramatsu A. Reproducibility of maxillofacial anatomic landmarks on 3-dimensional computed tomographic images determined with the 95% confidence ellipse method. Angle Orthod. 2008; 78:396–402.

Müller F, O'rahilly R. The human chondrocranium at the end of the embryonic period, proper, with particular reference to the nervous system. Developmental Dynamics, 1980, 159.1: 33-58.

Nanda SK. Patterns of vertical growth in the face. American Journal of Orthodontics and Dentofacial Orthopedics, 1988, 93.2: 103-116.

Niida H, Takeuchi K, Ueshima K, Okabe S. Vagally mediated acid hypersecretion and lesion formation in anesthetized rat under hypothermic conditions. Digestive diseases and sciences, 1991, 36.4: 441-448.

Ngan P, Moon W. Evolution of Class III treatment in orthodontics. American Journal of Orthodontics and Dentofacial Orthopedics, 2015, 148.1: 22-36.

Ngan P. Early timely treatment of Class III malocclusion. In: Seminars in Orthodontics. WB Saunders, 2005. p. 140-145.

Ngan P. Early treatment of Class III malocclusion: is it worth the burden. American Journal of OBEROI, Snehlata, Chigurupati, R, Gill P, Hoffman WY, Vargervik K. Volumetric assessment of secondary alveolar bone grafting using cone beam computed tomography. The Cleft palate-craniofacial journal, 2009, 46.5: 503-511.Orthodontics and Dentofacial Orthopedics, 2006, 129.4: S82-S85.

Ogle OE, Weinstock RJ, Friedman E. Surgical anatomy of the nasal cavity and paranasal sinuses. Oral and maxillofacial surgery clinics of North America, 2012, 24.2: 155-166.

Ogle OE, Weinstock RJ, Friedman E. Surgical anatomy of the nasal cavity and paranasal sinuses. Oral and maxillofacial surgery clinics of North America, 2012, 24.2: 155-166.

Ogle OE. The management of oronasal fistulas in the cleft palate patient. Oral and maxillofacial surgery clinics of North America, 2002, 14.4: 553-562.

Oliveira JMM, Alonso MBCC, De Sousa MJAP, Fuziy A, Scocate A, Costa A. Volumetric study of sphenoid sinuses: anatomical analysis in helical computed tomography. Surgical and Radiologic Anatomy, 2017, 39.4: 367-374.

Olszewski R, Reychler H. Three-dimensional surgical guide for frontal-nasal-ethmoid-vomer disjunction in Le Fort III osteotomy. Journal of Craniofacial Surgery, 2011, 22.5: 1791-1792.

O'rahilly R, Meyer DB. Roentgenographic investigation of the human skeleton during early fetal life. American Journal of Roentgenology, 1956, 76: 455-468.

Opperman LA. Cranial sutures as intramembranous bone growth sites. Developmental dynamics, 2000, 219.4: 472-485.

Park SB, Kim YI, Hwang DS, Lee JY. Midfacial soft-tissue changes after mandibular setback surgery with or without paranasal augmentation: cone-beam computed tomography (CBCT) volume superimposition. Journal of Cranio-Maxillofacial Surgery, 2013, 41.2: 119-123.

Park JW, Kim NK, Kim JW, Kim MJ, Chang YI. Volumetric, planar, and linear analyses of pharyngeal airway change on computed tomography and cephalometry after

mandibular setback surgery. American Journal of Orthodontics and Dentofacial Orthopedics, 2010, 138.3: 292-299.

Park SB, Yoon JK, Kim YI, Hwang DS, Cho BH, Son WS. The evaluation of the nasal morphologic changes after bimaxillary surgery in skeletal class III malocclusion by using the superimposition of cone-beam computed tomography (CBCT) volumes. Journal of Cranio-Maxillofacial Surgery, 2012, 40.4: e87-e92.

Pangrazio-kulbersh V, Berger JL, Janisse FN, Bayirli B. Long-term stability of Class III treatment: rapid palatal expansion and protraction facemask vs LeFort I maxillary advancement osteotomy. American Journal of Orthodontics and Dentofacial Orthopedics, 2007, 131.1: 7. E9-7. E19.

Paschetta C, De Azevedo S, Castillo L, Martínez-Abadías N, Hernández M, Lieberman DE, González-José R. The influence of masticatory loading on craniofacial morphology: a test case across technological transitions in the Ohio Valley. American journal of physical anthropology, 2010, 141.2: 297-314.

Patel S, Dawood A, Wilson R, Horner K, Mannocci F. The detection and management of root resorption lesions using intraoral radiography and cone beam computed tomography–an in vivo investigation. International endodontic journal, 2009, 42.9: 831-838.

Pauwels R, Beinsberger J, Collaert B, Theodorakou C, Rogers J, Walker A, Horner K. Effective dose range for dental cone beam computed tomography scanners. European journal of radiology, 2012, 81.2: 267-271.

Pelinsari LJ, Moura RCP, De Carvalho MV, Eduardo Alencar de Souza, P, Ricardo Manzi F, Campolina Rebello Horta M. Anatomic variations and lesions of the maxillary sinus detected in cone beam computed tomography for dental implants. Clinical oral implants research, 2012, 23.12: 1398-1403.

Pelo S, Deli R, Correra P, Boniello R, Gasparini G, Moro A. Evaluation of 2 different reference planes used for the study of asymmetric facial malformations. Journal of Craniofacial Surgery, 2009, 20.1: 41-45.

Periago D. Linear accuracy and reliability of cone beam CT derived 3-dimensional images constructed using an orthodontic volumetric rendering program. Angle Orthod. 2008; 78:387–95.

Perillo L, Cannavale R, Ferro F, Franchi L, Masucci C, Chiodini P, Baccetti T. Meta-analysis of skeletal mandibular changes during Fränkel appliance treatment. The European Journal of Orthodontics, 2010, 33.1: 84-92.

Perillo L, Masucci C, Ferro F, Apicella D, Baccetti T. Prevalence of orthodontic treatment need in southern Italian schoolchildren. The European Journal of Orthodontics, 2009, 32.1: 49-53.

Persson M, Sundell S. Facial morphology and open bite deformity in Amelogenesis Imperfecta: a roentgenocephalometric study. Acta Odontologica Scandinavica, 1982, 40.3: 135-144.

Pertovic, AG, Stutzman J. The biology of occlusal development. Monograph 6, cranial growth series. Center for human growth and development. University of Michigan Ann Arbor. Michigan 1977.

Peterlík I, Sedef M, Basdogan C, Matyska L. Real-time visio-haptic interaction with static soft tissue models having geometric and material nonlinearity. Computers & Graphics, 2010, 34.1: 43-54.

Plooij JM, Maal TJ, Haers P, Borstlap WA, Kuijpers-Jagtman AM, Bergé SJ. Digital three-dimensional image fusion processes for planning and evaluating orthodontics and orthognathic surgery. A systematic review. International journal of oral and maxillofacial surgery, 2011, 40.4: 341-352.

Polat OO, Kaya B. Changes in cranial base morphology in different malocclusions. Orthod Craniofacial Res. 2007; 10:216–21.

Proff PWF, Bokan I, Fanghänel J, Gedrange T. Cranial base features in skeletal Class III patients. The Angle Orthodontist, 2008, 78.3: 433-439.

Proffit WR, Fields HW. The etiology of orthodontic problems. Contemporary Orthodontic. 3ed. St. Louis: Mosby, 2000, 13-144.

Proffit WR, Bailey LTJ, Phillips C, Turvey TA. Long-term stability of surgical open-bite correction by Le Fort I osteotomy. The Angle Orthodontist, 2000, 70.2: 112-117.

Proffit WR, Fields HW. Biomechanics and mechanics. Contemporary orthodontics. St Louis: Mosby, 2000, 296-361.

Proffit WR, Sarver DM. Combined surgical and orthodontic treatment. Contemporary orthodontics, 2000, 607-645.

Proffit WR, Fields HW. and Sarver, D.M. (2007) Contemporary orthodontics. Mosby, St. Louis.   [Citation Time(s):1]

Rafferty MA, Siewerdsen JH, Chan Y, Daly MJ, Moseley DJ, Jaffray DA, Irish JC. Intraoperative cone-beam CT for guidance of temporal bone surgery. Otolaryngology—Head and Neck Surgery, 2006, 134.5: 801-808.

Rak D. Cephalometric analysis in cases with Class III malocclusions. Stomatol. Glas. Srb. 1989,36:277–287.

Ren S, Ma L, Sun Z, Qian J. Relationship between Palate-Vomer development and maxillary growth in submucous cleft palate patients. The Cleft Palate-Craniofacial Journal, 2014, 51.3: 314-319.

Ren S, Ma L, Zhou X, Sun Z. Bony defect of palate and vomer in submucous cleft palate patients. International journal of oral and maxillofacial surgery, 2015, 44.1: 63-66.

Ravassipour DB, Powell CM, Phillips CL, Hart PS, Hart TC, Boyd C, Wright JT. Variation in dental and skeletal open bite malocclusion in humans with Amelogenesis Imperfecta. Archives of Oral Biology, 2005, 50.7: 611-623.

Ricketts RM. New findings and concepts emerging from the clinical use of the computer. Transactions. European Orthodontic Society, 1973, 507.

Ricketts RM, Bench RW, Hilgers JJ, Schulhof R. An overview of computerized cephalometrics. American Journal of Orthodontics, 1972, 61.1: 1-28.

Roberts JA, Drage NA, Davies J, Thomas DW. Effective dose from cone beam CT examinations in dentistry. The British journal of radiology, 2009, 82.973: 35-40.

Rohr K. Landmark-based image analysis: using geometric and intensity models. Springer Science & Business Media, 2001.

Rohlf FJ, Slice D. Extensions of the Procrustes method for the optimal superimposition of landmarks. Syst. Zool. 1990,39:40–59.

Sadler TW. Langman's medical embryology. Lippincott Williams & Wilkins, 2011.

Sato S. A Treatment Approach to malocclusion under the consideration of craniofacial dynamics. Grace Printing Press Inc.; 2001.

Schaefer M, Black SM, Scheuer L. Juvenile osteology: a laboratory and field manual. Elsevier, Academic Press, 2009.

Silva FOG, Silva PRB, Rego MVNN, Silva FPL, Cavassan AO. Epidemiologia da má oclusão na dentadura decídua. Ortodontia 2002; 35: 22-33.

Swennen GRJ, Mollemans W, De Clercq C, Abeloos J, Lamoral P, Lippens F, Schutyser F. A cone-beam computed tomography triple scan procedure to obtain a three-dimensional augmented virtual skull model appropriate for orthognathic surgery planning. Journal of Craniofacial Surgery, 2009, 20.2: 297-307.

Subsol G, Thirion JP, Ayache N. A scheme for automatically building three-dimensional morphometric anatomical atlases: application to a skull atlas. Medical image analysis, 1998, 2.1: 37-60.

Suri S, Khandelwal N, Mago SK. Craniofacial computerized tomography analysis of the midface of patients with repaired complete unilateral cleft lip and palate. American Journal of Orthodontics and Dentofacial Orthopedics, 2008, 134.3: 418-429.

Sperber GH, Guttmann GD, Sperber SM. Craniofacial Development (Book for Windows & Macintosh). PMPH-USA, 2001.

Schendel SA, Walker G, Kamisugi A. Hawaiian craniofacial morphometrics: average Mokapuan skull, artificial cranial deformation, and the "rocker" mandible. American Journal of Physical Anthropology, 1980, 52.4: 491-500.

Sandikcioglu M, Mølsted K, Kjaer I. The prenatal development of the human nasal and vomeral bones. Journal of craniofacial genetics and developmental biology, 1994, 14.2: 124-134.

Siegel MI, Mooney MP, Kimes KR, Todhunter J. Developmental correlates of midfacial components in a normal and cleft lip and palate human fetal sample. The Cleft Palate-Craniofacial Journal, 1991, 28.4: 408-412.

Scammon RE. The measurement of man. The measurement of the body in childhood, 1930.

Savara BS, Thomas DR. Facial growth of children with cleft lip and/or palate. Cleft Palate J, 1972, 9: 119-131.

Scott JH. The analysis of facial growth: I. The anteroposterior and vertical dimensions. American Journal of Orthodontics, 1958, 44.7: 507-512.

Singh GD, McNamara JR, Lozanoff S. Morphometry of the cranial base in subjects with Class III malocclusion. J. Dent. Res. 1997a ,76:694–703.

Singh GD, McNamara JR, Lozanoff S. thin plate spline analysis of the cranial base in subjects with Class III malocclusion. Euro. J. Orthod. 1997b,19:341–353.

Singh GD, McNamara JR, Lozanoff S. Finite element analysis of the cranial base in subjects with Class III malocclusion. Brit. J. Orthod. 1997c 24:103–112.

Singh GD, Rivera-Robles J, DE JESUS-VINAS J. Longitudinal craniofacial growth patterns in patients with orofacial clefts: geometric morphometrics. The Cleft palate-craniofacial journal, 2004, 41.2: 136-143.

Singh GD. Morphologic determinants in the etiology of class III malocclusions: a review. Clinical anatomy, 1999, 12.5: 382-405.

Singh GD, MCNAMARA JR, LOZANOFF S. Finite-element morphometry of soft tissue morphology in subjects with untreated Class III malocclusions. The Angle Orthodontist, 1999, 69.3: 215-224.

Sassouni V. A classification of skeletal facial types. Am J Orthod 1969; 55: 109-23.

Silva Filho OG, Santos SC, Suguimoto RM. Má oclusão de Classe III: época oportuna de tratamento. Ortodontia 1995; 28: 74-84.

Siriwat PP, Jarabak JR. Malocclusion and facial morphology is there a relationship? An epidemiologic study. Angle Orthod. 1985,55:127–138.

Sarnat BG, Wexler MR. Growth of the face and jaws after resection of the septal cartilage in the rabbit. Developmental Dynamics, 1966, 118.3: 755-767.

Siegel MI. Mechanisms of early maxillary growth-implications for surgery. J Oral Surg. 1976; 34:106–112.

Smahel Z. Variations in craniofacial morphology with severity of isolated cleft palate. Cleft Palate J. 1984; 21:140–158.

Suri S, Utreja A, Khandelwal N, Mago SK. Craniofacial computerized tomography analysis of the midface of patients with repaired complete unilateral cleft lip and palate. Am J Orthod Dentofacial Orthop. 2008; 134:418–429.

Suda N, Ishii-Suzuki, M, Hirose K, Hiyama S, Suzuki S, Kuroda T. Effective treatment plan for maxillary protraction: is the bone age useful to determine the treatment plan?. American Journal of Orthodontics and Dentofacial Orthopedics, 2000, 118.1: 55-62.

Subburaj K, Ravi B, Agarwal M. Automated identification of anatomical landmarks on 3D bone models reconstructed from CT scan images. Computerized Medical Imaging and Graphics, 2009, 33.5: 359-368.

Santler G, Kärcher H, Ruda C. Indications and limitations of three-dimensional models in cranio-maxillofacial surgery. Journal of Cranio-Maxillofacial Surgery, 1998, 26.1: 11-16.

Scolozzi P, Herzog G. Computer-assisted virtual planning for surgical guide manufacturing and internal distractor adaptation in the management of midface hypoplasia in cleft patients. The Cleft Palate-Craniofacial Journal, 2017, 54.4: 457-464.

Schatz EC, Xia JJ, Gateno J, English JD, Teichgraeber JF, Garrett FA. Development of a technique for recording and transferring natural head position in 3 dimensions. Journal of Craniofacial Surgery, 2010, 21.5: 1452-1455.

Swenson KE. "Nasal septal deviation in a longitudinal growth sample." MS (Master of Science) thesis, University of Iowa, 2012. http://ir.uiowa.edu/etd/2995.

Schneiderman ED, Xu H, Salyer KE. Characterization of the maxillary complex in unilateral cleft lip and palate using cone-beam computed tomography: a preliminary study. Journal of Craniofacial Surgery, 2009, 20.8: 1699-1710.

Tanaka E, Sato S. Longitudinal alteration of the occlusal plane and development of different dentoskeletal frames during growth. Am L Orthod Dentofacial Orthop. 2008; 134(5):602.e1– 602.e11.

Takada K, Petdachai S, Sakuda M. Changes in dentofacial morphology in skeletal Class III children treated by a modified maxillary protraction headgear and a chin cup: a longitudinal cephalometric appraisal. Eur J Orthod. 1993; 15: 211-21.

Takahashi MJ, Jones JF, Reber BF, Catterall WA. Subunit structure of dihydropyridine-sensitive calcium channels from skeletal muscle. Proceedings of the National Academy of Sciences, 1987, 84.15: 5478-5482.

Takada K, Petdachai S, Sakuda M. Changes in dentofacial morphology in skeletal Class III children treated by modified maxillary protraction headgear and a chin cup: A longitudinal cephalometric appraisal. Euro. J. Orthod. 1993,15:211–221.

Tanne K, Matsubara S, Sakuda M. Location of the center of resistance for the nasomaxillary complex studied in a three-dimensional finite element model. Br. J. Orthod. 1995,22:227–232.

Tollaro IT, Baccetti L, Franchi L. Class III malocclusion in the deciduous dentition: a morphological and correlation study. Euro. J. Orthod.1994, 16:401–408.

Tollaro IT, Baccetti l, Franchi L. Craniofacial changes induced by early functional treatment of Class III malocclusion. Am. J. Orthod. Dentofac. Orthop. 1996,109:310–318.

Tweed CH. The Frankfort-Mandibular Plant Angle in Orthodontic Diagnosis, Classification, Treatment Planning, and Prognosis. Plastic and Reconstructive Surgery, 1947, 2.5: 513.

Trpkova B, Major P, Prasad N, Nebbe B. Cephalometric landmarks identification and reproducibility: a meta-analysis. American Journal of Orthodontics and Dentofacial Orthopedics, 1997, 112.2: 165-170.

Teke HY, Duran S, Canturk N, Canturk G. Determination of gender by measuring the size of the maxillary sinuses in computerized tomography scans. Surgical and Radiologic Anatomy, 2007, 29.1: 9-13.

Turley PK. Managing the developing Class III malocclusion with palatal expansion and facemask therapy. American Journal of Orthodontics and Dentofacial Orthopedics, 2002, 122.4: 349-352.

Tucker S, Cevidanes LHS, Styner M, Kim H, Reyes M, Proffit W, Turvey T. Comparison of actual surgical outcomes and 3-dimensional surgical simulations. Journal of oral and maxillofacial surgery, 2010, 68.10: 2412-2421.

Uribe LM, Moreno Vela KC, Kummet C, Dawson DV, Southard TE. Phenotypic diversity in white adults with moderate to severe Class III malocclusion. American Journal of Orthodontics and Dentofacial Orthopedics, 2013, 144.1: 32-42.

Uribe FPS, Allareddy V, Nanda R. Patients', parents', and orthodontists' perceptions of the need for and costs of additional procedures to reduce treatment time. American Journal of Orthodontics and Dentofacial Orthopedics, 2014, 145.4: S65-S73.

Uechi J, Okayama M, Shibata T, Muguruma T, Hayashi K, Endo K, Mizoguchi I. A novel method for the 3-dimensional simulation of orthognathic surgery by using a multimodal image-fusion technique. American Journal of Orthodontics and Dentofacial Orthopedics, 2006, 130.6: 786-798.

Van Loon B, Maal TJ, Plooij JM, Ingels KJ, Borstlap WA, et al. 3D Stereophotogrammetric assessment of pre-and postoperative volumetric changes in the cleft lip and palate nose. International journal of oral and maxillofacial surgery, 2010, 39.6: 534-540.

Van Vlijmen OJ, Berge SJ, Swennen GR. Comparison of cephalometric radiographs obtained from cone-beam computed tomography scans and conventional radiographs. J Oral Maxillofac Surg. 2009; 67(1):92–7.

Verwoerd CD, Verwoerd-Verhoef HL, Meeuwis CA. Stress and wound healing of the cartilaginous nasal septum. Acta oto-laryngologica, 1989, 107.5-6: 441-445.

Verwoerd CD, Urbanus NA, Mastenbroek GJ, Verwoerd-Verhoef HL. The influence of partial resection of the nasal septum on the outgrowth of nose and upper jaw [proceedings]. ORL J Otorhinolaryngol Relat Spec. 1977; 39:174.

Wada T, Kremenak CR, Miyazaki T. Midfacial growth effects of surgical trauma to the area of the vomer in beagles. J Osaka Dent School. 1980; 20:241–246.

William MR, Newton GN. Cranial base morphology in association with intentional cranial vault deformation. American Journal of Physical Anthropology, 1965, 23.3: 241-253.

Wylie WL. The assessment of anteroposterior dysplasia. Angle Orthod 1947; 17: 97-109.

Wilde F, Lorenz K, Ebner AK, Krauss O, Mascha F, Schramm A. Intraoperative imaging with a 3D C-arm system after zygomatico-orbital complex fracture reduction. Journal of Oral and Maxillofacial Surgery, 2013, 71.5: 894-910.

Wolford LM, Cassano DS, Goncalves JR. Common TMJ disorders: orthodontic and surgical management. Temporomandibular Disorders and Orofacial Pain: Separating

Controversy from Consensus. Ann Arbor, MI: Department of Orthodontics and Pediatric Dentistry, University of Michigan School of Medicine, 2009, 159-198.

Wealthall RJ, Herring SW. 2006. Endochondral ossification of the mouse nasal septum. Anat Rec 288A:1163–1172.

Yoshida I, Shoji T, Mizoguchi I. Effects of treatment with a combined maxillary protraction and chincap appliance in skeletal Class III patients with different vertical skeletal morphologies. The European Journal of Orthodontics, 2007, 29.2: 126-133.

Yu HS, Baik HS, Sung SJ, Kim KD, Cho YS. Three-dimensional finite-element analysis of maxillary protraction with and without rapid palatal expansion. The European Journal of Orthodontics, 2007, 29.2: 118-125.

Yüksel S, Üçem TT, Keykubat A. Early and late facemask therapy. The European Journal of Orthodontics, 2001, 23.5: 559-568.

Yang Li, Chen Z, Zhang X. A cone-beam computed tomography evaluation of facial asymmetry in unilateral cleft lip and palate individuals. Journal of oral science, 2016, 58.1: 109-115.

Zuroff JP, Chen SH, Shapiro PA, Little RM, Joondeph DR, Huang GJ. Orthodontic treatment of anterior open-bite malocclusion: stability 10 years postretention. American journal of orthodontics and dentofacial orthopedics, 2010, 137.3: 302. E1-302. e8.

10. BIOGRAPHY

I was born in Baghdad, Iraq, in October 1980. I obtained my Bachelor's degree in Dentistry from Baghdad University in August 2003. Between August 2003 and May 2005, I worked as a General Practioneer Dentist. From September 2005 to November 2008, I enrolled Maxillofacial Surgery Residency. Between February 2009 and February 2011, I enrolled Biogenetic Engineering Medicine Specialty to be specialist in February 2012. From September 2012 to the September 2013, I enrolled Turkish language preparation course as a requirement for PhD. degree scholarship. Since September 2013, I enrolled for PhD. in the Department of Dento-Maxillofacial Radiology, Faculty of Dentistry, Marmara University, Istanbul, Turkey.

PERSONAL INFORMATION:

Name	AMMAR	Surname	MOHI
Birth Place	Baghdad-IRAQ	Birth Date	18/10/1980
Citizen	IRAQI	ID Card	760413921
E-Mail	Ammar_19_80@yahoo.com	Contact NO.	0095389513315

EDUCATION LEVEL:

	INISTITUTION	GRADUATION YEAR
Higher Diploma	University Of Baghdad	2012
Maxillofacial Surgery Certified Residency	Iraqi Higher Supreme of Medical Specialty	2009
License	University Of Baghdad	2003
Higher School	Baghdad Collage Of Intelligent Students	1998

WORK EXPERIENCE:

Job	Institute	Duration
Oncology Specialist dentist	Early detection special care hospital	2011-2012
Iraqi Oral cancer committee member	Ministry of health	2009-2011
Maxillofacial specialist	Surgical medical hospital	2005-2008
Health planning manager	Baghdad medical city	2008-2009
General practioneer	Alwia Dental care center	2003-2005

LANGUAGE COMPETENCY:

Foreign languages	Comprehension	Speaking	Writing
English	Excellent	Excellent	Excellent
Turkish	Good	Good	Good
French	Good	Good	Good

Evaluated as Excellent, Good, Intermediate, and Invalid.

Foreign Language Competency Exam #								
YDS	ÜDS	**IELTS** (Academic)	TOEFL IBT	**TOEFL PBT**	TOEFL CBT	FCE	CAE	CPE
		6.6		595				

COMPUTER KNOWLEDGE:

Program	Ability
Microsoft Office	Excellent
Mimics 10,14,19 and InPrint 1.0 (Materialise, Leuven, Belgium)	Excellent
Head and Neck Ultrasound Program British association of Ultrasound (Leiden Medical University, Leiden, Netherland)	Good

Evaluated as Excellent, Good, Intermediate and Invalid.